AD NUMBER

ADB131156

LIMITATION CHANGES

TO:

Approved for public release; distribution is unlimited.

FROM:

Distribution authorized to U.S. Gov't. agencies and their contractors; Critical Technology; JAN 1989. Other requests shall be referred to U.S. Army Aviation Research and Technology Activity Attn: AVSCOM, Fort Eustis, VA 23604-5577. This document contains export-controlled technical data.

AUTHORITY

USAAVSCOM ltr, 22 Mar 1990

(2)

USAAVSCOM TR-88-D-14A

US ARMY
AVIATION
SYSTEMS COMMAND

AD-B131 156

DYNAMIC SYSTEM COUPLER PROGRAM (DYSCO 4.1)
VOLUME I - THEORETICAL MANUAL

Alex Berman, Shyi-Yuang Chen, Bruce Gustavson, Patricia Hurst

Kaman Aerospace Corporation
P.O. Box 2
Bloomfield, CT 06002-0002

January 1989

Final Report for Period September 1985 - May 1988

Prepared for

AVIATION APPLIED TECHNOLOGY DIRECTORATE
US ARMY AVIATION RESEARCH AND TECHNOLOGY ACTIVITY (AVSCOM)
Fort Eustis, VA. 23604-5577

AVIATION APPLIED TECHNOLOGY DIRECTORATE POSITION STATEMENT

This report documents the work performed to enhance the Dynamic System Coupler (DYSCO) computer program through the addition of advanced modeling capabilities. These capabilities include rotor blade damage modeling, Eigen analysis development, general time history solution development, frequency domain solution development, general modal representation of three-dimensional structures, lifting surface modal representation, landing gear, general force, linear constraints, lifting surface aerodynamics, calculation of component interface and internal loads, and a nonlinear spring and damper system. While the improvements incorporated into DYSCO, as a result of this work, increase the analytical capabilities of the program, it still has limitations in several areas. More correlation with flight test data or with similar proven analytical tools is needed to validate program results. A new or improved trim algorithm is needed to eliminate deficiencies in the current DYSCO trim algorithm. Also, DYSCO should be converted to double precision to increase the accuracy of program results.

Mr. Robert A. Lindholm of the Aeronautical Technology Division served as the project engineer for this contract.

The following notice applies to any unclassified (including originally classified and now declassified) technical reports released to "qualified U.S. contractors" under the provisions of DoD Directive 5230.25, Withholding of Unclassified Technical Data From Public Disclosure.

NOTICE TO ACCOMPANY THE DISSEMINATION OF EXPORT-CONTROLLED TECHNICAL DATA

1. Export of information contained herein, which includes, in some circumstances, release to foreign nationals within the United States, without first obtaining approval or license from the Department of State for items controlled by the International Traffic in Arms Regulations (ITAR), or the Department of Commerce for items controlled by the Export Administration Regulations (EAR), may constitute a violation of law.

2. Under 22 U.S.C. 2778 the penalty for unlawful export of items or information controlled under the ITAR is up to two years imprisonment, or a fine of $100,000, or both. Under 50 U.S.C., Appendix 2410, the penalty for unlawful export of items or information controlled under the EAR is a fine of up to $1,000,000, or five times the value of the exports, whichever is greater; or for an individual, imprisonment of up to 10 years, or a fine of up to $250,000, or both.

3. In accordance with your certification that establishes you as a "qualified U.S. Contractor", unauthorized dissemination of this information is prohibited and may result in disqualification as a qualified U.S. contractor, and may be considered in determining your eligibility for future contracts with the Department of Defense.

4. The U.S. Government assumes no liability for direct patent infringement, or contributory patent infringement or misuse of technical data.

5. The U.S. Government does not warrant the adequacy, accuracy, currency, or completeness of the technical data.

6. The U.S. Government assumes no liability for loss, damage, or injury resulting from manufacture or use for any purpose of any product, article, system, or material involving reliance upon any or all technical data furnished in response to the request for technical data.

7. If the technical data furnished by the Government will be used for commercial manufacturing or other profit potential, a license for such use may be necessary. Any payments made in support of the request for data do not include or involve any license rights.

8. A copy of this notice shall be provided with any partial or complete reproduction of these data that are provided to qualified U.S. contractors.

D E S T R U C T I O N N O T I C E

For classified documents, follow the procedures in DoD 5200.22-M, Industrial Security Manual, Section II-19 or DoD 5200.1-R, Information Security Program Regulation, Chapter IX. For unclassified, limited documents, destroy by any method that will prevent disclosure of contents or reconstruction of the document.

UNCLASSIFIED
SECURITY CLASSIFICATION OF THIS PAGE

REPORT DOCUMENTATION PAGE

1a. REPORT SECURITY CLASSIFICATION UNCLASSIFIED	1b. RESTRICTIVE MARKINGS
2a. SECURITY CLASSIFICATION AUTHORITY	3. DISTRIBUTION / AVAILABILITY OF REPORT Distribution authorized to U.S. Government agencies and their contractors, critical technology, January 1989. Other requests for this document shall be referred to the Aviation Applied Technology Directorate,U.S. Army Aviation Research & Technology Activity (AVSCOM), Fort Eustis, VA 23604-5577
2b. DECLASSIFICATION / DOWNGRADING SCHEDULE	
4. PERFORMING ORGANIZATION REPORT NUMBER(S) R-1790	5. MONITORING ORGANIZATION REPORT NUMBER(S) USAAVSCOM TR 88-D-14A
6a. NAME OF PERFORMING ORGANIZATION KAMAN AEROSPACE CORPORATION 6b. OFFICE SYMBOL (If applicable)	7a. NAME OF MONITORING ORGANIZATION AVIATION APPLIED TECHNOLOGY DIRECTORATE
6c. ADDRESS (City, State, and ZIP Code) P. O. BOX 2 BLOOMFIELD, CONNECTICUT 06002-0002	7b. ADDRESS (City, State, and ZIP Code) U.S. ARMY AVIATION RESEARCH AND TECHNOLOGY ACTIVITY (AVSCOM) FORT EUSTIS, VIRGINIA 23604-5577
8a. NAME OF FUNDING / SPONSORING ORGANIZATION 8b. OFFICE SYMBOL (If applicable)	9. PROCUREMENT INSTRUMENT IDENTIFICATION NUMBER DAAJ02-85-C-0033
8c. ADDRESS (City, State, and ZIP Code)	10. SOURCE OF FUNDING NUMBERS PROGRAM ELEMENT NO. 62209A; PROJECT NO. TL1622-09AH76; TASK NO. B; WORK UNIT ACCESSION NO. 43 EK

11. TITLE (Include Security Classification)
Dynamic System Coupler Program (DYSCO 4.1), Volume I - Theoretical Manual

12. PERSONAL AUTHOR(S)
Alex Berman, Shyi-Yuang Chen, Bruce Gustavson, Patricia Hurst

13a. TYPE OF REPORT	13b. TIME COVERED	14. DATE OF REPORT (Year, Month, Day)	15. PAGE COUNT
Final	FROM 13 Sep 85 TO 13 May 88	January 1989	143

16. SUPPLEMENTARY NOTATION
Volume I of a three-volume report.

17. COSATI CODES			18. SUBJECT TERMS (Continue on reverse if necessary and identify by block number)
FIELD	GROUP	SUB-GROUP	Dynamic analysis, Component coupling, Helicopter analysis.

19. ABSTRACT (Continue on reverse if necessary and identify by block number)

DYSCO is an interactive computer program which allows a user to model the dynamic and aerodynamic behavior of rotorcraft and other aerospace structures. The Program provides user-oriented modeling procedures and data base management for dynamic analyses of coupled systems of independently modeled components. Each component is a system of second-order ordinary differential equations. The user employs modules from an expandable library of algorithms to formulate and couple components and to obtain solutions of the coupled system.

20. DISTRIBUTION / AVAILABILITY OF ABSTRACT	21. ABSTRACT SECURITY CLASSIFICATION	
☐ UNCLASSIFIED/UNLIMITED ☐ SAME AS RPT. ☐ DTIC USERS		
22a. NAME OF RESPONSIBLE INDIVIDUAL R.A. Lindholm	22b. TELEPHONE (Include Area Code) (804) 878-3773	22c. OFFICE SYMBOL SAVRT-TY-ATA

DD FORM 1473, 84 MAR 83 APR edition may be used until exhausted. All other editions are obsolete.

SECURITY CLASSIFICATION OF THIS PAGE
UNCLASSIFIED

TABLE OF CONTENTS

TABLE OF CONTENTS (continued)

LIST OF ILLUSTRATIONS

LIST OF ILLUSTRATIONS

1.0 DYSCO OVERVIEW

DYSCO is a fully interactive computer program for modeling arbitrarily coupled dynamic and aerodynamic systems. It is designed to provide the automatic dynamic coupling of components and associated forces necessary to formulate the system equations of motion of a model and to execute user-selected solution algorithms. The program is composed of an executive which acts on user-oriented modeling commands to control execution, a data base management facility for input/output and data storage and retrieval, and an expandable technology library of component, force, and solution algorithms.

A component technology module ("component") is a group of program subroutines that represents a system of 2nd-order ordinary differential equations which may have constant, time-dependent, or nonlinear coefficients. The coefficients may be arbitrary (but computable) functions of the independent variable (time) and the system state vector. Thus, a "component" is an algorithm which defines the degrees of freedom and computes the coefficients of a system of differential equations from specified physical parameters, time, and the component state vector. A force technology module ("force") is an algorithm which computes the generalized force acting on the component as a function of the present or a past state vector of the component and other physical data (e.g., aerodynamic). A "model" is a coupled system of differential equations formulated from the component equations and associated forces specified by the user. A solution technology module can include any algorithm which operates on a system of differential equations (e.g., eigenanalysis, time history).

The user defines a model by selecting components and forces and identifying the data to be used. From the model definition, the coupled system equations are automatically formed independent of any solution algorithm. Solutions may then be selected for the model. Modeling will typically be accomplished over several interactive sessions using previous results as building blocks for forming variations in the models. Component and force input data are individually stored on permanent user data files. An existing input data set for a

component or force can be edited to form a different data set or to replace the original data set. Model definitions are also individually stored and may be edited to replace, delete, insert, or add components and forces for new model formulation.

DYSCO supports two types of data files: random access user data files and sequential external data files. A user data file contains the data resulting from interactive user modeling sessions and includes component, force, and model definitions and data, and auxiliary engineering data such as airfoil tables. The data on user data files is in a format that allows it to be recognized, listed, and appropriately manipulated by the executive. Examples of external data are induced velocity maps for rotor systems, airfoil tables, and plot files. While the executive has knowledge of and tracks the existence of external data during a session, it does not automatically attempt to handle the data. Special programming must be developed within technology modules to utilize the data as required. Some data, such as airfoil tables, although created externally and initially introduced as an external data file, are used frequently and are thus read, reformatted, and saved on a user data file via a special modeling command.

1.1 MATHEMATICS OF THE COMPONENT AND SYSTEM EQUATIONS

1.1.1 Assumptions. The general concept upon which DYSCO is based depends on the following assumptions:

1. The relevant physics of a system may be modeled as a set of second-order differential equations in the time domain. The equations are of the form

$$M\ddot{X} + C\dot{X} + KX = F$$

where X is the vector of the degrees of freedom of the system. M, C, and K are coefficient matrices and F is a force vector where M, C, K, and F are arbitrary functions of $\dot{X}$, X, and time.

2. It is possible to formulate the equations of a system based on the equations of the components of the system. The equations of the components are of the same form as the equations of the system as in 1, above. "Formulation" includes the establishment of the logic which will allow the computation of the varying coefficients (elements of M, C, and K) and forces (F) of the system equations based on the computed coefficients and forces of each component at any point in time.

3. It is possible to compute the state vector ($\dot{X}$ and X) of each component based on the state vector of the system. The state vectors of the components may be used to compute the coefficients and forces of the equations of the components at each point in time. These coefficients and forces may then be used to compute the coefficients and forces of the system equations as in 2, above.

1.1.2 Component Equations. Any portion of the system which can be represented by a set of second-order differential equations, subject to the conditions stated below, may be considered to be a "component" represented in its own local coordinate system. The equation of component I may be written

$$M_I \ddot{X}_I + C_I \dot{X}_I + K_I X_I = F_I + F_{IR}$$

where X_I is a vector containing the degrees of freedom of the component. The coefficient matrices, M_I, C_I, and K_I, and the force vector, F_I, may be arbitrary functions of X_I, $\dot{X}_I$, and time. F_{IR} is a vector of the reaction forces at the interfaces to other components. The elements of F_I may also be functions of X and $\dot{X}$ of other components. "Arbitrary function" as used above means that it is possible to write a program to compute the numerical value of the function at any point in time given numerical values of the appropriate variables. This functionality includes linear, nonlinear analytical, periodic, and tabular functions.

The individual degrees of freedom must represent independent (generalized) coordinates. The degrees of freedom may be actual physical displacements in coordinate systems which are fixed or moving at a uniform velocity or rotating at a constant velocity. They may also represent modal displacements or any other generalized coordinate. X_I may contain any combination of the allowable types of degrees of freedom.

The coupling treated in DYSCO involves equating physical displacements of two or more components. These physical displacements may or may not be generalized coordinates of the components; however, they must be expressible as a linear combination of degrees of freedom of each of the components to be coupled. Thus, the vector, X_I, must contain appropriate degrees of freedom to allow desired coupling to other components.

1.1.3 System Equations. The system coefficient matrices and generalized force vector are formed from the component matrices and vectors. The degree of freedom vector of the system, X, must contain only independent coordinates. This vector is formed by assembling the degrees of freedom of all of the components and eliminating duplications when specific degrees of freedom are coupled or eliminating a degree of freedom whenever linear combinations of degrees of freedom are coupled. Also, the reaction forces between components cancel when the system equations are assembled. Thus, they may be neglected.

1.1.4 Coordinate Transformations. Each degree of freedom of a component is equal to a degree of freedom of the system or is a linear combination of degrees of freedom. This relationship may be expressed as a matrix equation

$$X_I = T_I X$$

where T_I is an $n_I x n$ matrix. n_I and n are the number of degrees of freedom of the component and the system. Since the coupling treated in DYSCO physically joins components, T_I may not be a function of time and, therefore,

$$\dot{X}_I = T_I \dot{X}$$

$$\ddot{X}_I = T_I \ddot{X}$$

When the system contains degrees of freedom in fixed and moving coordinate systems, any necessary transformations are to be modeled within the component representations. This will result in time dependent coefficients, which is consistent with the component equations as previously defined.

Using the transformation relationships, the equation for a component can be written in terms of the system degrees of freedom

$$M_I T_I \ddot{X} + C_I T_I \dot{X} + K_I T_I \dot{X} = F_I$$

This matrix equation, however, is not a proper dynamic representation since the coefficient matrices are rectangular and F_I is not the generalized force vector corresponding to X. The generalized force vector is defined as the vector that yields work done by the external forces when the product $X_I^T F_I$ is formed where X_I^T is X_I transpose.

The work done cannot depend on the coordinate system; that is, the work due to the component degrees of freedom must be equal to the work due to the system degrees of freedom. Then, since

$$X_I^T F_I = X^T T_I^T F_I$$

the right side of the transformed matrix equation must be $T_I^T F_I$. This is achieved by premultiplying by T_I^T, yielding

$$T_I^T M_I T_I \ddot{X} + T_I^T C_I T_I \dot{X} + T_I^T K_I T_I X = T_I^T F_I$$

When this transformation is performed on each component set of equations, they are consistent and may be added to form the equations of the coupled system

$$M\ddot{X} + C\dot{X} + KX = F$$

where

$$M = \sum_I T_I^T M_I T_I$$

$$C = \sum_I T_I^T C_I T_I$$

$$K = \sum_I T_I^T K_I T_I$$

$$F = \sum_I T_I^T F_I$$

These equations are not limited to linear equations. It should be noted, however, that when the coefficients and forces are functions of time or are nonlinear, they must be evaluated numerically at discrete values of time, or when the component state vectors have been evaluated if the coefficients or forces are nonlinear.

(A global reference system, which permits the application of consistent gravitational and centrifugal force vectors to component degrees of freedom, has been developed as an adjunct to several component and solution technology modules and is discussed in paragraph 3.4, Volume II.)

1.2 SOLUTION TECHNIQUES

The solutions currently available in DYSCO are of three types:

1. Eigenanalysis
2. Frequency domain
3. Time history.

The eigenanalysis and frequency domain solutions are purely mathematical operations on the system constant M, C, and K matrices. Time history solutions involve solutions of the differential equations in the time domain.

A time history solution is an integration algorithm which takes the accelerations at a given time, t, and computes the velocities and displacements at the next time increment, $t + \Delta t$. The acceleration is obtained by solving

$$\ddot{X} = M^{-1} (F - C\dot{X} - KX)$$

at time, t. The values of $\dot{X}$ and X were obtained on the previous execution of the integration and M, C, K, and F are obtained as previously computed constants and time-dependent values, if any.

The time-dependent component coefficients are computed, transformed, and added to the system constant matrices at each time step. The calculation of nonlinear coefficients and forces requires information derived from local velocities and displacements of the component (and possibly other components). This information is obtained from the system state vector by use of the transformation data as previously described.

1.3 TECHNOLOGY MODULES

The technology module library contains the component, force, and solution algorithms available for formulating and analyzing a model. Each technology module is a group of program subroutines called technical modules that implement a given algorithm. The technology module library is designed for expansion, allowing new methods to be added in a consistent and well-defined manner. A technology module has multiple interfaces with the executive corresponding to specific steps in the modeling process and is thus composed of a specific set of technical modules, depending on whether it represents a component, force, or solution. Technology modules are given a four-character name. The first character is C, F, or S, depending on whether the technology module is a component, force, or solution. The second and third characters are used as a description and the fourth character indicates a general level of complexity.

Technical Modules - The type and number of technical modules required for implementation of a technology module depend on the technology module type. Each technical module has specific functions to perform although the data required, the algorithms, and the output data vary. The name of a technical module is five characters - the technology module name plus a character that indicates the function to be performed. A brief description of the required technical modules is shown below (full detail may be found in Volume II of this report):

Component Technical Modules

Input	C---I	Defines the user input data requirements
Definition	C---D	Defines the degrees of freedom and implicit relationships for a particular usage
Coefficient	C---C	Computes the constant coefficients and forces of the component equations
Active	C---A	Computes time varying coefficients and forces of the component equations based on component state vector. Accesses optional "force module" for computation of applied forces.
Block	C---B	Reads/writes private common block /C---/
Loads	C---L	Optional. Computes time history component loads based on component state vector.

Force Technical Modules

Input	F---I	Defines the user input data requirements
Coefficient	F---C	Performs preliminary calculations
Active	F---A	Computes time varying applied forces of the associated component equation
Block	F---B	Reads/writes private common block /F---/

Solution Technical Modules

Input	S---I	Defines the user input data requirements
Active	S---A	Performs the solution and outputs the results

C---B and F---B are utilities for the preparation of a "case," which is automatically formed as a user option. A case includes a model, user input for a selected solution, and any required auxiliary data (e.g., airfoil tables). Thus, the CASE command allows the user to execute a solution which has been previously defined.

During an interactive session, degree of freedom names are either automatically formed in a standard format or they may be supplied by the user, depending on the formulation of the technology module for a given component. Components are automatically coupled into a model either by recognition of identical degree of freedom names or by generated or supplied linear constraint relations. The degrees of freedom may represent physical displacements or generalized modal displacements. Each component is represented independently, the only requirement being that necessary interface coordinates be included as degrees of freedom.

1.4 COMMUNICATION

Mechanisms are provided for communication between the executive and technology modules, between technology modules, and within technology modules.

Between the Executive and Technology Modules - The executive controls data related to a model being formed or executed with a chosen solution. Technical modules may require this data as input or may be required to compute it and send it to the executive for storage. These requirements are specific to the particular technical module. A design feature which prohibits the passage of physical data into the executive allows the independent implementation of

technology modules. All physical data associated with a technology module are treated as local data, and only abstract data (e.g., equation coefficients) are passed to the executive. The mechanisms utilized are:

1. Argument Lists - Provide input from the Executive and output to the Executive.
2. XBG Utilities - Provide for retrieval of Base and Global Variables (user input for Component and Force modules).
3. /AFTAB/ - A common block used by the Executive to store all airfoil tables required for a model. /AFTAB/ is incorporated into specific Technical Modules for accessing the tables.

Between Technology Modules - Communication between technology modules is via special "shared" common blocks. Communication between the technical modules of a particular component or between a component and a force or solution module is through a shared common block. The name of a shared common block is descriptive of its usage.

Within a Technology Module - Communication strictly between the technical modules for a specific technology module is through a "private" common block. The name of a private common block is the same as the component, force, or solution module with which it is used.

1.5 INSTALLATION OF NEW TECHNOLOGY MODULES

Whenever a new technology module is added to the DYSCO library, certain information must be provided to the executive. This information is provided by "installing" the technology module into the common block, /XTM/, which contains master variables and arrays describing the limitations and usages of

that technology module. In addition, FORTRAN "calls" are inserted into specific predeveloped subroutines for each of the technical modules developed. A new shared common block is similarly installed via the common block, /XTM/, and insertion of appropriate "calls."

1.6 THEORETICAL BASIS

The basic concepts and procedures for the practical use of DYSCO have been presented in this general discussion. The following sections include detailed descriptions of component and force modules which augment material presented in Volume II. The results of validation analyses for advanced helicopter simulations are presented and are compared with results from other sources.

Except where noted otherwise, the accuracy of the analyses is only dependent upon the limitations of the approximations made by the user in the development of specific component representations (data sets).

Volume II contains a complete description of the features and uses of the program and the necessary information for the development and installation of new components, forces, and solutions. Volume III contains examples of input and output data for each technology module and several modeling examples.

2.0 DYSCO ANALYSES

2.1 ADVANCED ELASTIC BLADE ANALYSIS - CRE3

A comprehensive development of the equations of motion of a rotor blade was first published by Houbolt and Brooks (Reference 1) in 1958. These equations were reformulated by Hodges and Dowell (Reference 2) in 1974, their major contribution being improved generality, including nonlinear terms and the independent verification of the earlier work. Berman, Giansante, and Flannelly (Reference 3) expanded these previous works by the addition of five hub degrees of freedom.

The present research uses the equations of motion for a flexible hingeless rotor blade, as derived in Reference 2, as a starting point. The mathematical model considered for the rotor blade is a straight, slender, nonuniform beam with distributed pretwist. The elastic axis (shear center), the mass center, and the area centroid are considered as noncoincident. Offset at $r = \bar{e}$ is included to allow for consideration of the hinge offset of an articulated rotor, or a very stiff hub of a hingeless rotor. Different offsets, e_F and e_L, are used for flap and lead-lag motion.

The rotor blade can undergo combined in-plane bending, out-of-plane bending, and torsion, and the rotor hub is assigned six degrees of freedom. Hamilton's law of varying action (Reference 4) has been used to derive the equations of motion in a generalized coordinate system which allows a direct solution without the consideration of force equilibrium. It may be noted that the above approach is equivalent to the Lagrange approach if the shape function in time domain is not being used.

2.1.1 Ordering Scheme. In order to avoid high order terms that might overly complicate the equations of motion, a systematic ordering scheme was adopted

to determine which terms should be ignored. The ordering scheme employed in this study for the various parameters is given below:

$u/R = 0(\epsilon^2)$ $\quad\quad$ $\eta, \zeta/R = 0(\epsilon)$

$v/R = 0(\epsilon)$ $\quad\quad$ $c, t/R = 0(\epsilon)$

$w/R = 0(\epsilon)$ $\quad\quad$ $e/R = 0(\epsilon)$

$x/R = 0(1)$ $\quad\quad$ $\beta_{pc} = 0(\epsilon)$

$\phi = 0(\epsilon)$

$X_H, Y_H, Z_H, \alpha_x, \alpha_y, \alpha_z = 0(\epsilon)$

In the total energy equation, if any terms are two or more orders higher than the lowest order term, then the higher order terms are discarded.

2.1.2 Coordinate System and Motion Variable. As demonstrated in Figure 1, the coordinate system used to describe the blade and hub motion in the present analysis is as follows:

1. Triplet X, Y, Z represents an inertia frame, R. The R system coordinates are the rotor shaft axes when there is no hub motion.
2. Triplet x_p, y, z is fixed in a reference frame B_1 which rotates with respect to R frame at constant angular velocity Ω.
3. x, y, z axes are also fixed in B_1, in which x, the elastic axis of the undeformed beam, is inclined to x_p axis at the precone angle β_{pc}. This system is referred to as B frame.
4. x′, y′, z′ are a blade fixed coordinate system. x′ is tangent to the deformed elastic axis, and y′, z′ are the principal axes of local cross section. Note that the torsion deformation of the blade cross section is about the x′ axis.

The deformations of elastic axes u, v, and w are defined with respect to the B system, while the linear and angular motion of the rotor hub, X_H, Y_H, Z_H, α_x, α_y, α_z (Figure 2) are defined with respect to the inertia frame, R.

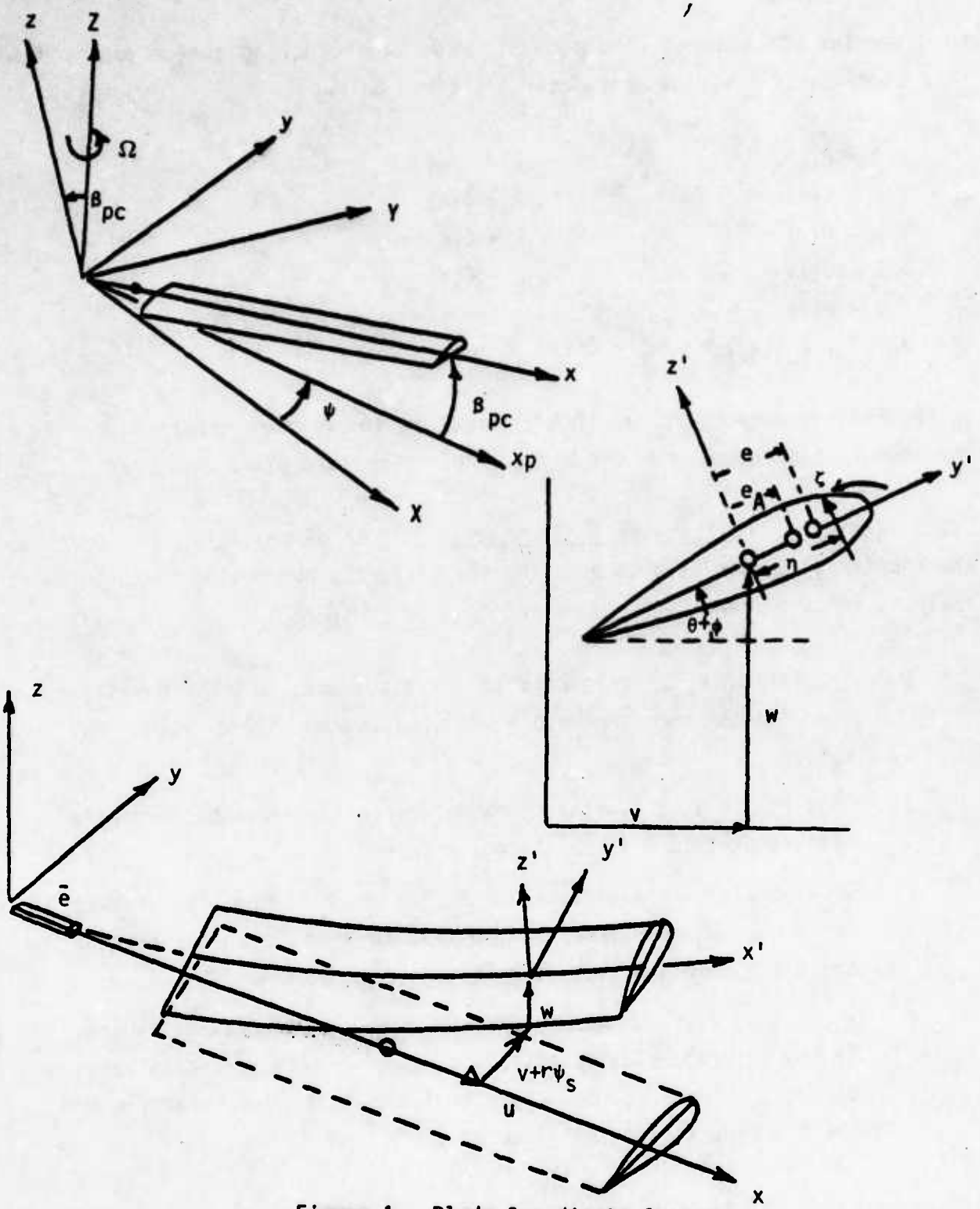

Figure 1. Blade Coordinate System.

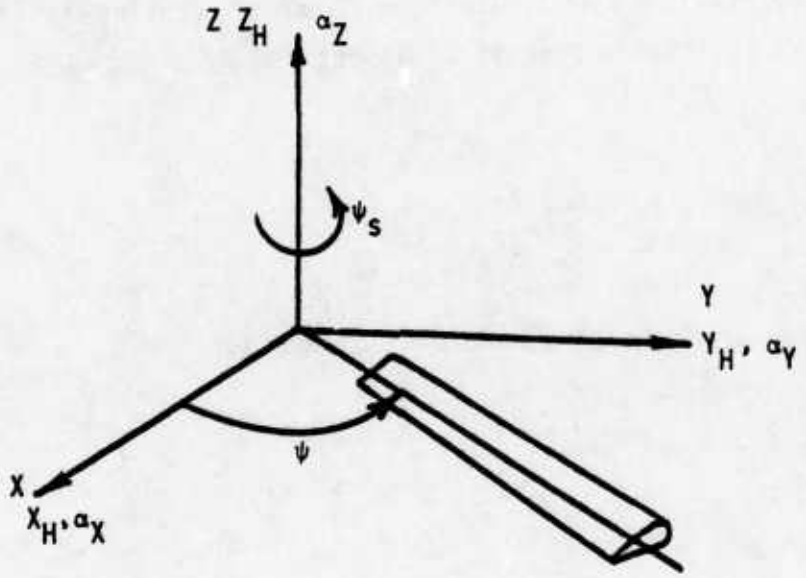

Figure 2. Hub and Perturbation Rotational Degrees of Freedom.

2.1.3 Hamilton's Law of Varying Action. "Hamilton's Principle," used in Reference 2 to derive equations of motion of the rotor blade, can be expressed as

$$\int_{t_1}^{t_2} [\delta (U - T) - \delta W] \, dt = 0 \tag{1}$$

where U is the strain energy, T is the kinetic energy, and δW is the virtual work of the external forces. Hamilton's law of varying action, which is a special case of Hamilton's Principle, is defined by

$$\int_{t_1}^{t_2} [\delta (U - T) - \delta W] \, dt - \frac{\partial T}{\partial \dot{q}_i} \delta q_i \Big|_{t_1}^{t_2} = 0 \tag{2}$$

which can reduce to Equation 1 under the assumption

$$\frac{\partial T}{\partial \dot{q}_i} \delta q_i \Big|_{t_1}^{t_2} = 0 \tag{3}$$

i.e., "stationary" in calculus of variation's terminology.

The Lagrange equation

$$\int_{t_1}^{t_2} \left[\frac{d}{dt} \frac{\partial T}{\partial \dot{q}_i} - \frac{\partial T}{\partial q_i} + \frac{\partial U}{\partial q_i} - \frac{\delta W}{\partial q_i} \right] \delta q_i dt = 0 \tag{4}$$

can be obtained from either Equation 2 without any assumptions or Equation 1 with the "stationary" assumption.

It should be emphasized here that Hamilton's law of varying action, Equation 2, is not merely an alternative form of the Lagrangian equation, Equation 4, but is much more general. Equation 2 allows one to pursue the solutions of a system without consideration of force equilibrium and the theory of partial differential equations (References 4 and 5), while Equation 4 does not. Unfortunately, a detailed discussion of the differences among Equations 1, 2, and 4 is beyond the scope of this study.

2.1.4 Strain Energy Contributions. Using the derivations of Reference 2 with the addition of root springs, the strain energy contribution can be expressed as

$$\delta U = \int_{\bar{e}}^{r} \left\{ Y_{v''}\delta v'' + Y_{v'}\delta v' + Y_{w''}\delta w'' + Y_{w'}\delta w' + Y_{\phi''}\delta\phi'' + Y_{\phi'}\delta\phi' + Y_{\phi}\,\delta\phi + Y_{u'}\delta u' \right\} dx + \left[K_F w'\delta w' + K_L v'\delta v' + K_\phi \phi\delta\phi \right] \Big|_{r=\bar{e}} \qquad (5)$$

where K_F, K_L, and K_ϕ are flap, lag, and torsion spring rate, respectively, and

$$\left.\begin{aligned} Y_{v''} &= M_{z'}\cos(\theta+\phi) + M_{y'}\sin(\theta+\phi) \\ Y_{v'} &= V_{x'}v' \\ Y_{w''} &= M_{z'}\sin(\theta+\phi) - M_{y'}\cos(\theta+\phi) \\ Y_{w'} &= V_{x'}w' \\ Y_{\phi''} &= P_{x'} \\ Y_{\phi'} &= S_{x'} + T_{x'} \\ Y_{\phi} &= Y_{v''}w'' - Y_{w''}v'' \\ Y_{u'} &= V_{x'} \end{aligned}\right\} \qquad (6)$$

From Equation 34 of Reference 2

$$
\left.
\begin{aligned}
V_{x'} &\equiv \iint_A \sigma_{xx}\, d\eta\, d\zeta = EA\left\{u' + \frac{v'^2}{2} + \frac{w'^2}{2} + k_A^2\,\theta'\phi' - e_A\,[v''\cos(\theta+\phi) \right. \\
&\qquad \left. + w''\sin(\theta+\phi)]\right\} \\
S_{x'} &\equiv \iint_A (\hat{\eta}\sigma_{x\zeta} - \hat{\zeta}\sigma_{x\eta})\, d\eta\, d\zeta = GJ\phi' \\
T_{x'} &\equiv \iint_A (\theta+\phi)'\sigma_{xx}(\eta^2+\zeta^2)\, d\eta\, d\zeta = EAk_A^2(\theta+\phi)'\left[u' + \frac{v'^2}{2} + \frac{w'^2}{2}\right] \\
&\qquad + EB_1^*\theta'^2\phi' - EB_2^*\theta'\,(v''\cos\theta + w''\sin\theta) \\
P_{x'} &\equiv -\iint_A \lambda\sigma_{xx}\, d\eta\, d\zeta = EC_1\phi'' + EC_1^*\,(w''\cos\theta - v''\sin\theta) \\
M_{y'} &\equiv \iint_A \zeta\sigma_{xx}\, d\eta\, d\zeta = EI_{y'}[v''\sin(\theta+\phi) - w''\cos(\theta+\phi)] - EC_1^*\phi'' \\
M_{z'} &\equiv -\iint_A \eta\sigma_{xx}\, d\eta\, d\zeta = EI_{z'}[v''\cos(\theta+\phi) + w''\sin(\theta+\phi)] \\
&\qquad - EAe_A\left[u' + \frac{v'^2}{2} + \frac{w'^2}{2}\right] - EB_2^*\theta'\phi'
\end{aligned}
\right\} \quad (7)
$$

From Equation 35 of Reference 2, the section integrals in Equation 7 are defined as follows:

$$\left.\begin{aligned} A &\equiv \iint_A d\eta\, d\zeta & Ae_A &\equiv \iint_A \eta\, d\eta\, d\zeta \\ I_{y'} &\equiv \iint_A \zeta^2\, d\eta\, d\zeta & I_{z'} &\equiv \iint_A \eta^2\, d\eta\, d\zeta \\ Ak_A^2 &\equiv \iint_A (\eta^2 + \zeta^2)\, d\eta\, d\zeta & J &\equiv \iint_A (\hat{\eta}^2 + \hat{\zeta}^2)\, d\eta\, d\zeta \\ B_1^* &\equiv \iint_A (\eta^2 + \zeta^2)^2\, d\eta\, d\zeta & B_2^* &\equiv \iint_A \eta(\eta^2 + \zeta^2)\, d\eta\, d\zeta \\ C_1 &\equiv \iint_A \lambda^2\, d\eta\, d\zeta & C_1^* &\equiv \iint_A \zeta\lambda\, d\eta\, d\zeta \end{aligned}\right\} \quad (8)$$

2.1.5 Kinetic Energy Contribution. The position vector $\vec{\rho}$ of a blade element, after deformation, in the rotating frame B is

$$\begin{aligned} \vec{\rho} &= x_1 \vec{i} + y_1 \vec{j} + z_1 \vec{k} \\ &= \Big\{ x + u - \lambda\phi' - (v' + \psi_s)\,[\eta \cos(\theta + \phi) - \zeta \sin(\theta + \phi)] \\ &\qquad - w'\,[\eta \sin(\theta + \phi) + \zeta \cos(\theta + \phi)] \Big\} \vec{i} \\ &\quad + \Big\{ v + r\psi_s + \eta \cos(\theta + \phi) - \zeta \sin(\theta + \phi) \Big\} \vec{j} \\ &\quad + \Big\{ w + \eta \sin(\theta + \phi) + \zeta \cos(\theta + \phi) \Big\} \vec{k} \end{aligned} \quad (9)$$

The rotational velocity of frame B is

$$\vec{\omega}_B = [T] \begin{Bmatrix} \dot{\alpha}_x \\ \dot{\alpha}_y \\ \dot{\alpha}_z + \Omega \end{Bmatrix} \tag{10}$$

where

$$[T] = \begin{bmatrix} \cos\beta_{pc}\cos\psi & \cos\beta_{pc}\sin\psi & \sin\beta_{pc} \\ -\sin\psi & \cos\psi & 0 \\ -\sin\beta_{pc}\cos\psi & -\sin\beta_{pc}\sin\psi & \cos\beta_{pc} \end{bmatrix} \tag{10a}$$

The translational velocity of the origin of frame B is

$$\vec{V}_{oB} = [T] \begin{Bmatrix} \dot{X}_H \\ \dot{Y}_H \\ \dot{Z}_H \end{Bmatrix} \tag{11}$$

Then, the total velocity, $\vec{V}_B$ of a blade element can be expressed as

$$\vec{V}_B = \vec{V}_{oB} + \dot{\vec{\rho}} + \vec{\omega}_B \times \vec{\rho} \tag{12}$$

where $\dot{\vec{\rho}}$ is the relative velocity of a blade element with regard to rotating frame B. $\vec{V}_{oB}$ and $\vec{\omega}_B \times \vec{\rho}$ are contributions from the motion of hub degrees of

freedom. Thus, from Equations 9 and 11, the total velocity $\vec{V}_B$ of a blade element is given by

$$\left.\begin{aligned}
\vec{V}_B &= V_x\vec{i} + V_y\vec{j} + V_z\vec{k} \\
&= (\dot{x}_1 - \Omega y_1 \cos\beta_{pc} + \cos\beta_{pc}\cos\psi\,\dot{X}_H + \cos\beta_{pc}\sin\psi\,\dot{Y}_H \\
&\quad + \sin\beta_{pc}\,\dot{Z}_H + \Omega_y z_1 - \Omega_z y_1)\,\vec{i} \\
&\quad + (\dot{y}_1 + \Omega x_1 \cos\beta_{pc} - \Omega z_1 \sin\beta_{pc} - \sin\psi\,\dot{X}_H + \cos\psi\,\dot{Y}_H \\
&\quad - \Omega_x z_1 + \Omega_z x_1)\,\vec{j} \\
&\quad + (\dot{z}_1 + \Omega y_1 \sin\beta_{pc} - \sin\beta_{pc}\cos\psi\,\dot{X}_H - \sin\beta_{pc}\sin\psi\,\dot{Y}_H \\
&\quad + \cos\beta_{pc}\,\dot{Z}_h + \Omega_x y_1 - \Omega_y x_1)\,\vec{k}
\end{aligned}\right\} \quad (13)$$

where

$$\begin{Bmatrix}\Omega_x\\ \Omega_y\\ \Omega_z\end{Bmatrix} = [T]\begin{Bmatrix}\dot{\alpha}_x\\ \dot{\alpha}_y\\ \dot{\alpha}_z\end{Bmatrix} \quad (14)$$

The variation of kinetic energy is

$$\delta T = \int_0^R \iint_A \vec{V}_B \cdot \delta\vec{V}_B \, dm\, dx \quad (15)$$

Following the ordering scheme of Reference 2, with the additional assumption that the order of hub degrees of freedom and perturbation shaft speed are $O(\epsilon)$, then, from Equations 13, 14, 15 and the application of Hamilton's law, the following equation can be obtained:

$$\left.\begin{aligned} &\delta \int_{t_1}^{t_2} T\,dt - \frac{\partial T}{\partial \dot{q}_i}\,\delta q_i \Bigg|_{t_1}^{t_2} \\ &= \int_{t_1}^{t_2} \int_0^R \left(X_u\,\delta u + X_v\,\delta v + X_w\,\delta w + X_\phi\,\delta\phi\right. \\ &\qquad + X_{v'}\,\delta v' + X_{w'}\,\delta w' + X_{\phi'}\,\delta\phi' + X_{\psi_S}\,\delta\psi_S \\ &\qquad + X_{Y_H}\,\delta Y_H + X_{Z_H}\,\delta Z_H + X_{\alpha_X}\,\delta\alpha_X + X_{\alpha_Y}\,\delta\alpha_Y \\ &\qquad \left. + X_{\alpha_Z}\,\delta\alpha_Z\, X_{X_H}\,\delta X_H\right)\,dx\,dt \end{aligned}\right\} \quad (16)$$

where

$$X_u = m\left[\Omega^2 r + 2\Omega\left(\dot{v} + r\dot{\psi}_S\right)\right] - m\sin\psi\,\ddot{Y}_H - m\cos\psi\,\ddot{X}_H + mr\Omega\Omega_Z \quad (16a)$$

$$
\begin{aligned}
X_v = {} & m\Omega^2(v + r\psi_s + e\cos(\theta + \phi)) + 2m\Omega(\beta_{pc}\dot{w} - \dot{u}) \\
& + 2me\Omega(\dot{v}'\cos\theta + \dot{\psi}_s\cos\theta + \dot{w}'\sin\theta) - m(\ddot{v} + r\ddot{\psi}_s) \\
& + me\ddot{\phi}\sin\theta + m(v + r\psi_s)\,\Omega_z\,\Omega + me\Omega_z\,\Omega\cos(\theta + \phi) \\
& - m\Omega_y\,\Omega w - me\sin\theta\,\Omega_y\,\Omega + m(v + r\psi_s)\,\Omega_z\,\Omega + me\cos\theta\,\Omega_z\,\Omega \\
& + m\ddot{X}_H\sin\psi - m\ddot{Y}_H\cos\psi + mw\dot{\Omega}_x + me\sin\theta\,\dot{\Omega}_x + m\dot{w}\Omega_x \\
& + m\dot{w}\Omega_x - mx\dot{\Omega}_z + m\dot{Z}_H\,\Omega_x - mr\beta_{pc}\,\Omega_y\,\Omega - mr\Omega_x
\end{aligned}
\qquad (16b)
$$

$$
\begin{aligned}
X_w = {} & -m\beta_{pc}(\Omega^2 r + 2\Omega(\dot{v} + r\dot{\psi}_s)) - m\ddot{w} - me\cos\theta\,\ddot{\phi} - mr\Omega_x\,\Omega \\
& - m\ddot{Z}_H - m(\dot{v} + r\dot{\psi}_s)\,\Omega_x + mr\dot{\Omega}_y \\
& + m\dot{X}_H\sin\psi\,(\Omega\beta_{pc} + \Omega_x) - m\dot{Y}_H\cos\psi\,(\Omega\beta_{pc} + \Omega_x) \\
& - mr\Omega_z\,(\Omega\beta_{pc} + \Omega_x)
\end{aligned}
\qquad (16c)
$$

$$
\begin{aligned}
X_{\phi} = &- mK_m^2 \ddot{\phi} - m\Omega^2 (K_{m2}^2 - K_{m1}^2) \cos(\theta+\phi) \sin(\theta+\phi) \\
&- me\Omega^2 r (w' \cos\theta - v' \sin\theta - \psi_s \sin\theta) \\
&- me \sin\theta \, \Omega^2 (v + r\psi_s) - me\Omega^2 \beta_{pc} r \cos\theta \\
&+ me (\ddot{v} \sin\theta + r\ddot{\psi}_s \sin\theta - \ddot{w} \cos\theta) \\
&- \Omega\Omega_z m(K_{m2}^2 - K_{m1}^2) \cos\theta \sin\theta - me \sin\theta \ddot{X}_H \sin\psi \\
&+ me \sin\theta \ddot{Y}_H \cos\psi + me \sin\theta \, r \dot{\Omega}_z - me \cos\theta \, r \, \Omega_x \Omega \\
&- me \cos\theta \ddot{Z}_H + me \cos\theta \, r \dot{\Omega}_y
\end{aligned}
\qquad (16d)
$$

$$
\begin{aligned}
X_{v'} = &- me (\Omega^2 r \cos(\theta+\phi) + 2\Omega (\dot{v} + r\dot{\psi}_s) \cos\theta) \\
&+ me \cos\theta \ddot{X}_H \cos\psi + me \cos\theta \ddot{Y}_H \sin\psi - me \cos\theta \, r \, \Omega\Omega_z
\end{aligned}
\qquad (16e)
$$

$$
\begin{aligned}
X_{w'} = &- me (\Omega^2 r \sin(\theta+\phi) + 2\Omega (\dot{v} + r\dot{\psi}_s) \sin\theta) \\
&+ me \sin\theta \ddot{X}_H \cos\psi + me \sin\theta \ddot{Y}_H \sin\psi - me \cos\theta \, r \, \Omega\Omega_z
\end{aligned}
\qquad (16f)
$$

$$
X_{\phi'} = 0 \qquad (16g)
$$

$$
X_{\psi_s} = r X_v + X_{v'} \qquad (16h)
$$

$$X_{\alpha_x} = \frac{d}{dt}\Big\{V_x\,(\sin\psi\, z_1 + \cos\psi \sin\beta_{pc}\, y_1) + V_y\,(\cos\beta_{pc}\cos\psi\, z_1 - \sin\beta_{pc}\cos\psi\, x_1) - V_z\,(\cos\beta_{pc}\cos\psi\, y_1 + \sin\psi\, x_1)\Big\} \tag{16i}$$

$$X_{\alpha_y} = \frac{d}{dt}\Big\{-V_x\,(\cos\psi\, z_1 + \sin\psi \sin\beta_{pc}\, y_1) + V_y\,(\cos\beta_{pc}\sin\psi\, z_1 + \sin\beta_{pc}\sin\psi\, x_1) + V_z\,(\cos\beta_{pc}\sin\psi\, x_1 + \cos\psi\, x_1)\Big\} \tag{16j}$$

$$X_{\alpha_z} = \frac{d}{dt}\Big\{V_x\cos\beta_{pc}\, y_1 + V_y\,(\sin\beta_{pc}\, z_1 - \cos\beta_{pc}\, x_1) - V_z\sin\beta_{pc}\, y_1\Big\} \tag{16k}$$

$$X_{X_H} = -\frac{d}{dt}\Big\{V_x\cos\beta_{pc}\cos\psi - V_y\sin\psi - V_z\sin\beta_{pc}\cos\psi\Big\} \tag{16l}$$

$$X_{Y_H} = -\frac{d}{dt}\Big\{V_x\cos\beta_{pc}\sin\psi + V_y\cos\psi - V_z\sin\beta_{pc}\sin\psi\Big\} \tag{16m}$$

$$X_{Z_H} = -\frac{d}{dt}\Big\{V_x\sin\beta_{pc} + V_z\cos\beta_{pc}\Big\} \tag{16n}$$

2.1.6 Virtual Work of External Forces. The virtual work for generalized nonconservative forces may be expressed as

$$\left.\begin{aligned}\delta W = \int_0^R (L_u\,\delta u + L_v\,\delta v + L_w\,\delta w + M_\phi \delta\phi + M_{\psi_S}\,\delta\psi_S)\,dx + L_{X_H}\,\delta X_H \\ + L_{Y_H}\,\delta Y_H + L_{Z_H}\,\delta Z_H + M_{\alpha_x}\,\delta\alpha_x + M_{\alpha_y}\,\delta\alpha_y + M_{\alpha_z}\,\delta\alpha_z\end{aligned}\right\} \quad (17)$$

where L and M are generalized forces and moments for each degree of freedom.

2.1.7 Governing Equations in Physical Coordinate System. Combining Equations 2, 5, 16, and 17 yields the following governing equations:

δu Equation

$$\int_0^R (Y_{u'}\,\delta u' - X_u\,\delta u - L_u\,\delta u)\,dx = 0 \quad (18)$$

δv Equation

$$\int_0^R (Y_{v''}\,\delta v'' + Y_{v'}\,\delta v' - X_{v'}\,\delta v' - X_v\,\delta v - L_v\,\delta v)\,dx$$

$$+ [K_L\,v'\,\delta v']_{r=e} = 0 \quad (19)$$

δw Equation

$$\int_0^R (Y_{w''}\,\delta w'' + Y_{w'}\,\delta w' - X_{w'}\,\delta w' - X_w\,\delta w - L_w\,\delta w)\,dx$$

$$+ [K_F\,w'\,\delta w']_{r=e} = 0 \quad (20)$$

$\delta\phi$ Equation

$$\int_0^R \left(Y_{\phi''}\,\delta\phi'' + Y_{\phi'}\,\delta\phi' + Y_{\phi}\,\delta\phi - X_{\phi}\,\delta\phi - M_{\phi}\,\delta\phi\right) dx$$

$$+ \left[K_{\phi}\,\phi\,\delta\phi\right]_{r=e} = 0 \tag{21}$$

$\delta\psi_s$ Equation

$$-\int_0^R \left[X_{\psi_s}\,\delta\psi_s - M_{\psi_s}\,\delta\psi_s\right] dx = 0 \tag{22}$$

δX_H Equation

$$\int_0^R X_{X_H}\,dx + L_{X_H} = 0 \tag{23}$$

δY_H Equation

$$\int_0^R X_{Y_H}\,dx + L_{Y_H} = 0 \tag{24}$$

δZ_H Equation

$$\int_0^R X_{Z_H}\,dx + L_{Z_H} = 0 \tag{25}$$

$\delta\alpha_x$ Equation

$$\int_0^R X_{\alpha_x}\,dx + M_{\alpha_x} = 0 \tag{26}$$

$\delta\alpha_y$ Equation

$$\int_0^R X_{\alpha_y} dx + M_{\alpha_y} = 0 \tag{27}$$

$\delta\alpha_z$ Equation

$$\int_0^R X_{\alpha_z} dx + M_{\alpha_z} = 0 \tag{28}$$

If hub mass, damping, and spring rate are also included, then Equations 23 - 28 can easily be rewritten as

δX_H Equation

$$M_{X_H} \ddot{X}_H + C_{X_H} \dot{X}_H + K_{X_H} X_H = \int_0^R X_{X_H} dx + L_{X_H} \tag{23a}$$

δY_H Equation

$$M_{Y_H} \ddot{Y}_H + C_{Y_H} \dot{Y}_H + K_{Y_H} Y_H = \int_0^R X_{Y_H} dx + L_{Y_H} \tag{24a}$$

δZ_H Equation

$$M_{Z_H} \ddot{Z}_H + C_{Z_H} \dot{Z}_H + K_{Z_H} Z_H = \int_0^R X_{Z_H} dx + L_{Z_H} \tag{25a}$$

$\delta\alpha_x$ Equation

$$I_{\alpha_x} \ddot{\alpha}_x + C_{\alpha_x} \dot{\alpha}_x + K_{\alpha_x} \alpha_x = \int_0^R X_{\alpha_x} dx + M_{\alpha_x} \tag{26a}$$

$\delta\alpha_y$ Equation

$$I_{\alpha_y} \ddot{\alpha}_y + C_{\alpha_y} \dot{\alpha}_y + K_{\alpha_y} \alpha_y = \int_0^R X_{\alpha_y} \, dx + M_{\alpha_y} \tag{27a}$$

$\delta\alpha_z$ Equation

$$I_{\alpha_z} \ddot{\alpha}_z + C_{\alpha_z} \dot{\alpha}_z + K_{\alpha_z} \alpha_z = \int_0^R X_{\alpha_z} \, dx + M_{\alpha_z} \tag{28a}$$

As suggested in Reference 2, the tension, T, and the longitudinal deflection, u, can be eliminated from the equations. Considering ϕ to be small, with ϕ ignored where compared to θ in the nonlinear terms, the equation for the tension in the blade becomes

$$T = EA \left\{ u' + \frac{v'^2}{2} + \frac{w'^2}{2} + K_A^2 \, \theta'\phi' - e_A \left(v'' \cos(\theta + \phi) + w'' \sin(\theta + \phi) \right) \right\} \tag{29}$$

Integrating with respect to x and solving for u yields

$$u = \int_0^x u' dx = \int_0^x \frac{T}{EA} - K_A^2 \, \theta'\phi' + e_A \left(v'' \cos(\theta + \phi) + w'' \sin(\theta + \phi) \right) dx$$

$$- \int_0^x \left(\frac{v'^2}{2} + \frac{w'^2}{2} \right) dx \tag{30}$$

with boundary condition $u(0) = 0$.

From Equation 18, neglecting elastic displacement, u, as suggested by Reference 2, the force equilibrium in u direction can be expressed as

$$T' = - L_u - m(\Omega^2 r + 2\Omega (\dot{v} + r\dot{\psi}_s)) \tag{31}$$

Integrating Equation 31 and using $\tau = \int_x^R m\xi \, d\xi$, the resulting equation is

$$T = T^* + 2\Omega\lambda \tag{32}$$

where

$$T^* = \int_x^R L_u \, dx + \Omega^2 \tau$$

$$\lambda = \int_x^R m(\dot{v} + r\dot{\psi}_s) \, d\xi$$

Equations 31, 32, and an expression for u' developed from Equation 30 are substituted into Equations 19 - 28 and, noting that

$$\int \equiv \int_0^R ( ) \, dx \, , \quad p = me \sin\theta \, , \quad \text{and } q = me \cos\theta \, ,$$

the equations of motion for a one-bladed rotor can be obtained as

δv Equation

$$
\begin{aligned}
&\Bigg\{ \left[\iint m\ddot{v}\ \delta v - \int p\ddot{\phi}\ \delta v + \int mx\ddot{\psi}_s\ \delta v - \left[\iint m\ddot{X}_H\ \delta v \sin\psi + \int q\ddot{X}_H\ \delta v' \cos\psi\right]\right. \\
&\quad + \left[\iint m\ddot{Y}_H\ \delta v \cos\psi - \int q\ddot{Y}_H\ \delta v' \sin\psi\right] - \int \left[P + mX\beta_{pc}\right] \ddot{\alpha}_x\ \delta v \cos\psi \\
&\quad \left. - \int \left[P + mX\beta_{pc}\right] \ddot{\alpha}_y\ \delta v \sin\psi + \int mx\ddot{\alpha}_z\ \delta v\right] \\
&\quad + \left[\left[\iint 2q\Omega\dot{v}\ \delta v' - \int 2e_A\Omega\lambda \cos\theta\ \delta v'' + \int 2m\Omega\ e_A\ \dot{v}''\ \delta v - \int 2q\Omega\dot{v}'\ \delta v\right]\right. \\
&\quad + \left[\iint 2m\Omega\ \left(\int e_A \sin\theta\ \dot{w}''\right)\ \delta v - \int 2p\Omega\dot{w}'\ \delta v - \int 2m\Omega\beta_{pc}\dot{w}\ \delta v\right] \\
&\quad - \int 2m\Omega\ \left(\int K_A^2\ \theta'\dot{\phi}'\right)\ \delta v + \left[\iint 2qx\Omega\ \dot{\psi}_s\ \delta v' - \int 2q\Omega\ \dot{\psi}_s\ \delta v\right] \\
&\quad \left. + \left[\iint 2qx\Omega\ \dot{\alpha}_z\ \delta v' - \int 2q\Omega\ \dot{\alpha}_z\ \delta v\right]\right] + \left[\left[\iint T^*v'\ \delta v' + \int E_v\ v''\ \delta v''\right.\right. \\
&\quad \left. - \int m\Omega^2\ v\ \delta v + K_L\ v'\ \delta v'\Big|_{r=e}\right] + \int E_{vw}\ w''\ \delta v'' + \left[\iint P\Omega^2\phi\ \delta v\right. \\
&\quad - \int px\Omega^2\phi\ \delta v' + \int EC_1^*\ \sin\theta\ \phi''\ \delta v'' + \int E_1\ \theta'\phi'\ \delta v'' \\
&\quad \left.\left. + \int e_A\ T^*\ \sin\theta\ \phi\ \delta v''\right]\right]\Bigg\} + (CONST)_v + (NONLIN)_v = \int L_v\ \delta v
\end{aligned}
\tag{33}
$$

where

$$(\text{CONST})_v = \int - e_A T^* \delta v'' - \int q\Omega^2 \delta v + \int q\Omega^2 x \delta v'$$

$$(\text{NONLIN})_v = \int 2\Omega \left[\int_x^R m(\dot{v} + r\dot{\psi}_s)\right](v' + \psi_s) \delta v'$$

$$- \int 2m\Omega \left[\int\left[(v' + \psi_s)(\dot{v}' + \dot{\psi}_s) + w'\dot{w}'\right] dx\right] \delta v$$

$$- \int 2m\Omega (v' + r\psi_s) \dot{\alpha}_z \delta v + \int m(\dot{X}_H \cos\psi + \dot{Y}_H \sin\psi) \dot{\alpha}_z \delta v$$

$$+ \int m\Omega w (-\dot{\alpha}_x \sin\psi + \dot{\alpha}_y \cos\psi) \delta v + \int - mw\dot{\Omega}_x \delta v$$

$$- \int 2m\dot{w}\Omega_x \delta v - \int m\dot{Z}_H \Omega_x \delta v + \int mx \Omega_x \Omega_y \delta v$$

$$+ \int (EA\, e_A^2 \sin\theta - \Delta E \sin 2\theta) v'' \phi \delta v''$$

$$+ \int (EA\, e_A^2 \cos\theta - \Delta E \cos 2\theta) w'' \phi \delta v''$$

δw Equation

$$
\begin{aligned}
\Bigg\{ \Bigg[\Bigg[\iint \ddot{mw}\, \delta w + \int q\ddot{\phi}\, \delta w - \Bigg(\iint P\ddot{X}_H\, \delta w' + \int m\beta_{pc}\, \ddot{X}_H\, \delta w \Bigg) \cos\psi - \Bigg(\iint P\ddot{Y}_H\, \delta w' \\
+ \int m\beta_{pc}\, \ddot{Y}_H\, \delta w \Bigg) \sin\psi + \int m\, \ddot{Z}_H\, \delta w + \Bigg(\iint mx\, \ddot{\alpha}_x\, \delta w \sin\psi \\
+ \int q\, \ddot{\alpha}_x\, \delta w \cos\psi \Bigg) + \Bigg[- \Bigg(\int mx\, \ddot{\alpha}_y\, \delta w \cos\psi + \int q\, \ddot{\alpha}_y\, \delta w \sin\psi \Bigg) \Bigg] \\
+ \Bigg[\Bigg(\iint - 2e_A \sin\theta\, \Omega\lambda\, \delta w'' + \int 2m\Omega\, \beta_{pc}\, \dot{v}\, \delta w + \int 2P\Omega\, \dot{v}\, \delta w' \Bigg) \\
+ \Bigg(\iint 2mx\Omega\, \beta_{pc}\, \dot{\psi}_s\, \delta w + \int 2Px\Omega\, \dot{\psi}_s\, \delta w' \Bigg) + \Bigg(\iint 2mx\Omega\, \dot{\alpha}_x\, \delta w \cos\psi \\
- \int 2q\Omega\, \dot{\alpha}_x\, \delta w \sin\psi \Bigg) + \Bigg(\iint 2mx\Omega\, \dot{\alpha}_y\, \delta w \sin\psi + \int 2q\Omega\, \dot{\alpha}_y\, \delta w \cos\psi \Bigg) \\
+ \Bigg(\iint 2mx\Omega\, \beta_{pc}\, \dot{\alpha}_z\, \delta w + \int 2px\, \Omega\dot{\alpha}_z\, \delta w' \Bigg) \Bigg] \\
+ \Bigg[\iint E_{wv}\, v''\, \delta w'' + \Bigg(\iint T^*\, w'\, \delta w' + \int E_w\, w''\, \delta w'' + K_F\, w'\, \delta w' \Big|_{r=e} \Bigg)
\end{aligned}
\tag{34}
$$

(Equation 34 continued on next page)

(Equation 34, continued)

$$+ \left\{ \left[\left[- e_A T^* \phi \, \delta w'' + \int EC_1^* \phi'' \, \delta w'' + \int E_1 \theta' \, \theta \, \phi' \, \delta w'' \right. \right. \right.$$

$$\left. \left. \left. + \int me\Omega^2 x \, \phi \, \delta w' \right] \right] \right\} + (CONST)_w + (NONLIN)_w = \int L_w \, \delta w$$

where

$$(CONST)_w = \int - e_A \, \theta T^* \, \delta w'' + \int m\Omega^2 \, \beta_{pc} \, x \, \delta w + \int P\Omega^2 \, x \, \delta w'$$

$$(NONLIN)_w = \int 2\Omega \left[\int_x^R m \, (\dot{v} + r\dot{\psi}_s) \, dx \right] w' \, \delta w' - \int e_A \, \phi \, 2\Omega \left[\int_x^R m \, (\dot{v} + r\dot{\psi}_s) \, dx \right] \delta w''$$

$$+ \int m \, (\dot{v} + r\dot{\psi}_s) \, \Omega_x \, \delta w + \int m \, (-\dot{X}_H \sin \psi + \dot{Y}_H \cos \psi) \, \Omega_x \, \delta w$$

$$+ \int mx \, \dot{\alpha}_z \, \Omega_x \, \delta w + \int m \, (v + r\psi_s) \, \Omega\Omega_y \, \delta w$$

$$- \int m \, (\dot{X}_H \cos \psi + \dot{Y}_H \sin \psi) \, \Omega_y \, \delta w + \int m \, (v + r\psi_s) \, \dot{\Omega}_x \, \delta w$$

$$+ \int m \, (\dot{v} + r\dot{\psi}_s) \, \Omega_x \, \delta w + \int (EA \, e_A^2 \, \theta \sin \theta - \Delta E \cos 2\theta) \, v'' \, \phi \, \delta v''$$

$$+ \int w'' \, \phi \, \Delta E \sin 2\theta \, \delta w''$$

δφ Equation

$$
\left\{\left[\left[- \int \ddot{pv}\delta\phi + \int \ddot{qw}\delta\phi + \int mK_m^2\, \ddot{\phi}\delta\phi - \int px\, \ddot{\psi}_s\, \delta\phi + \int \ddot{PX}_H\, \delta\phi \sin\psi \right.\right.
$$

$$
- \int \ddot{PY}_H\, \delta\phi \cos\psi + \int \ddot{qZ}_H\, \delta\phi + \int mex\, \ddot{\alpha}_x\, \delta\phi \sin\psi - \int mex\, \ddot{\alpha}_y\, \delta\phi \cos\psi
$$

$$
\left. - \int px\, \ddot{\alpha}_z\, \delta\phi \right] + \left[\iint K_A^2\, \theta'\, 2\Omega\lambda\, \delta\phi' + \int m\Omega\, (K_{m2}^2 - K_{m1}^2)\, \theta\dot{\psi}_s\, \delta\phi \right.
$$

$$
+ 2 \int mex\Omega\, \dot{\alpha}_x\, \delta\phi \cos\psi + \int 2mex\, \Omega\, \dot{Y}_H\, \delta\phi \sin\psi
$$

$$
\left. + \int m\Omega\, (K_{m2}^2 - K_{m1}^2)\, \theta\, \dot{\alpha}_z\, \delta\phi \right] + \left[\iint E_1\, \theta'\, v''\, \delta\phi' - \int EC_1^*\, \theta\, v''\, \delta\phi'' \right. \qquad (35)
$$

$$
+ \int e_A\, T^*\, \theta\, v''\, \delta\phi + \int P\Omega^2 v\, \delta\phi - \left. \int P\Omega^2\, x\, v'\, \delta\phi \right] + \iint E_1\, \theta\theta' w''\, \delta\phi'
$$

$$
+ \int EC_1^*\, w''\, \delta\phi'' - \left[\int e_A\, T^*\, w''\, \delta\phi + \int me\Omega^2\, x\, w'\, \delta\phi \right] + \left[\iint E_\phi\, \phi'\, \delta\phi' \right.
$$

$$
\left. \left. + \int EC_1^*\, \phi''\, \delta\phi'' + \int m\Omega^2\, (K_{m2}^2 - K_{m1}^2) \cos 2\theta\, \phi\delta\phi + K_\phi\, \phi\, \delta\phi \Big|_{r=e} \right] \right\}
$$

$$
+ (CONST)_\phi + (NONLIN)_\phi = \int M_\phi\, \delta\phi
$$

where

$$(\text{CONST})_\phi = \int K_A^2\, \theta'\, T^*\, \delta\phi' + \int m\Omega^2 \left(K_{m2}^2 - K_{m1}^2\right) \cos\theta \sin\theta\, \delta\phi$$

$$+ \int me\Omega^2 \beta_{pc}\, x \cos\theta\, \delta\phi$$

$$(\text{NONLIN})_\phi = \int\Bigg[K_A^2\, \phi' \left[2\Omega \int_x^R m\left(\dot{v} + r\dot{\psi}_s\right)\right] - EAK_A^4\, \theta'\, \phi'^2$$

$$+ EAK_A^2\, \phi'\, e_A \left(v'' + w''\theta\right)\Bigg] \delta\phi'$$

$$+ \int\Bigg[-2e_A\, \Omega \int_x^R m\left(\dot{v} + r\dot{\psi}_s\right) + EA\, e_A \Big[K_A^2\, \theta'\, \phi'$$

$$- e_A \left(v'' + w''\theta\right)\Big]\Bigg] \left(w' - v''\theta\right) \delta\phi$$

$$+ \int \Delta EI \left[\left(w''^2 - v''^2\right) \cos\theta \sin\theta + v''\, w'' \cos 2\theta\right] \delta\phi$$

$\delta\psi_s$ Equation

$$
\begin{aligned}
&\Bigg\{\Bigg[\iint m\ddot{x}\ddot{v} - \int px\ddot{\phi} + \int mx^2\ddot{\psi}_s - \left(\iint mx\ddot{X}_H \sin\psi + \int q\ddot{X}_H \cos\psi\right) + \left(\iint mx\ddot{Y}_H \cos\psi\right. \\
&\qquad \left. - \int q\ddot{Y}_H \sin\psi\right) - \left(\iint mx^2 \beta_{pc}\ddot{\alpha}_x \cos\psi + \int px\ddot{\alpha}_x \cos\psi\right) \\
&\qquad - \left(\iint mx^2 \beta_{pc}\ddot{\alpha}_y \sin\psi + \int px\ddot{\alpha}_y \sin\psi\right) + \int mx^2\ddot{\alpha}_z \Bigg] \\
&\qquad + \Bigg[\Bigg(-2\int qx\Omega\dot{v}' + 2\int q\Omega\dot{v}\Bigg) - \Bigg(2\int px\Omega\dot{w}' + 2\int mx\Omega\beta_{pc}\dot{w}\Bigg) \\
&\qquad + \int m\Omega\theta\left[K_{m2}^2 - K_{m1}^2\right]\phi\Bigg]\Bigg\} + (\text{CONST})_{\psi_s} + (\text{NONLIN})_{\psi_s} = \int M_{\psi_s}
\end{aligned}
\tag{36}
$$

where

$$(CONST)_{\psi_s} = 0$$

$$(NONLIN)_{\psi_s} = \int 2\Omega \left[\int_x^R \dot{m}v\,dx\right](v' + \delta\psi_s)\,\delta\psi_s$$

$$- \int 2m\Omega \left[\int_0^x [(v' + \psi_s)\,(\dot{v}' + \dot{\psi}_s) + w'\dot{w}']\,dx\right] r\,\delta\psi_s$$

$$- \int 2m\Omega\,(v + r\psi_s)\,\dot{\alpha}_z\,r\delta\psi_s + \int m\,(\dot{X}_H \cos\psi + \dot{Y}_H \sin\psi)\,\dot{\alpha}_z r\,\delta\psi_s$$

$$+ \int m\,\Omega w\,\Omega_y\,r\delta\psi_s - \int mw\,\Omega_x\,r\delta\psi_s - \int 2\,m\dot{w}\,\Omega_x\,r\delta\psi_s - \int m\dot{Z}_H\,\Omega_x\,r\delta\psi_s$$

$$+ \int mx\,\Omega_x\,\Omega_y\,r\delta\psi_s$$

δX_H Equation

$$
\begin{aligned}
&\Bigg\{\Bigg[\Bigg[-\left(\iint m\ddot{v}\sin\psi + \int q\ddot{v}'\cos\psi\right) - \left(\iint m\beta_{pc}\ddot{w}\cos\psi + \int p\ddot{w}'\cos\psi\right) \\
&\quad + \int p\ddot{\phi}\sin\psi - \left(\iint mx\ddot{\psi}_s\sin\psi + \int q\ddot{\psi}_s\cos\psi\right) + \left(\iint m + m_{x_H}\right)\ddot{X}_H \\
&\quad + \left(\iint p + \int mx\beta_{pc}\right)\ddot{\alpha}_y - \left(\iint mx\ddot{\alpha}_z\sin\psi + \int q\ddot{\alpha}_z\cos\psi\right)\Bigg] \\
&\quad + \Bigg[\Bigg(-2\int m\Omega\dot{v}\cos\psi + 2\int q\Omega\dot{v}'\sin\psi\Bigg) + \Bigg(2\int p\Omega\dot{w}'\sin\psi \\
&\quad + 2\int m\Omega\beta_{pc}\dot{w}\sin\psi\Bigg) + 2\int p\Omega\dot{\phi}\cos\psi + \Bigg(-2\int mx\Omega\dot{\psi}_s\cos\psi \\
&\quad + 2\int q\Omega\dot{\psi}_s\sin\psi\Bigg) + \Bigg(-2\int mx\Omega\dot{\alpha}_z\cos\psi + 2\int q\Omega\dot{\alpha}_z\sin\psi\Bigg)\Bigg] \\
&\quad + \Bigg[\left(\iint m\Omega^2 v\sin\psi + \int q\Omega^2 v'\cos\psi\right) + \left(\iint m\Omega^2\beta_{pc}w + \int p\Omega^2 w'\right)\cos\psi \\
&\quad + \left(\iint mx\Omega^2\psi_s\sin\psi + \int q\Omega^2\psi_s\cos\psi\right) + K_{X_H}\Bigg]\Bigg\} \\
&\quad + \int (CONST)_{X_H} + \int (NONLIN)_{X_H} = L_{X_H}
\end{aligned}
\tag{37}
$$

where

$$\int (\text{CONST})_{X_H} = \int q\,\Omega^2 \sin\psi + \left[- \int mx\Omega^2 \cos\beta_{pc} + \int P\Omega^2\,\beta_{pc} \right] \cos\psi$$

$$\int (\text{NONLIN})_{X_H} = - \int mx\,(\dot{\alpha}_z^2 \cos\psi - \int m\,(v + r\psi_s)\,\ddot{\alpha}_z \cos\psi$$

$$+ 2 \int m\Omega\,(v + r\psi_s)\,\dot{\alpha}_z \sin\psi + \int m\Omega\, w\,\dot{\alpha}_x$$

$$- 2 \int m\Omega\,(\dot{v} + r\dot{\psi}_s)\,\dot{\alpha}_z \cos\psi + \int m\, w\,\ddot{\alpha}_y$$

$$+ 2 \int m\,\dot{w}\,\dot{\alpha}_y - \int mx\,\dot{\alpha}_y\,\dot{\Omega}_y$$

δY_H Equation

$$
\begin{aligned}
&\Bigg\{\Bigg[\Bigg[\left(\iint m\ddot{v}\cos\psi - \int q\ddot{v}'\sin\psi\right) - \left(\iint m\beta_{pc}\ddot{w} + \int p\ddot{w}'\right)\sin\psi - \int p\ddot{\phi}\cos\psi \\
&\quad + \left(\iint mx\ddot{\psi}_s\cos\psi - \int q\ddot{\psi}_s\sin\psi\right) + \left(\iint m + m_{Y_H}\right)\ddot{Y}_H - \left(\iint mx\beta_{pc} + \int p\right)\ddot{\alpha}_y \\
&\quad + \left(\iint mx\ddot{\alpha}_z\cos\psi - \int q\ddot{\alpha}_z\sin\psi\right)\Bigg] + \Bigg[-\iint 2m\Omega\dot{v}\sin\psi \\
&\quad + \int 2q\Omega\dot{v}'\cos\psi - \left(\iint 2p\Omega\dot{w}' + \int 2m\Omega\beta_{pc}\dot{w}\right)\cos\psi + \int 2p\Omega\dot{\phi}\sin\psi \\
&\quad - \left(\iint 2mx\Omega\dot{\psi}_s\sin\psi + \int 2q\Omega\dot{\psi}_s\cos\psi\right) - \iint 2mx\Omega\dot{\alpha}_z\sin\psi \\
&\quad + \int 2q\Omega\dot{\alpha}_z\cos\psi\Bigg]\Bigg] + \Bigg[\Bigg[-\int m\Omega^2 v\cos\psi + \int q\Omega^2 v'\sin\psi\Bigg] \\
&\quad + \left(\iint m\Omega^2\beta_{pc}w + \int p\Omega^2 w'\right)\sin\psi + \Bigg[-\int mx\Omega^2\psi_s\cos\psi \\
&\quad + \int q\Omega^2\psi_s\sin\psi\Bigg] + K_{Y_H}Y_H\Bigg]\Bigg\} + \int(\text{CONST})_{Y_H} + \int(\text{NONLIN})_{Y_H} = L_{Y_H}
\end{aligned}
\tag{38}
$$

where

$$\int (\text{CONST})_{Y_H} = \int q\,\Omega^2 \cos\psi + \left[- \int mx\Omega^2 \cos\beta_{pc} + \int P\Omega^2\,\beta_{pc} \right] \sin\psi$$

$$\int (\text{NONLIN})_{Y_H} = - \int mx\,(\dot{\alpha}_z^2 \sin\psi - \int m\,(v + r\psi_s)\,\ddot{\alpha}_z \sin\psi$$

$$- 2 \int m\Omega\,(v + r\psi_s)\,\dot{\alpha}_z \cos\psi + \int m\Omega\, w\,\dot{\alpha}_y$$

$$- 2 \int m\Omega\,(\dot{v} + r\dot{\psi}_s)\,\dot{\alpha}_z \sin\psi - \int m\, w\,\ddot{\alpha}_x$$

$$- 2 \int m\,\dot{w}\,\dot{\alpha}_x + \int mx\,\dot{\alpha}_x\,\Omega_y$$

δZ_H Equation

$$\left\{\left[\left[\int m\ddot{w} + \int q\ddot{\phi} + \left[\int m + M_{Z_H}\right]\ddot{Z}_H + \left[\int q\ddot{\alpha}_x \cos\psi + \int mx\ddot{\alpha}_x \sin\psi\right]\right.\right.\right.$$

$$\left.\left.\left. + \left[\int q\ddot{\alpha}_y \sin\psi - \int mx\ddot{\alpha}_y \cos\psi\right]\right] + \left[\left[-\int 2q\,\Omega\dot{\alpha}_x \sin\psi + \int 2mx\,\Omega\dot{\alpha}_x \cos\psi\right]\right.\right.$$

$$\left.\left. + \left[\int 2q\,\Omega\dot{\alpha}_y \cos\psi + \int mx\,\Omega\dot{\alpha}_y \sin\psi\right]\right] + \left[K_{Z_H} Z_H\right]\right\} \qquad (39)$$

$$+ \int (CONST)_{Z_H} + \int (NONLIN)_{Z_H} = L_{Z_H}$$

where

$$\int (CONST)_{Z_H} = 0$$

$$\int (NONLIN)_{Z_H} = \int m\,(v + r\psi_s)\,\Omega\Omega_y + \int 2m\,(\dot{v} + r\dot{\psi}_s)\,\Omega_x + \int 2mx\,\dot{\alpha}_z\Omega_x$$

$\delta\alpha_x$ Equation

$$
\begin{aligned}
&\Bigg\{\Bigg[\Bigg[\Bigg(-\int mx\,\beta_{pc}\,\ddot{v}\cos\psi - \int p\ddot{v}\cos\psi\Bigg) + \Bigg(\int mx\ddot{w}\sin\psi + \int q\ddot{w}\cos\psi\Bigg)\\
&+ \int qx\,\ddot{\phi}\cos\psi - \Bigg(\int mx^2\,\beta_{pc} + \int px\Bigg)\ddot{\psi}_s\cos\psi - \Bigg(\int mx\,\beta_{pc} + \int p\Bigg)\ddot{Y}_H\\
&+ \Bigg(\int q\,\ddot{Z}_H\cos\psi + \int mx\,\ddot{Z}_H\sin\psi\Bigg) + \Bigg(\int qx\,\ddot{\alpha}_x\sin 2\psi + \frac{1}{2}\int mx^2\,\ddot{\alpha}_x\\
&- \frac{1}{2}\int mx^2\,\ddot{\alpha}_x\cos 2\psi + I_{\alpha_x}\ddot{\alpha}_x\Bigg) + \Bigg(-\int qx\,\ddot{\alpha}_y\cos 2\psi - \int\frac{1}{2}mx^2\,\ddot{\alpha}_y\sin 2\psi\Bigg)\\
&- \Bigg(\int mx^2\,\beta_{pc} + \int px\Bigg)\ddot{\alpha}_z\cos\psi\Bigg] + \Bigg[\Bigg(\int 2\,mx\,\beta_{pc}\,\Omega\dot{v} + \int 2p\,\Omega\dot{v}\Bigg)\sin\psi\\
&+ \Bigg(\int 2mx^2\Omega\,\beta_{pc} + \int 2px\,\Omega\Bigg)\dot{\psi}_s\sin\psi + \Bigg(\int 2qx\,\Omega\dot{\alpha}_x\cos 2\psi + \int mx^2\Omega\,\dot{\alpha}_x\sin 2\psi\\
&- \int mx^2\,\Omega\,\dot{\alpha}_y\cos 2\psi\Bigg) + \Bigg(\int 2mx^2\,\Omega^2\,\beta_{pc} + \int 2px\,\Omega\Bigg)\dot{\alpha}_z\sin\psi\Bigg]\\
&+ \Bigg[\Bigg(\int mx\,\Omega^2\,\beta_{pc} + \int p\Omega^2\Bigg)v\cos\psi + \Bigg(\int mx\,\Omega^2\,w\sin\psi + \int q\Omega^2\,w\cos\psi\Bigg)\\
&+ \Bigg(\int px\,\Omega^2\,\psi_s\cos\psi\Bigg) + K_{\alpha_x}\alpha_x\Bigg]\Bigg\} + \int(\text{CONST})_{\alpha_x} + \int(\text{NONLIN})_{\alpha_x} = M_{\alpha_x}
\end{aligned}
\tag{40}
$$

where

$$\int (\text{CONST})_{\alpha_x} = \int x \sin \psi \, (\text{CONST})_{Z_H} - \int x \, \beta_{pc} \, (\text{CONST})_{Y_H} + \int px \, \Omega^2 \sin \psi$$

$$+ \int \frac{m}{2} \left[K_{m2}^{\,2} - K_{m1}^{\,2} \right] \sin 2 (\theta + \phi) \, \Omega^2 \cos \psi$$

$$\int (\text{NONLIN})_{\alpha_x} = \int (\text{NONLIN})_{Z_H} \, x \sin \psi + \int m \, (v + r\psi_s) \, \ddot{Z}_H \cos \psi$$

$$- \int w \left[m\ddot{Y}_H + m \cos \psi \, (\ddot{v} + r\ddot{\psi}) - 2m \, \Omega \sin \psi \, (\dot{v} + r\dot{\psi}) \right.$$

$$\left. - m\Omega^2 \, (v + r\psi_s) \cos \psi + mx \cos \psi \, \ddot{\alpha}_z - 2mx \, \Omega \sin \psi \, \dot{\alpha}_z \right]$$

$\delta\alpha_y$ Equation

$$
\begin{aligned}
&\Bigg\{\Bigg[- \left(\int mx\, \beta_{pc}\, \ddot{v} + \int p\bar{v}\right) \sin\psi + \left(- \int mx\ddot{w} \cos\psi + \int q\ddot{w} \sin\psi\right) \\
&\quad - \int qx\, \ddot{\phi} \cos\psi - \left(\int mx^2\, \beta_{pc} + \int px\right) \ddot{\psi}_s \sin\psi + \left(\int p + \int mx\, \beta_{pc}\right) \ddot{X}_H \\
&\quad + \left(\int q\, \ddot{Z}_H \sin\psi - \int mx\, \bar{Z}_H \cos\psi\right) + \left(\int px\, \ddot{\alpha}_x \cos 2\psi - \int \tfrac{1}{2} mx^2\, \ddot{\alpha}_x \sin 2\psi\right) \\
&\quad - \left(\int qx\, \ddot{\alpha}_y \sin 2\psi + \tfrac{1}{2}\int mx^2\, \bar{\alpha}_y - \tfrac{1}{2}\int mx^2\, \bar{\alpha}_y \cos 2\psi + I_{\alpha_y}\, \ddot{\alpha}_y\right) \\
&\quad - \left(\int mx^2\, \beta_{pc} + \int px\right) \ddot{\alpha}_z \sin\psi\Bigg] + \Bigg[- \left(\int 2\, mx\, \beta_{pc}\, \Omega\dot{v} \cos\psi\right. \\
&\quad \left. + \int 2p\, \Omega\dot{v} \cos\psi\right) - \left(\int 2mx^2\, \Omega\, \beta_{pc} + \int 2px\, \Omega\right) \dot{\psi}_s \cos\psi \\
&\quad + \left(\int 2qx\, \Omega\, \dot{\alpha}_x \sin 2\psi - \int mx^2\, \Omega\, \dot{\alpha}_x - \int mx^2\, \Omega\, \dot{\alpha}_x \cos 2\psi\right) \\
&\quad + \left(- \int 2qx\, \Omega\, \dot{\alpha}_y \cos 2\psi - \int mx^2\, \Omega\, \dot{\alpha}_y \sin 2\psi\right) - \left(\int 2mx^2\, \Omega\, \beta_{pc}\right.
\end{aligned}
\tag{41}
$$

(Equation 41 continued)

Equation 41 (continued)

$$+ 2\left[px\Omega\right]\dot{\alpha}_z \cos\psi\Big] + \Big[\Big[\Big[mx\,\Omega^2\,\beta_{pc}\,v + \left[p\Omega^2\,v\right]\sin\psi$$

$$+ \Big[- \left[mx\,\Omega^2\,w\cos\psi + \left[q\,\Omega^2\,w\sin\psi\right] + \Big[\Big[px\,\Omega^2\,\psi_s\sin\psi\Big]$$

$$+ K_{\alpha_y}\,\alpha_y\Big]\Big]\Big] + \left[(CONST)_{\alpha_y} + \left[(NONLIN)_{\alpha_y} = M_{\alpha_y}\right.\right.$$

where

$$\left[(CONST)_{\alpha_y} = \left[- x\cos\psi\,(CONST)_{Z_H} + \left[x\,\beta_{pc}\,(CONST)_{X_H} - \left[px\,\Omega^2\cos\psi\right.\right.\right.\right.$$

$$+ \left[\frac{m}{2}\left[K_{m2}^{\,2} - K_{m1}^{\,2}\right]\sin 2(\theta+\phi)\,\Omega^2\sin\psi\right.$$

$$\left[(NONLIN)_{\alpha_y} = \left[- x\cos\psi\,(NONLIN)_{Z_H} + \left[mv\,\ddot{Z}_H\sin\psi\right.\right.\right.$$

$$+ \left[w\left[m\ddot{X}_H - m\sin\psi\,(\ddot{v} + r\ddot{\psi}_s) - 2m\,\Omega\cos\psi\,(\dot{v} + r\dot{\psi}_s)\right.\right.\right.$$

$$+ m\Omega^2\,(v + r\psi_s)\sin\psi - mx\sin\psi\,\ddot{\psi}_s - 2mx\,\Omega\cos\psi\,\dot{\alpha}_z\Big)$$

$\delta\alpha_z$ Equation

$$
\begin{aligned}
&\Bigg\{\Bigg[\Bigg[\int mx\,\ddot{v} - \int px\,\ddot{\phi} + \int mx^2\,\ddot{\psi}_s - \Bigg[\int mx\,\ddot{X}_H \sin\psi + \int q\,\ddot{X}_H \cos\psi\Bigg] \\
&\quad + \Bigg[\int mx\,\ddot{Y}_H \cos\psi - \int q\,\ddot{Y}_H \sin\psi\Bigg] - \Bigg[\int mx^2\,\beta_{pc} + \int px\Bigg]\,\ddot{\alpha}_x \cos\psi \\
&\quad - \Bigg[\int mx^2\,\beta_{pc} + \int px\Bigg]\,\ddot{\alpha}_y \sin\psi + \Bigg[\int mx^2 + I_{\alpha_x}\Bigg]\,\ddot{\alpha}_z\Bigg] \\
&\quad + \Bigg[\Bigg[-\int 2qx\,\Omega\dot{v}' + \int 2q\,\Omega\dot{v}\Bigg] - \Bigg[\int 2px\,\Omega\dot{w}' + \int 2m\,\Omega x\,\beta_{pc}\,\dot{w}\Bigg] \\
&\quad - \int m\Omega\,\theta\left[K_{m2}^2 - K_{m1}^2\right]\phi\Bigg] + \left[K_{\alpha_z}\,\alpha_z\right] + \int (CONST)_{\alpha_z} \\
&\quad + \int (NONLIN)_{\alpha_z} = M_{\alpha_z}
\end{aligned}
\qquad (42)
$$

where

$$
\int (CONST)_{\alpha_z} = \int x\cos\psi\cos\beta_{pc}\,(CONST)_{Y_H} - \int x\sin\psi\cos\beta_{pc}\,(CONST)_{X_H}
$$

$$
+ \int qx\,\Omega^2 - \int px\,\Omega^2\,\beta_{pc}\sin\psi\cos\psi
$$

$$\int (\text{NONLIN})_{\alpha_z} = \int x \cos\psi \cos\beta_{pc} (\text{NONLIN})_{Y_H} - \int x \sin\psi \cos\beta_{pc} (\text{NONLIN})_{X_H}$$

$$- \int m (v + r\psi_s) \left[\ddot{Y}_H \sin\psi + \ddot{X}_H \cos\psi \right] + \int 2m (v + r\psi_s) \times\Omega \dot{\alpha}_z$$

$$+ \int 2m\Omega (v + r\psi_s) (\dot{v} + r\dot{\psi}_s)$$

2.1.8 Rayleigh-Ritz/Galerkin Method. According to the Rayleigh-Ritz method, arbitrary functions for the blade elastic displacement can be separated into a sum of products of functions of r and t only:

$$v(r,t) = \sum_i y_i(t)\, Y_i(r) = \sum y_i\, Y_i \tag{43}$$

$$w(r,t) = \sum_j z_j(t)\, Z_j(r) = \sum z_j\, Z_j \tag{44}$$

$$\phi(t,r) = \sum_k \phi_k(t)\, \Phi_k(r) = \sum \phi_k\, \Phi_k \tag{45}$$

where $Y_i(r)$, $Z_j(r)$, $\Phi_k(r)$ are modal functions and y_i, z_j, ϕ_k are generalized coordinates. Substituting these sums into Equations 33 - 42 yields the equations of motion for all the generalized degrees of freedom. These can be automatically handled by the computer program. Therefore, Equations 33 - 42 represent the final form of the equations of motion and no further derivation is necessary. Note that the modal functions are chosen as any complete set of linear independent functions that satisfy all the geometry boundary conditions (but not necessarily the force boundary conditions), and are piecewise twice differentiable.

It can be shown that this Rayleigh Ritz approach is equivalent to the Galerkin method as applied to equations of motion, including all the "trailing terms" (Reference 6). Note, however, that if the Galerkin method applies to equations of motion only and does not include the "trailing terms," then the modal functions have to satisfy all geometry and force boundary conditions. This is not always possible when masses or dampers are at the boundaries. In addition to this, the modal functions have to be differentiable to the degree required by the differential equations (for the present study, fourth differentiable), which is two degrees higher than the usage of energy method.

2.1.9 Program Features of CRE3. Three physical degrees of freedom are assigned to each blade: out-of-plane bending, in-plane bending, and torsion. The rotor speed perturbation is treated as an additional rotor degree of freedom which may couple with transmission and fuel systems to reflect the feedback relationship between power supply and rotor speed. However, component representations of these systems are not yet available. All four blade physical degrees of freedom mentioned above are optional in CRE3, except that at least one blade elastic degree of freedom must be chosen. The bending and torsion motion of the blade is expanded as series of the product of decoupled modes and generalized degrees of freedom (as in Equations 43, 44, and 45).

Up to five modes for out-of-plane bending and three modes for in-plane bending and torsion may be used. The user has the option of either inputting the mode shape and its first and second derivatives, or letting the program generate the mode shape automatically based on the normal modes of a nonrotating beam and the user-selected boundary conditions. Because the derivation of equations of motion in this present study is based on the energy method, the satisfaction of geometric boundary conditions for each mode shape may not be required, although it is always a plus if all boundary conditions are satisfied.

Theoretically, a mode shape may be obtained by integrating its 2nd derivative twice while applying the appropriate displacement and slope boundary conditions. However, for a discretized system, this approach results in numerical

problems, especially for higher order modes. So, a more complicated input procedure has been adopted. The mode shape and its first and second derivatives must be input, instead of the second derivative and its associated boundary condition.

The mode shape data are defined at blade stations, starting at the blade root and ending at the tip. Hinge and bearing locations are input as indices of the blade station. Based on the derivation of Reference 2, the blade rotation order is in-plane, out-of-plane, and torsion. Care must be taken when simulating an articulated rotor to ensure that hinge and bearing locations are consistent with the blade rotation order.

In CRE3, six hub degrees of freedom in the fixed system (none of which is mandatory) are assigned to the hub. In a model, these hub degrees of freedom may automatically couple with a fuselage component (CFM2) if the component number of the rotor coincides with any one of the assigned rotor numbers in component CFM2. The hub degrees of freedom may also couple with any degree of freedom with the same name through the DYSCO naming convention.

CRE3 can couple with the control system (CCEØ, CCE1) only if the torsional degree of freedom is activated. In that case, pitch horn length and pitch horn station data will be requested. If a model is formed by including both the rotor component and control system, the same component number has to be assigned to each in order to successfully couple them. In addition to coupling with the control system, the blade may also couple with CSF1, CFM2, or CES1 via the DYSCO naming convention, if the blades' implicit degrees of freedom are chosen, or through the use of component CLC1. Although programmatically DYSCO will perform the coupling, logically the mass coupling of these components with the rotor will not be correct unless the component mass matrices are derived for a rotating system.

In CRE3, if a term in the mass matrix depends on the acceleration of a degree of freedom, the delay acceleration of the DOF is used in order to avoid any iterative procedure in the solution method. This approach is justifiable if

the nonlinear term is not the lowest order term in an equation. This is the case in the present study.

CRE3 may also couple with any one of the aerodynamic force modules FRAØ, FRA2 and FRA3. FRAØ is the simplest aerodynamic force module and deals only with the linear aerodynamics. FRA2 can handle airfoil tables, and can read the inflow distribution from an outside sequential file. Both FRAØ and FRA2 consider only steady aerodynamics without yaw flow correction. The C81 type of aerodynamics is installed in FRA3. A detailed description of FRA3 is given in the next section. In addition to aerodynamic force modules, CRE3 may also couple with the vibration shaker, FSS1, to get useful information about the rotor under harmonic excitation.

2.2 ADVANCED ROTOR AERODYNAMIC ANALYSIS - FRA3

The basic rotor aerodynamic analysis used in the present study is based on the report by McLarty (Reference 7). The steady state lifting coefficient C_L, drag coefficient C_D, and moment coefficient C_M can be either calculated or looked up in a table. For either option, the angle of attack and Mach number, based on the two-dimensional strip theory, are modified by the yaw flow angle to account for the three-dimensional aerodynamic effect. The analysis and experimental work presented in References 8 and 9 are used to find the induced velocity distribution across the rotor disk.

The unsteady aerodynamic effects on the pitching moment coefficient (Reference 10), on the lift coefficients (References 11 and 12), and on the drag coefficient (Reference 12) are included to modify the steady lift, drag, and moment coefficients. Figure 3 shows the flowchart for the rotor aerodynamics logic. The equations in the following sections can be found in Reference 7 but are reproduced in this report for the sake of clarity.

2.2.1 Induced Velocity by Equation. The theoretical basis of the induced velocity calculation in this paragraph is given in Reference 9. Several

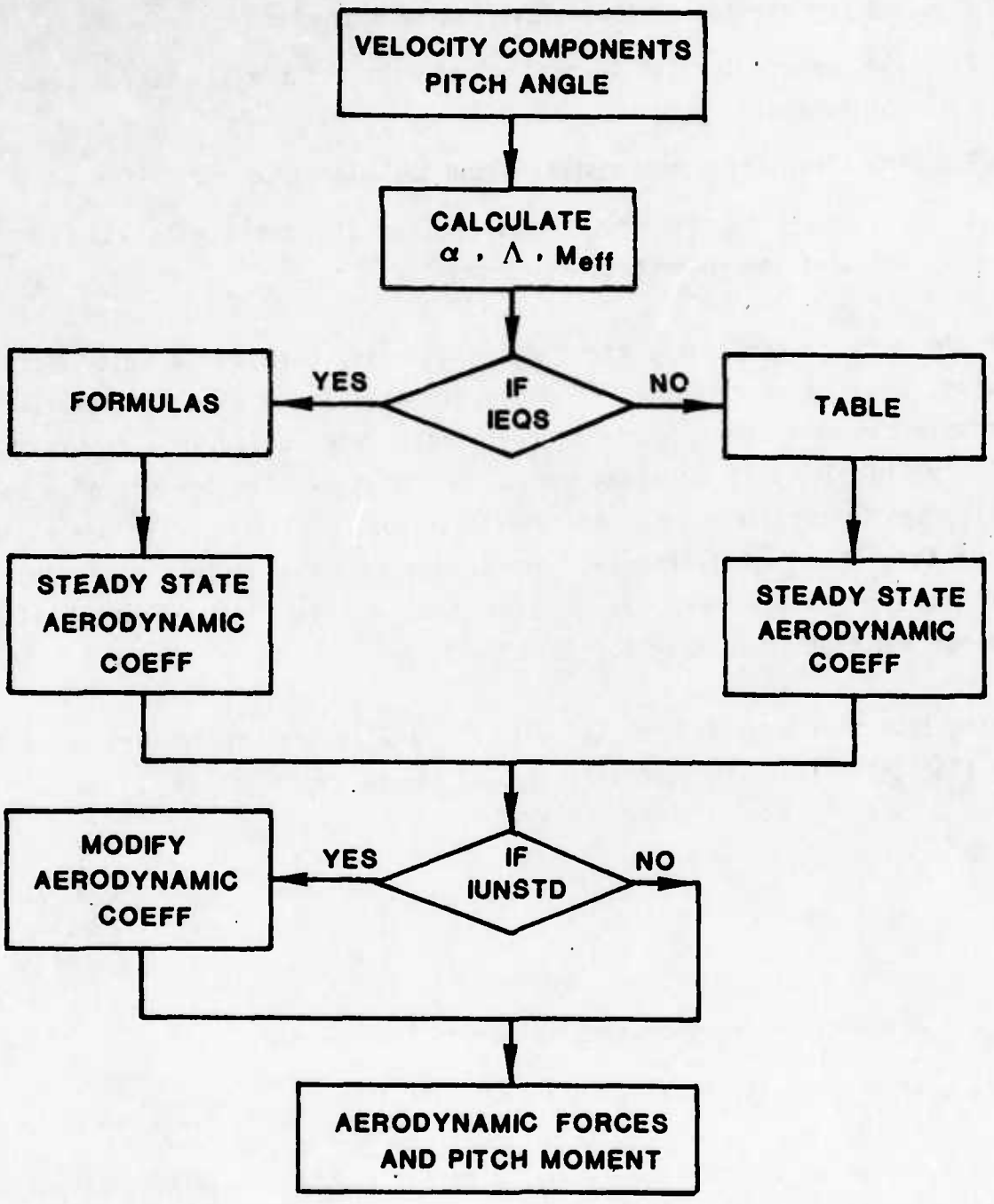

Figure 3. Rotor Aerodynamic Logic.

assumptions of the vortex theory adopted in Reference 9 are:

1. The contraction of the slipstream is neglected.
2. The number of rotor blades is infinite and the slipstream does not rotate.
3. The circulation is constant along the blade radius.
4. The angle between the slipstream and the rotor disc at each point of the rotor disc is constant.

Under the above assumptions, the induced velocity across the rotor is then computed from the contribution of bound, free tip, and shed vortices. Like the simple momentum theory, this approach fails when μ (advance ratio) and λ (inflow ratio) are both equal to zero. In that case, the concept of a solid disk is used to replace a rotor to make the result realistic. Further refinement of this theory (Reference 8) permits its application to a wide range of rotor operating states such as autorotation, vortex ring, windmill state, climbing, and high speed flight.

Assuming that the rotor-induced velocity is parallel to the centerline of the rotor shaft, the local induced velocity, ν, can be expressed as

$$\nu = \bar{\nu} F_N \tag{46}$$

where

$\bar{\nu}$ = the average induced velocity across the rotor disk

F_N = an induced velocity distribution function.

F_N is a function of the advance ratio, μ, radial station, x, blade azimuth, ψ, and inflow ratio, λ. It may be either calculated or looked up in a data table

(see paragraph 2.2.5). The equation used to represent F_N is

$$F_N = \frac{4}{3} \times [1 + f_1(\mu) \cos \psi]$$

$$+ f_2(x,\psi)\ f_1(\mu)\ K_{27} \sqrt{-.5\ V_N^2 + \sqrt{.25\ V_N^4 + (\bar{\nu}_i)_N^2}} \qquad (47)$$

where

$\bar{\nu}$ is the average induced velocity across the rotor disc

x is the nondimensional station

ψ is the blade azimuth angle

K_{27} is the tip vortex coefficient

V_N is the flight path airspeed in ft/s divided by 1.0 ft/s

$(\bar{\nu})_N$ is $\bar{\nu}$ in ft/s divided by 1.0 ft/s

and $f_1(\mu)$ is defined as

$$f_1(\mu) = \begin{cases} .5, \text{ if } \Omega < 1 \text{ rad/s} \\ 11.25\ \mu, \text{ if } \Omega \geq 1 \text{ and } \mu < .1067 \\ 1.36 - 1.5\ \mu, \text{ if } \Omega \geq 1 \text{ and } .1067 \leq \mu < .5733 \\ .5, \text{ if } \Omega \geq 1 \text{ and } \mu \geq .573 \end{cases} \qquad (48)$$

Function $f_2(x,\psi)$ is given by

$$f_2(x,\psi) = \begin{cases} 0, \text{ if } (x > .7) \\ \quad \text{or } (105^\circ < \psi < 255^\circ) \\ \quad \text{or } (315^\circ < \psi < 360^\circ) \\ \quad \text{or } (0^\circ < \psi < 45^\circ) \\ \sin [6(\psi - 45^\circ)], \text{ if } (x \geq .7) \text{ and} \\ \qquad \text{if } (45^\circ \leq x \leq 105^\circ) \\ \qquad \text{or } [(225^\circ \leq \psi \leq 351^\circ)] \end{cases} \qquad (49)$$

The average induced velocity, is given as

$$\bar{\nu} = \frac{C_B}{\sqrt{0.886\ \lambda^2 + \mu^2} + \dfrac{0.6|C_B|^{1.5}\ (|C_B| + 8\ \lambda|\lambda|/3)}{(C_B + 8\ \lambda^2)\ (C_B + 8\ \mu^2)}} \qquad (50)$$

C_B is defined as

$$C_B = C_T/(B^2 - X_h^2) \tag{51}$$

where

C_T is the thrust coefficient

X_h is the hub extent divided by rotor radius

B is tip loss factor.

The ground effect is included if the center of gravity of the vehicle is between one-fourth and one rotor diameter above the ground and the airspeed is less than 30 ft/s:

$$\bar{\nu}^* = \bar{\nu}\ [1 + (G - 1)\ ((v - 30)/30)^2] \tag{52}$$

where

$\bar{\nu}^*$ is the induced velocity with the ground effect included

G is 0.25, plus the altitude of the CG divided by the rotor diameter

V is the flight path velocity in ft/s.

2.2.2 Steady State Aerodynamics. If the relative velocity of a blade element with regard to the air is the vector sum of tangential velocity U_T (in the hub plane, positive in the blade drag direction), the vertical velocity U_p (perpendicular to the hub plane, positive downward), and the radial velocity U_R (positive outward), then the standard two-dimensional strip theory gives us the inflow angle ϕ_A defined by

$$\phi_A = \tan^{-1} \frac{U_P}{U_T} \tag{53}$$

and the angle of attack

$$\alpha = \theta_A + \phi + \phi_A \tag{54}$$

where

ϕ is the torsion deformation and θ_A is the sum of the root pitch angle and built-in twist.

The three-dimensional effect of aerodynamics may be included by the consideration of yaw flow angle, Λ, which is defined as

$$\Lambda = \tan^{-1} \frac{U_R}{U_T} \tag{55}$$

If $|\Lambda| > 60°$, then Λ is given by

$$\Lambda = 60° \cdot \sin(\Lambda) \tag{56}$$

Then the modified angle of attack, α_{mod}, and the effective Mach number, M_{eff}, are expressed as

$$\alpha_{mod} = \alpha \cos \Lambda \tag{57}$$

$$M_{eff} = \frac{U_R^2 + U_T^2 + U_P^2}{V_{sound}} (\cos q_1 \Lambda)^{q_2} \tag{58}$$

As suggested by References 12 and 13, Equations 55 - 58 should be adopted in all aspects of the steady state lift determination. Both q_1 and q_2 in Equation 58 must be supplied by the user and should be determined carefully. Note that Hoerner's result (Reference 13) can be approximated by assuming $q_1 = 2$, $q_2 = 1$, or $q_1 = 1$, $q_2 = .5$.

The steady state lift coefficient is then expressed as

$$C_{L_S} = C_L (\alpha_{mod}, M_{eff})/\cos \Lambda \tag{59}$$

Equation 59 is valid whether C_L is derived or looked up in a table.

According to Harris (Reference 12), the blade drag coefficient in the blade element plane is

$$C_{D_N} = C_D (\alpha, M_{eff}) \tag{60}$$

and the drag coefficient in the radial direction, based on U_R, is given by

$$C_{D_R} = C_D \ (\alpha = 0, M = .3) \tag{61}$$

Equation 61 is used in addition to Equation 60 because the resultant drag force should be in the same direction as the total wind velocity.

The steady state moment coefficient is

$$C_{M_S} = C_M \ (\alpha, M_{eff}) \tag{62}$$

The program provides the option of using either formulas or lookup tables to determine the steady state coefficients C_L, C_D, and C_M. Details of the formulas are given in paragraph 2.2.4.

2.2.3 BUNS Unsteady Aerodynamic Model. As stated in References 10, 11, and 12, the assumption of quasi-steady aerodynamics, which ignores the time rate of change of the blade angle of attack and the virtual mass effect of the air, is too crude to be adequate in certain situations. Also, it is impractical to obtain meaningful wind tunnel test data over the full range of angles of attack and yaw angles, or to construct a theoretically general unsteady aerodynamic model. Therefore, a procedure based on limited wind tunnel data and a simplified, unsteady two-dimensional theory is used to determine the unsteady aerodynamic coefficients as described in the following paragraphs.

2.2.3.1 Pitching Moment Coefficient - The determination of pitching moment coefficient is based on the work of Carta, et al. (Reference 10). (The theoretical basis for their unsteady aerodynamics can be found in Reference 14.) Their test data was obtained from differential pressure transducers mounted on a 2-ft-chord NACA 0012 model. Testing was performed in the two-dimensional channel of the UARL 8-ft wind tunnel.

Carta, et al., assume that "...sinusoidal data could be generalized, through cross plots, to functions of instantaneous angle of attack, angular velocity

parameter, A, and angular acceleration parameter, B, for a given Mach number." From Reference 10, A and B are given by

$$A = \left(\frac{c}{2U}\right) \dot{\alpha} \tag{63}$$

$$B = \left(\frac{c}{2U}\right)^2 \ddot{\phi} \tag{64}$$

where c is chord length, U is wind velocity perpendicular to airfoil leading edge, $\dot{\alpha}$ is time rate change of angle of attack, and $\ddot{\phi}$ is the blade torsion acceleration. Carta's table, adopted here, excludes the contribution from the steady state aerodynamics, i.e., $\Delta C_M = 0$ when $A = B = 0$, and is based on Mach number equal to zero. The effect of Mach number on the stall point is included by computing a shift in the angle of attack argument before entering the A - B tables as follows (Reference 6):

$$\alpha_{Carta} = |\alpha| \text{ for } M_{eff} \leq .2 \tag{65}$$

$$\alpha_{Carta} = |\alpha| \frac{13.5}{13.5 - 16.25\,(M_{eff} - .2)} \quad \text{for } .2 \leq M_{eff} < .6 \tag{66}$$

$$\alpha_{Carta} = |\alpha| \cdot 1.93 \text{ for } M_{eff} \geq .6 \tag{67}$$

Then ΔC_M is determined as

$$\Delta C_M = (\sin \alpha)\, \Delta C_M\,(A, B, \alpha_{Carta})/N \tag{68}$$

where N is used to consider the compressibility effect:

$$N = \sqrt{1 - M_{eff}^2} \quad \text{for } M_{eff} < .6 \tag{69}$$

$$N = .8 \text{ for } M_{eff} \geq .6 \tag{70}$$

The total pitching moment coefficient, C_M, can then be expressed as

$$C_M = C_M \text{ (steady state)} + \Delta C_M \tag{71}$$

2.2.3.2 Lift Coefficient - The lift coefficient determination is based on the work of Scanlan and Rosenbaum (Reference 11) and the assumption that the frequency of oscillation of the rotor blade is small (i.e., the value of circulation function is equal to 1). The lift coefficient increment of a flat plate airfoil due to the effect of unsteady aerodynamics in an unstalled region is

$$\Delta C_L = 2\pi \left[-\frac{b\ddot{z}}{2U^2} - \frac{ab^2\ddot{\phi}}{2U^2} - (a - \frac{1}{2})\frac{b\dot{\phi}}{U} + \frac{b\dot{\alpha}}{2U} \right] \tag{72}$$

where

$\ddot{z}$ is vertical acceleration
$\ddot{\phi}$ is torsion acceleration
$\dot{\phi}$ is torsion velocity
U is the resultant wind velocity
$\dot{\alpha}$ is angle of attack change rate
b is the semichord
a is the distance from midchord to the elastic axis, divided by b.

The first and second terms on the right side of Equation 72 represent the virtual mass effect of the air due to the acceleration of the rotor blade in the vertical and torsion directions, respectively. The third term is the effect of blade torsion velocity on the angle of attack. The last term is a damping term based on rate of change of the angle of attack $\dot{\alpha}$. If the elastic axis is located at the quarter chord, the value of a in Equation 72 is minus one-half.

As suggested in Reference 12, the dynamic stall effect should be included as follows:

For $\alpha_{mod} > \alpha_{stall}$

$$\alpha_{RL} = \alpha_{mod} - (\text{sign } \dot{\alpha}) \quad \text{Min} \left\{ \begin{matrix} \Delta\alpha \\ |.2\ \alpha_{mod}| \end{matrix} \right\} \tag{73}$$

where

$$\Delta\alpha = 61.5\ \ell n\ (.6/MM) \sqrt{|\dot{\alpha}\ b/U|}$$

$$MM = \begin{cases} .3 \text{ for } M_{eff} \leq .3 \\ M_{eff} \text{ for } .3 < M_{eff} < .6 \\ .6 \text{ for } M_{eff} \geq .6 \end{cases} \tag{74}$$

If $\alpha_{mod} \leq \alpha_{stall}$

then

$$\alpha_{RL} = \alpha_{mod} \tag{75}$$

The total lifting coefficient is given by

$$C_{L_T} = C_L\ (\alpha_{RL}, M_{eff}) \quad \frac{\alpha}{\alpha_{RL}} + \Delta C_L \tag{76}$$

where $C_L\ (\alpha_{RL}, M_{eff})$ is the lift coefficient corresponding to α_{RL} and M_{eff} under stationary conditions.

2.2.3.3 Drag Coefficient - According to Reference 12, the C_{D_N} should be modified as

$$C_{D_N} = C_D\ (\alpha_{RD}, M_{eff}) \tag{77}$$

where

$$\alpha_{RD} = \alpha - (\sin \dot{\alpha})\ \text{Min} \left\{ \begin{matrix} \Delta\alpha \\ |.2\ \alpha| \end{matrix} \right\} \tag{78}$$

2.2.4 Steady State Aerodynamics by Equations. It is noted that all the equations in this paragraph are reproduced from Reference 6 for the sake of completeness. In order to facilitate the derivation which follows, an array Y is first defined as shown below.

Y (1)	Drag divergence Mach number for $\alpha = 0$	
Y (2)	Mach number for lower boundary of supersonic region	
Y (3)	Maximum C_L, normal flow, $M = 0$	
Y (4), Y (5), Y (6)	Coefficients of Mach number in maximum C_L equation, normal flow	
Y (7)	Maximum C_L, reversed flow, $M = 0$	
Y (8)	Slope of lift curve for $M = 0$	(/deg)
Y (9), Y (10), Y (11)	Coefficients of Mach number for lift curve slope in subsonic region	(/deg), (/deg), (/deg)
Y (12)	C_D for $\alpha = 0$, $M = 0$	(/deg)
Y (13), Y (14)	Coefficients of α in nondivergent drag equation	(/deg), (/deg^2)
Y (15)	Coefficient in supersonic drag equation	
Y (16)	Maximum nondivergent C_D	
Y (17)	Thickness/chord ratio	
Y (18)	Not used	
Y (19)	Drag rise coefficient	(/deg)
Y (20)	Coefficient of yaw angle in Mach number equation	
Y (21)	Exponent in Mach number equation for yawed flow	
Y (22), Y (23), Y (24)	Coefficients of α for Mach critical in steady C_M equation	(/deg^2), (/deg)
Y (25)	C_M for $\alpha = 0$, $M = 0$	

2.2.4.1 Lift and Drag Coefficient - The slopes of lift curve in subsonic, transonic, and supersonic flow regions are defined as

$$a_1 = Y(8) + Y(9)\, M + Y(10)\, M^2 + Y(11)\, M^3 \quad \text{(subsonic)} \tag{79}$$

$$a_2 = B_0 + B_1\, M + B_2\, M^2 \quad \text{(transonic)} \tag{80}$$

$$a_3 = 4/(57.3\sqrt{M^2 - 1}) \qquad \text{(supersonic)} \qquad (81)$$

where M is the effective Mach number defined by Equation 58. The lift curve slope corresponding to the critical Mach number (in the subsonic region) is

$$a_{1_{CR}} = a_1\ (Y(1)) \qquad (82)$$

The Mach number, M_{SC}, used in calculating the lift curve slope (in the supersonic region) can be found from Equation 81 as

$$M_{SC} = \sqrt{1 + ((.0698)/(a_1)_{CR})^2} \qquad (83)$$

Then, the Mach number of the transonic region is defined between Y(1) and M_S, where

$$M_S = \text{Max}\ \{Y(2),\ M_{SC}\} \qquad (84)$$

The three coefficients B_0, B_1, B_2 in the transonic region are determined by the following three equations:

$$a_2\ (Y(1)) = a_1\ (Y(1)) \qquad (85)$$

$$a_2\ (M_S) = a_3\ (M_S) \qquad (86)$$

$$\frac{da_2}{dM}\ (M_S) = \frac{da_3}{dM}\ (M_S) \qquad (87)$$

The modified angle of attack is given as

$$\alpha_1 = \begin{cases} \alpha \cos \Lambda & \text{if } |\alpha| < 90° \\ \alpha & \text{if } |\alpha| > 90° \end{cases} \qquad (88)$$

The typical curve of C_L versus α is shown in Figure 4.

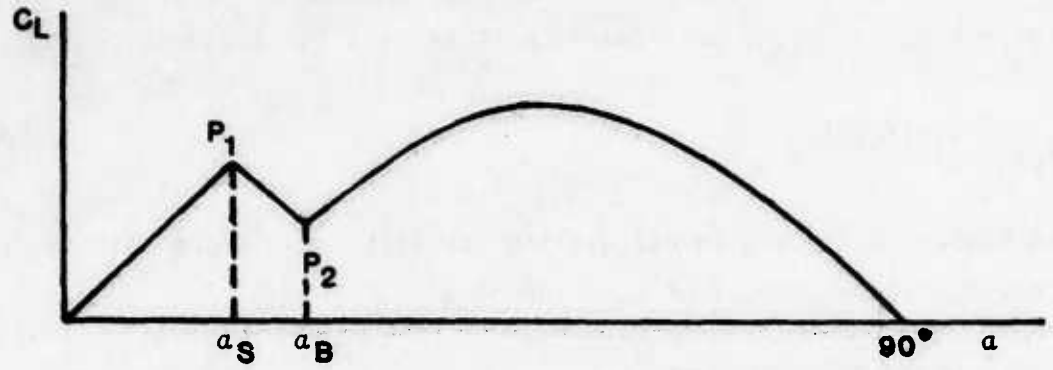

Figure 4. General Lift Coefficient Versus Angle of Attack Curve.

In the normal flow region, $|\alpha_1| \leq 90\_$:

$$\alpha = |\alpha_1|$$

$$C_L = Y(3) + Y(4)\ M + Y(5)\ M^2 + Y(6)\ M^3$$

$$\alpha_S = C_L/a$$

$$\alpha_B = \alpha_S + 5\_$$

In the reverse flow region, $|\alpha| > 90°$:

$$\alpha = 180° - |\alpha_1|$$

$$C_L = Y(7)$$

$$\alpha_B = C_L/a + 5°$$

For $\alpha_B \leq \alpha \leq 90°$

$$C_L = [(1.876 \sin \alpha - (.581))\ K + .81] \cos \alpha$$

where

$$K = \begin{cases} 1 + .25\ M^4 & , \text{ if } M \leq 1 \\ .85 + .82/(M - .8), & \text{if } M > 1 \end{cases}$$

The curve of C_D against α is seen in Figure 5. The corresponding C_D and α at P_3 are C_{DX} and α_X, respectively. At P_3, either $\alpha_X = \alpha_S$ and $C_{DX} < Y(16)$, or $\alpha_X < \alpha_S$ and $C_{DX} = Y(16)$.

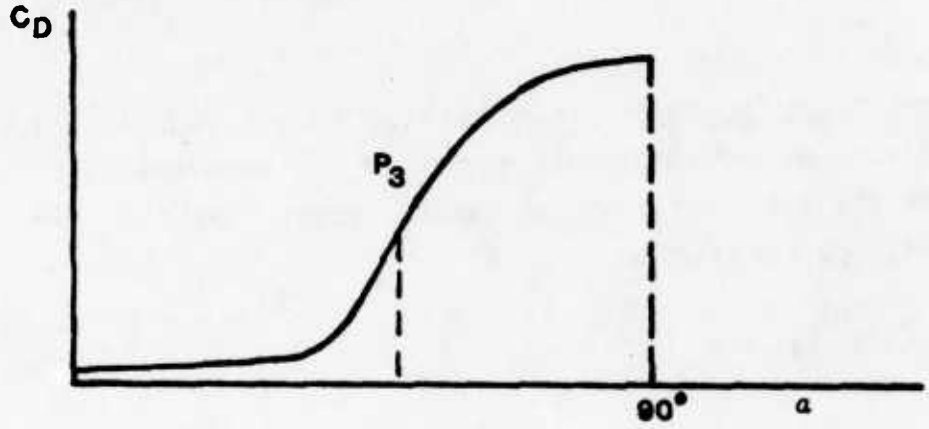

Figure 5. General Drag Coefficient Versus Angle of Attack Curve.

Unlike the lift coefficient, determination of the drag coefficient requires the definition of drag characteristics in only two regions: the subsonic and the supersonic. In the subsonic region, C_D is expressed as

For $\alpha_X \geq \alpha \geq 0$

$$C_D = \text{Min}\ \{Y(16),\ (Y(12) + Y(13)\alpha + Y(14)\alpha^2 + \text{Max}\ \{0,\ Y(19)\alpha - Y(1) + \text{Max}\ (M,\ .35))))$$

For $90° \geq \alpha \geq \alpha_X$

$$C_D = K_4 \sin^2 \alpha + (C_{DX} - K_4 \sin^2 \alpha_X) \cos \alpha / \cos \alpha_X$$

where

$$K_4 = 2.1\ K$$

In the supersonic region, $M \geq M_S$, C_D is the function of both α and M and is given as

$$C_D = \text{Min} \left\{ Y(16),\ \left[Y(12) + 4\ [(\alpha/57.3)^2 + Y(15)] / \sqrt{M^2 - 1} \right] \right\}$$

2.2.4.2 Moment Coefficient - The moment coefficient, C_M, is a function of angle of attack, α, effective Mach number, M_{eff}, and some input constants which define the characteristics of the C_M curve. The Mach number of the break point can be expressed as

$$M_b = A_3 + A_2 |\alpha| + A_1 |\alpha|^2$$

$$= Y(24) + Y(23) |\alpha| + Y(22) |\alpha|^2$$

which is defined as Mach number at the point where C_M breaks rapidly away from an input constant A_4 or Y(25). The angle of attack corresponding to a particular M_b in this equation is α_B. The value of α_B at $M_b = 0$ is defined as A_5. Then, the determination of C_M is described as below:

For $\alpha_B > \alpha$

$$C_M = Y(25)$$

For $A_5 > \alpha > \alpha_B$

$$C_M = (|\alpha| - \alpha_B)\,\bar{d}\ \text{sign}\ (\alpha) + Y(25)$$

where $\bar{d}$ depends on M_{eff} and an input critical value, Y(24), which is the point on the break curve for $\alpha = 0$:

$$\bar{d} = -.045 + .0425\,M_{eff} \qquad \text{for } M_{eff} \leq A_3$$

$$\bar{d} = -.01 - .2\,(M_{eff} - A_3) \qquad \text{for } M_{eff} > A_3$$

For $|\alpha| > A_5$

$$C_M = (A_5 - \alpha_B)\,\bar{d} - .00646\,(|\alpha| - A_5)\ \text{sign}\ (\alpha) + Y(25)$$

For $|\alpha| \geq 90°$

$$C_M = -.5\,(C_L \cos\alpha + C_D \sin\alpha) + Y(25)$$

It is assumed that the aerodynamic center is located at the .75 chord, rather than at the .25 chord. Under this assumption, the pitching moment is mainly due to lift and drag forces.

2.2.5 Induced Velocity by Data Table. When a data table is used, the local induced velocity, ν_i, can be expressed as a function of advance ratio, μ, average inflow ratio, λ, radial blade station, r/R, and blade azimuth angle, ψ,

$$\nu_i\ (\mu,\lambda,r/R,\psi) = \bar{\nu}_i \left[a_0 + \sum_{n=1}^{NH} a_n \cos\ (n\psi) + b_n \sin\ (n\psi) \right]$$

where

ν_i is the average induced velocity across the rotor disc

a_n, b_n are coefficients of the harmonics

NH is the highest harmonic.

For a data table, the permissible number of advance ratios is 3, the number of inflow ratios is 2, and the number of harmonics is 6. If μ, or λ, or r/R is not the same as used in FRA3A, then subroutine WKFIND interpolates the values wherever the computed values are within the range of their respective input. If the computed value is outside the range of its input, the procedure uses the input value which is closest to the computed value.

2.2.6 Program Features of FRA3. In FRA3, the user has the option to choose whether the steady state aerodynamic coefficients are to be calculated by equation or through table look-up. The basic independent variables used by both the equations and the table look-up procedure are angle of attack and Mach number. As shown in the preceding section, the angle of attack and Mach number are modified based on yaw flow angle, furthermore, the blade drag in the radial direction is also considered.

The BUN's unsteady aerodynamics described by Equations 63 - 78 are also implemented in FRA3 as an option under the assumption that the rotor reduced frequency is small. It is emphasized here to caution the user that, according to Reference 7, "...for rotors with cambered airfoils where the chord line and zero lift line are not coincident, it is advisable to use data table rather than equations to compute the aerodynamic coefficients," because the original equations were developed based on the symmetric airfoil. Note that both options take the effect of the yaw flow into consideration and include the blade drag in the radial direction.

The same options (equation or data table) are also available for the rotor induced velocity calculation. According to Reference 7, the induced velocity

equations described in Equations 46 - 52 are supposed to be valid for a very wide range of rotor operating states, including autorotation, vortex ring, windmill state, and climbing, as well as high speed flight. However, inside FRA3, a factor is introduced to make the induced velocity calculation more flexible due to the apparent discrepancy between Equations 50 - 51 and their counterparts which appear in a report of the Bell Helicopter Company (Reference 8).

Whenever the table option for induced velocity is chosen, an outside wake program has to be run first and the result stored in a sequential file, the appropriate format of which is depicted in the User's Manual (Volume II).

2.3 MODAL LIFTING SURFACE - CLS2

A lifting surface structure is represented as a linear combination of orthogonal modes. These modes are defined as displacement and slope functions of the structure spanwise coordinate. The displacement at some point on the surface is given by the summation of the products of the modal displacements at that point and the associated time-dependent generalized coordinates (modal amplitudes):

$$w_j = \sum_{i=1}^{n} \phi_{ij} \, q_i(t)$$

where w_j is the total displacement at the point of interest, ϕ_{ij} is the ith modal displacement, and $q_i(t)$ is the ith generalized coordinate. The slope is given by

$$w'_j = \sum_{i=1}^{n} \phi'_{ij} \, q_i(t)$$

A control surface angle degree of freedom is defined independently of the modal degrees of freedom and is coupled to them through implicit coupling.

2.4 LIFTING SURFACE AERODYNAMICS - FLA2

The lifting surface aerodynamics algorithm is based on the subsonic lifting surface theory of H. Multhopp (References 15 and 16). This is a theoretical method of analyzing finite wings that has received wide acceptance for its accuracy and adaptability to a wide range of fixed-wing applications (References 17 and 18).

The algorithm treats what is commonly referred to as the inverse problem: i.e., given the shape and attitude of a wing of finite aspect ratio, find the corresponding loading. A number of features have been included which allow the user much latitude in its application. Aerodynamics forces can be computed for full wings of two semispans or for wings of a single semispan (as in the case of a vertical tail). The wing may be swept or unswept, tapered or untapered, with or without twist. The user retains full control of the choice of the wing section aerodynamic characteristics and is free to vary them in the spanwise direction.

The algorithm includes the option of control surfaces deflected symmetrically or antisymmetrically for cases involving two semispans. The effects of flaps or ailerons with chords of approximately 20 percent of the total sectional chord may be computed. The user is free to specify arbitrarily the spanwise location of the limits of these control surfaces.

The algorithm automatically adjusts for the loss of aerodynamic efficiency at the spanwise limits of the control surface when those spanwise limits occur within a tolerance of the pivotal stations at which the downwash is computed. The loss of aerodynamic efficiency is due to the absence of endplating in usual control surface applications. This adjustment takes the form of a linear reduction of the control surface deflection such that if the edge of the control surface were to coincide with the spanwise pivotal point, the control surface deflection would be adjusted to one-half its inputted value. The spanwise range over which this adjustment occurs varies from about 10 percent of the semispan, inboard, to about 1.7 percent at the tip.

Input consists of the parameters describing the three-dimensional wing planform (aspect ratio, taper ratio, sweep), two-dimensional angle of attack and sectional properties (including control surface characteristics) at each of many spanwise stations, plus the free-stream conditions. The coordinates of the wing are transformed by the Prandtl-Glauert compressibility law to allow applicability of the solution up to the critical Mach number.

A matrix of 2 chordwise and 15 spanwise pivotal points is automatically computed over the extent of the planform (see Figure 6). It is at these locations that the integral equation for the downwash is evaluated. The choice of two chordwise points (at 34.55 and 90.45 percent chord) at each spanwise station is necessary to fully incorporate the information of the sectional lift and moment coefficients in the loading distribution. The choice of the number of spanwise stations of 15 is adequate for wings of simple planform geometry and of moderate aspect ratio. H. Multhopp suggested, in Reference 15, that for two chordwise points the number of spanwise points, M, exceed the minimum expressed in Equation 89 in terms of aspect ratio, AR, and Mach number:

$$M > 3 * AR * \sqrt{1 - Mach^2} \tag{89}$$

In Reference 18, J. E. Lamar studied the effect of varying the number of pivotal points and found that the aerodynamic center was the parameter most sensitive to the number of these points. The following formula was offered for determining the optimal number of pivotal points (N X M), where N is the number of chordwise points:

$$M = (4 \text{ TO } 5) * AR * \frac{N}{4} * \sqrt{1 - Mach^2} \tag{90}$$

This equation (which does not include sweep) indicates that, for aspect ratios from 4 to 9 and Mach numbers up to 0.6, the 2 X 15 combination should be an acceptable choice for most, but highly specialized planforms, i.e., very low and very high aspect ratios with highly swept or otherwise specialized leading edge shapes.

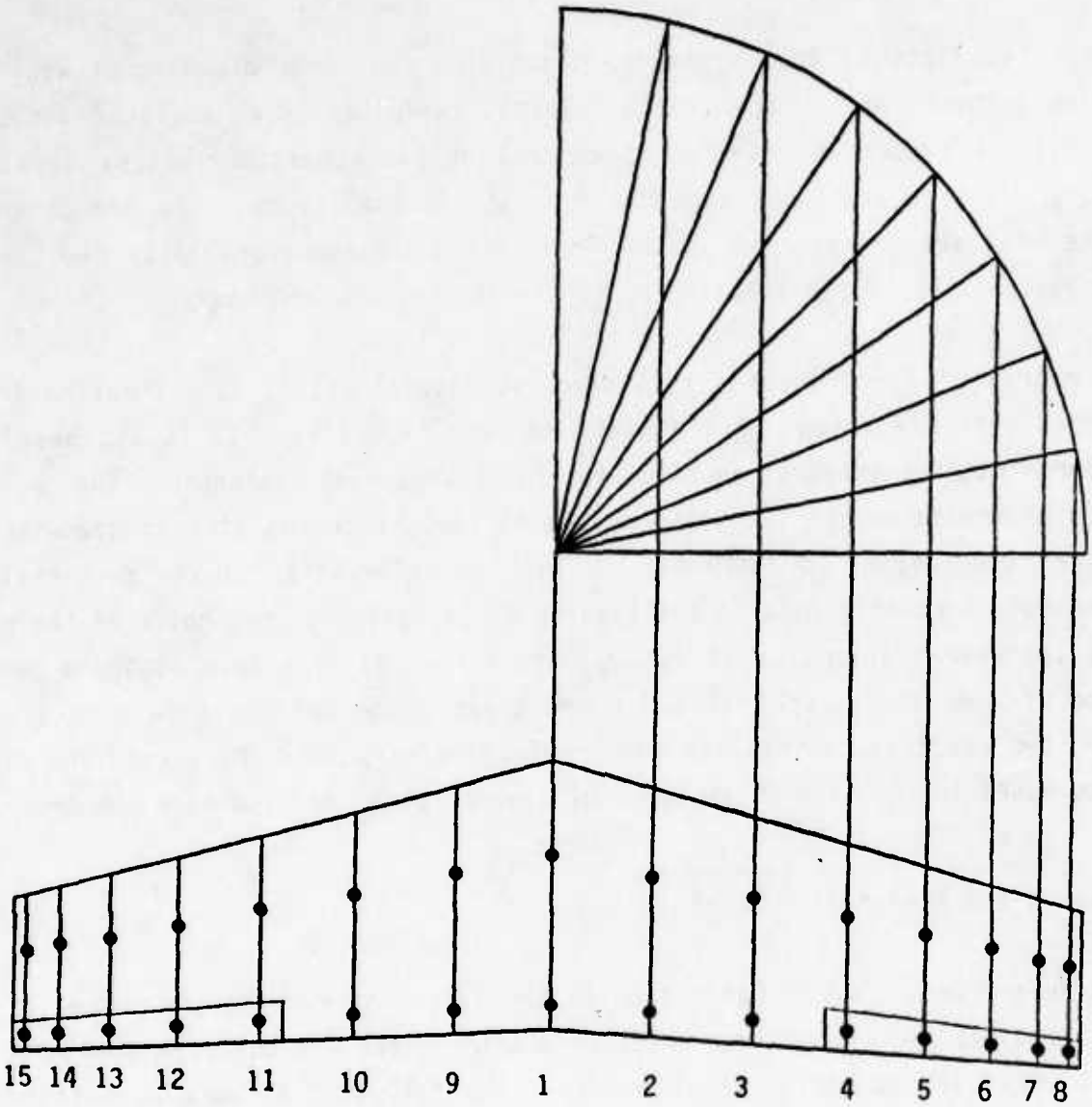

STATION NO.	NONDIMENSIONAL STATION
1	0.
2	0.1951
3	0.3827
4	0.5556
5	0.7071
6	0.8315
7	0.9239
8	0.9808

Figure 6. Lifting Surface Pivotal Points.

Selection of somewhat less than the optimal number of spanwise stations was not found to significantly detract from the results.

The lift and moment coefficients are automatically determined from the angle of attack at each of the spanwise stations computed by the dynamics package, and from the user-provided aerodynamic characteristics (lift and moment linear slopes versus angle of attack, control surface effectiveness, and control surface deflection).

The solution consists of representing the mean cambered surface of the wing by a sheet of doublets using fluid potential theory. The strengths of the doublets are subsequently computed at each of the pivotal points of the planform (as indicated in Figure 6). Euler's equation is used to solve the downwash, w, resulting from the loading distribution, $\ell(x_0,y_0)$, where x_0 and y_0 are points in the planform as in Equation 91:

$$w(x,y) = \frac{U_\infty}{8\pi}\int\int \frac{\ell(x_0,\ y_0)}{(y - y_0)^2}\left\{1 + \frac{(x - x_0)}{\sqrt{(x - x_0)^2 + (1 - \text{Mach}^2)(y - y_0)^2}}\right\} dx_0 dy_0 \tag{91}$$

With the solution of the downwash field of the wing, the induced angle of attack, and then the induced drag, can be computed by equations (92) and (93), respectively:

$$\alpha_i(x,y) = -\frac{w(x,y)}{U_\infty} \tag{92}$$

$$C_{Di} = \frac{1}{S}\int_{-b/2}^{b/2} c_\ell \cdot c \cdot \alpha_i \, dy \tag{93}$$

Thus, the solution involves the evaluation of the effect of each sectional station on the aerodynamic performance of every other section of the complete planform.

Special features incorporated in Reference 15 are employed such as the adjustment in the discontinuity of the sweep at the center line of swept wings, the correction of the logarithmic singularity in the influence functions, the choice of the interpolation polynomials, etc. Chordwise integration of the two influence functions is performed by a subroutine that uses Weddle's rule using 24 angular intervals, which was found to be adequate. The solution in the spanwise direction was carried out by the iterative solution of successive differences in the circulation and moment per unit span as described in Reference 18. The number of iterations was limited to 12, and the truncation terms were then added into the final summation of circulation and moment per unit span. From these sums, the integrated lift, drag, pitching and rolling moments, and center of pressure for the given planform were computed. Inasmuch as the Multhopp method is well documented, more detailed discussion of the solution of Equation 91 has not been included.

In addition to the limits of applicability noted above, the user should not expect to apply this algorithm to conditions that produce flow separation, shock waves or otherwise violate the limits of linearity engendered in the use of small perturbation analysis.

2.5 3-D MODAL STRUCTURE - CFM3

A three-dimensional structure is represented as a linear combination of orthogonal modes. Modal translations and rotations are specified at points defined in a Cartesian coordinate system. The displacement at a point in the structure is given by the summation of the products of the modal displacements at that point and the associated time-dependent generalized coordinates (modal amplitudes):

$$w_j = \sum_{i=1}^{n} \phi_{ij} \; q_i(t)$$

where w_j is the total displacement at the point of interest, ϕ_{ij} is the ith modal displacement, and $q_i(t)$ is the ith generalized coordinate.

2.6 LINEAR CONSTRAINTS - CLC2

Given a set of arbitrary relationships between degrees of freedom,

$$[\underset{mxn}{D}]\{x\} = \{0\},\ m < n$$

where m is the number of constraint equations and n is the number of degrees of freedom, m implicit degrees of freedom can be solved for (eliminated). m degrees of freedom are selected from x, and D is partitioned for retained and eliminated degrees of freedom:

$$\left[\begin{array}{c|c} D_{rr} & D_{re} \\ \hline D_{er} & D_{ee} \end{array}\right] \left\{\begin{array}{c} X_r \\ \hline X_e \end{array}\right\} = \left\{\begin{array}{c} 0 \\ \hline 0 \end{array}\right\}$$

Solving for X_e:

$$\{X_e\} = -\underset{mxm}{[D_{ee}]^{-1}} \underset{mx(n-m)}{[D_{er}]} \{X_r\}$$

$$\{X_e\} = \underset{mx(n-m)}{[T]} \{X_r\}$$

2.7 GENERAL FORCE - CGF2

All three types of forcing function (see paragraph 3.1.13, Volume II) are applied periodically. Start and end times define the period of each force

application, and the cycle is repeated automatically in the following manner. T_1 and T_2 are the specified start and end times, and T is the current time. The time argument is defined as

$$\bar{T} = \text{remainder}\left[\frac{T - T_1}{T_2 - T_1}\right]$$

$$= (T - T_1) - \left[\frac{T - T_1}{T_2 - T_1}\right](T_2 - T_1)$$

where the bracketed quantity is the largest integer whose magnitude does not exceed the magnitude of $(T - T_1)/(T_2 - T_1)$.

2.8 DAMAGED (NONIDENTICAL) ROTOR BLADES - CRD3

The CRD3 equations of motion are identical to those of CRE3. Changes in the properties of a blade or blades of an existing rotor are specified, and the coefficients of the component equations of motion computed from the changes are explicitly coupled to the original system.

Air loads are computed separately for the damaged blade(s).

2.9 LANDING GEAR - CLG2

A schematic of the landing gear is shown in Figure 7. x_s, y_s, z_s, α_x, α_y are the degrees of freedom of the strut attachment point. z_s is along the axis of the strut. The strut oleo is modeled as an elongation degree of freedom, ΔL, elastically coupled to the attachment degrees of freedom. x_t, y_t, z_t are tire degrees of freedom rigidly coupled to ΔL. The value of z_t determines whether or not the tire is in contact with the ground. When contact is made, the tire degrees of freedom are elastically coupled to the ground (vertical). Further,

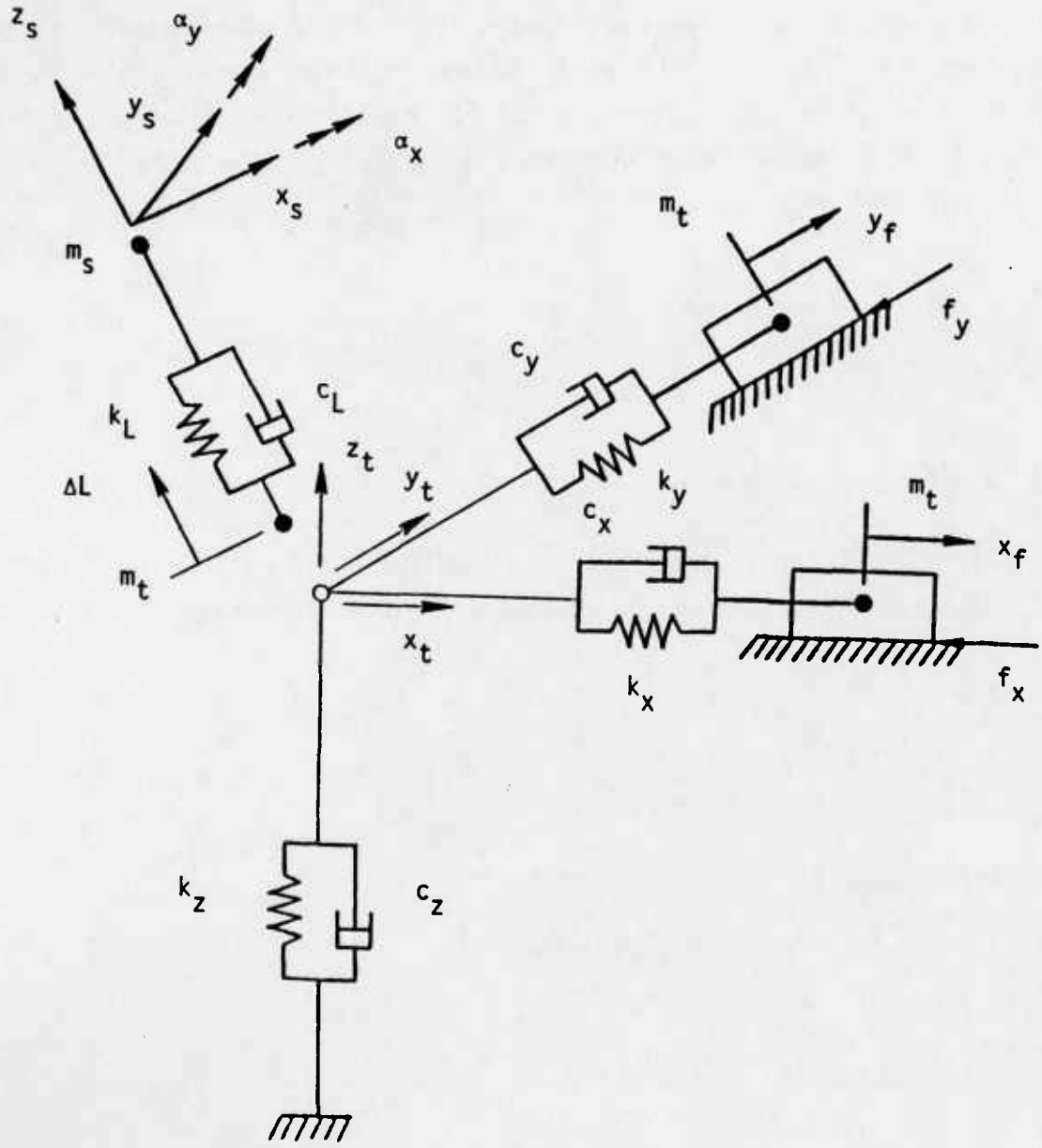

Figure 7. Landing Gear.

if friction is considered, the tire degrees of freedom are elastically coupled to longitudinal and lateral scrubbing degrees of freedom, x_f, y_f. The mass of the strut is assigned to the attachment degrees of freedom and the tire mass is assigned to ΔL and the scrubbing degrees of freedom.

The tire and scrubbing degrees of freedom are defined with respect to some fuselage coordinate system. The strut degrees of freedom need not be defined in the fuselage coordinate system and must be transformed. (X_s, Y_s, Z_s) are the local coordinates of the attachment point. Writing the strut vectors in terms of fuselage coordinates,

$$\vec{x}_s = a_x\vec{i} + a_y\vec{j} + a_z\vec{k}$$

$$\vec{y}_s = b_x\vec{i} + b_y\vec{j} + b_z\vec{k}$$

$$\vec{z}_s = c_x\vec{i} + c_y\vec{j} + c_z\vec{k}$$

where $\vec{i}$, $\vec{j}$, $\vec{k}$ are the unit vectors of the fuselage coordinate system. Letting (x_t, y_t, z_t) represent fuselage coordinates, the transformation can be written

$$\begin{Bmatrix} x_t \\ y_t \\ z_t \end{Bmatrix} = \begin{bmatrix} a_x & b_x & c_x \\ a_y & b_y & c_y \\ a_z & b_z & c_z \end{bmatrix} \begin{Bmatrix} x_s \\ y_s \\ z_s \end{Bmatrix}$$

and, accounting for translation and rotation of the strut,

$$\begin{Bmatrix} x_t \\ y_t \\ z_t \end{Bmatrix} = \begin{bmatrix} a_x & b_x & c_x & b_xL & -a_xL & c_x \\ a_y & b_y & c_y & b_yL & -a_yL & c_y \\ a_z & b_z & c_z & b_zL & -a_zL & c_z \end{bmatrix} \begin{Bmatrix} x_s \\ y_s \\ z_s \\ \alpha_x \\ \alpha_y \\ \Delta_L \end{Bmatrix}$$

where L is the undeformed length of the strut (small displacements assumed). Note that x_t, y_t, z_t can be treated as implicit degrees of freedom.

The transformation is then applied to the component coefficient matrices.

During a time history solution, the transformation is applied to the component state vector to determine whether the tire is in contact with the ground and to determine the tire damping and stiffness coefficients as a function of velocity and displacement. Strut damping and stiffness is computed directly from the state vector.

When Coulomb friction is greater than or equal to the stiffness and damping forces of the tire, the tire is considered to be elastically coupled to the ground (no scrubbing); when Coulomb friction is less than the combined stiffness and damping forces, the tire scrubbing force is equal to the friction:

<u>longitudinal - brakes on</u>

If: $u_x k_z |z_t| \geq |c_x (\dot{x}_f - \dot{x}_t) + k_x (x_f - x_t)|$

then: $f_x = m_t \ddot{x}_f + c_x (\dot{x}_f - \dot{x}_t) + k_x (x_f - x_t)$

else: $f_x = + u_x k_z |z_t| , \quad \dot{x}_f < 0$

$f_x = - u_x k_z |z_t| , \quad \dot{x}_f \geq 0$ (u_x = coefficient of friction)

<u>lateral</u>

If: $u_y k_z |z_t| \geq |c_y (\dot{y}_f - \dot{y}_t) + k_y (y_f - y_t)|$

then: $f_y = m_t \ddot{y}_f + c_y (\dot{y}_f - \dot{y}_t) + k_y (y_f - y_t)$

else: $f_y = + u_y k_z |z_t| , \quad \dot{y}_f < 0$

$f_y = - u_y k_z |z_t| , \quad \dot{y}_f \geq 0$ (u_y = coefficient of friction)

2.10 GENERAL TIME HISTORY SOLUTION - STH4

STH4 performs a Runge-Kutta integration of the system equations of motion. Input parameters are:

Start time
Initial increment
End time
Error check value
Initial velocity, displacement of system DOF

Evaluation is done by means of fourth-order Runge-Kutta formulae with the modification of Gill (Reference 19). Accuracy is tested by comparing the results of the procedure for single and double increments. The increment is adjusted during the solution by halving or doubling. If more than 10 bisections of the increment are necessary to achieve satisfactory accuracy, the solution is terminated.

A component state vector can be obtained by

$$\left\{ Y_I \right\} = \left[T_I \right] \left\{ Y \right\}, \quad \left\{ Y \right\} = \begin{Bmatrix} \dot{x} \\ x \end{Bmatrix}$$

where Y_I and Y are the component and system state vectors at a given time and T_I is the component transformation matrix.

2.11 COMPONENT INTERFACE AND INTERNAL LOADS - SII3

The complete equations of motion for a component are

$$\left[M_I \right] \left\{ \ddot{X}_I \right\} + \left[C_I \right] \left\{ \dot{X}_I \right\} + \left[K_I \right] \left\{ X_I \right\} = \left\{ F_I \right\} + \left\{ F_{IR} \right\}$$

where M_I, C_I, and K_I are the coefficient matrices of the Ith component, F_I is the forcing function vector, and F_{IR} is the vector of the reaction loads at the interfaces to other components. All of the F_{IR} cancel out when a system is assembled and thus are not included in the component formulation.

SII3 computes the interface loads acting on a component at a given time:

$$\left\{ F_{IR} \right\} = \left[M_I \right] \left\{ \ddot{X}_I \right\} + \left[C_I \right] \left\{ \dot{X}_I \right\} + \left[K_I \right] \left\{ X_I \right\} - \left\{ F_I \right\}$$

where

$$\left\{ X_I \right\} = \left[T_I \right] \left\{ X \right\}$$

$$\left\{ \dot{X}_I \right\} = \left[T_I \right] \left\{ \dot{X} \right\}$$

$$\left\{ \ddot{X}_I \right\} = \left[T_I \right] \left\{ \ddot{X} \right\}$$

$$\left\{ F_I \right\} = \left[T_I \right] \left\{ F \right\}$$

X and F are the system displacement and force vectors and T_I is the component transformation matrix.

Given M_I, C_I, K_I, X_I, $\dot{X}_I$, and $\ddot{X}_I$, internal parameters can then be computed (see paragraph 3.3.9, Volume II).

2.12 GENERAL EIGENANALYSIS - SEA5

The equation

$$[M]_{nxn}\{\ddot{X}\} + [C]\{\dot{X}\} + [K]\{X\} = \{0\}$$

can be transformed into

$$[\bar{M}]\{\dot{Y}\} + [\bar{K}]\{Y\} = \{0\}$$

where

$$\{Y\} = \begin{Bmatrix} \dot{X} \\ X \end{Bmatrix}$$

$$[\bar{M}] = \begin{bmatrix} [0] & [M] \\ [M] & [C] \end{bmatrix}$$

$$[\bar{K}] = \begin{bmatrix} -[M] & [0] \\ [0] & [K] \end{bmatrix}$$

(Reference 20)

The eigenvalue problem is defined by

$$[\bar{K}]\{Y\} = \omega_r^2 [\bar{M}]\{Y\} \quad , \quad r = 1, 2, \ldots, 2n$$

where $\bar{K}$ and $\bar{M}$ are real and may be nonsymmetric, and ω_r^2 are the eigenvalues.

SEA5 computes the eigenvalues and eigenvectors Y_r of the above equation. $\bar{K}$ is reduced to upper Hessenberg form and M to upper triangular form. K is further transformed to quasi-upper triangular form (upper Hessenberg with no two consecutive subdiagonal elements being nonzero). The rth eigenvalue is the complex number given by the ratio of the rth diagonal elements of the transformed K and M matrices (Reference 21).

3.0 INTERFACE TO IMPROVED NONUNIFORM INFLOW ANALYSES

A dummy module called FRWØ has been created to handle the interface between DYSCO and a wake program. FRWØ provides the following data: flapping angle, azimuth angle of blades, blade radius, flapping hinge location, number of calculation points, nondimensional radial location of calculation points, average chord, average thickness ratio, advance ratio (shaft reference), inflow ratio (shaft reference), air density, rotor speed, rotor thrust, vortex core size, radial location of root vortex (nondimensional), and radial location of tip vortex (nondimensional).

Like other aerodynamic force modules, i.e., FRAØ, FRA2 and FRA3, FRWØ may be coupled with the rotor modules CRR2 and CRE3 which, in turn, may be coupled with any other component modules to form a model within the limitations of DYSCO.

FRWØ consists of four modules: input module FRWØI, constant module FRWØC, active module FRWØA, and module FRWØB. A more detailed description of each of these modules is given in the following paragraphs.

3.1 MODULE FRWØI

The values of the following parameters in this module must be provided by the user:

1. Component of wind velocity, with regard to hub system (for a trim case, the wind velocity should be set to zero because it is replaced by vehicle velocity and wind velocity with regard to ground system in the input module of trim solution input module)
2. Number of nondimensional stations (calculation points)
3. Nondimensional stations (r/R)
4. Rotor thrust

5. Average thickness ratio

6. Vortex core size

7. Nondimensional station of root vortex

8. Nondimensional station of tip vortex.

3.2 MODULE FRWØC

In this module, all input data are retrieved and stored. Information concerning wind velocity and rotor thrust, air density ratio, average thickness ratio, vortex core size, station of root vortex and tip vortex are stored in common /FRWØ/, and data concerning number of stations and nondimensional stations are stored in common /ROT/. Both /FRWØ/ and /ROT/ also appear in module FRWØA.

If coupled with elastic rotor CRE3, this module also constructs mode shape and blade pitch angle based on the aerodynamic stations using the interpolation method.

3.3 MODULE FRWØA

Using the data in /FRWØ/ and /ROT/, calculations of advance ratio and inflow ratio about the shaft reference axis are performed in this module. These calculations, together with information about number of blades, azimuth angle of blades, blade radius, flapping hinge location, and flapping angle of each blade, which according to the DYSCO convention should be provided by the rotor component, provide all the data required by this contract.

3.4 MODULE FRWØB

When the 'CASE' command is activated, FRWØB is called to store all the information concerning /FRWØ/ into a user data file for batch purposes.

3.5 SUMMARY

Details of the computed parameters are listed below:

Geometric Parameters

NB(NROT)	- Number of blade of NROTth rotor, provided by rotor component stored in /ROT/.
SLOZ(K,L)	- Flapping angle of Kth Station of Lth blade, provided by rotor component through argument list.
PSIN	- Azimuth angle of Lth blade, provided by rotor component through argument list.
R	- Blade radius, provided by rotor component, stored in /ROT/ as XC(NX, NROT) where NX is number of dynamic stations.
EFC(IREF)	- Flapping hinge location, provided by rotor component, stored in /ROT/.
NXA	- Number of aerodynamic stations (calculation points), provided by FRWØI stored in /ROT/ as NAERO(FREF) where FREF is the FREFth use of FRWØ.
X(I)	- Radial location of calculation points, provided by FRWØI, stored in /ROT/ as XAERO(I,NROT).
CHORDC(I)	- Average blade chord, provided by FRWØI, stored in /ROT/.
TRTO(FREF)	- Average thickness ratio, provided by FRWØI, stored in /ROT/.

Flight Condition Parameters

AMUN - Advance ratio (shaft reference), calculated in FRWØA.

AINFWN - Inflow ratio (shaft reference), calculated in FRWØA.

FACT - Air density, provided by FRWØI and stored in /FRWØ/.

OM(NROT) - Rotor rpm, provided by rotor component and stored in /ROT/.

RCT(FREF) - Rotor thrust, provided by FRWØI and stored in /FRWØ/ as RCTC(FREF). Note that for trim case this value should be replaced by CT in /TRIM/ after 1st iteration.

Wake Parameters

VCS(FREF) - Vortex core size, provided by FRWØI and stored in /FRWØ/.

RVR(FREF) - Radial location (nondimensional) of root vortex, provided by FRWØI and stored in /FRWØ/.

RVT(FREF) - Radial location (nondimensional) of tip vortex, provided by FRWØI and stored in /FRWØ/.

4.0 VALIDATION OF ADVANCED HELICOPTER ANALYSIS

The primary goal of this validation effort is to compare DYSCO computed trim control parameters and horsepower consumption with those measured in the Operational Loads Survey test flight of the Bell AH-1G in order to determine the program's capabilities and accuracy (Reference 22). In addition, the results obtained from the elastic blade analysis, using both the advanced aerodynamic analysis and the simplified aerodynamic analyses currently in DYSCO, are compared with each other to observe differences between them. The model vehicle is the Bell AH-1G, a teetering single-rotor helicopter with anti-torque tail rotor.

The general input data for the AH-1G associated with C81 (Reference 23) are presented in the appendix.

4.1 DYSCO TRIM ALGORITHM

In DYSCO, the trim condition is defined for a fuselage flying at a steady state condition with the blades and fuselage in periodic motion. The trim algorithm by D. A. Peters and A. P. Izadpanah, called "Periodic Shooting With Newton-Raphson Iteration," Reference 24, has been adapted to include a complete helicopter, nonlinear aerodynamics, and such flight conditions as steady turn, steady climb, and autorotation. This method requires only numerical integration of nonlinear equations and the inversion of an approximate partial-derivative matrix formed from successive numerical integrations through one period for every perturbation in controls and initial conditions. This algorithm has the following characteristics:

1. On a computational basis, it is superior to any other transition-matrix method in that it requires less computer storage and computation.
2. It is superior to the harmonic balance method, except for a linear system with few harmonics in the coefficients.
3. It is superior to a direct numerical integration for a case with small damping.

As far as control strategy is concerned, four independent direct controls and two indirect controls are used. The choice of direct controls depends on the rotor type and flight condition. The two indirect controls are two of the three Euler angles of a ground fixed coordinate system with respect to the body fixed system. This algorithm treats all the controls and initial conditions of blade degrees of freedom as unknowns and adjusts them simultaneously to achieve force and moment balance in the concerned directions, as well as steady vibration of all the degrees of freedom of the system.

The helicopter trim solution module (STR3) involves an analysis which is somewhat more specialized than the general dynamic or aerodynamic analyses often carried out with DYSCO. That is, the trim algorithm includes large angular motions with respect to a fixed coordinate system, variations in the relationship of the body axis to the wind vector, and automatic treatment of the gravity vectors. For these reasons, the present applications require adherence to certain considerations not necessary in other DYSCO analyses.

At present, it is recommended that users apply STR3 to single dynamic rotor, single fuselage combinations because a set of independent trim variables must be introduced for more complex systems.

4.2 GENERAL CONSIDERATION OF THE MODEL FOR THE TRIM SOLUTION

4.2.1 CRR2, CRE3 (Rotor Component). Use a single rotor only. The number of blades is arbitrary. A teetering rotor may be modeled by the additional use of a CLC1 module (BETA1200 = -1 * BETA1100 for CRR2, or OP 1110 = -1 * OP 1210 for CRE3). A "single blade analysis' may be performed for efficiency of computations. The blade degrees of freedom are arbitrary, except for the flap or out-of-plane degree of freedom. If pitch or torsion is a DOF, CCEØ or CCE1 must also be used to provide controls for the rotor.

All other parameters are optional; the hub degrees of freedom must be consistent with the overall model.

4.2.2 FRA1, FRA2, FRA3 (Rotor Aerodynamic Module). The wind velocity should be entered as zero since it is an input to STR3. Care must be exercised in selecting the nondimensional stations for the aerodynamics which represent tip and root loss effects. The safest procedure, at present, is to select values that correspond to the aerodynamic stations.

4.2.3 CFM2 (Fuselage Component). The first CFM2 in the model is the "reference" fuselage. (At present, it is recommended that only one be used in a trim analysis. Contact Kaman for guidance if it is desired to use additional CFM2 modules.) The rotor should be coupled to this component using the standard input.

The reference axes are the principal axes of the fuselage. Note that the CG is that of the component, not of the entire vehicle. The mass and gravitational effects of the rotor and fuselage are automatically managed by STR3.

The rigid body degrees of freedom selected determine which forces and moments are to be balanced during trim. Only three options are presently allowed:

1. XCG, ZCG, ROLL, PTCH
2. XCG, YCG, ZCG, ROLL, PTCH
3. XCG, YCG, ZCG, ROLL, PTCH, YAW.

All options allow level flight or steady climb or descent. Options 2 and 3 may also be used for steady turn. Option 3 may be used for autorotation.

4.2.4 FFC2 (Fuselage Aerodynamic Module). This aerodynamic force module should be used with the reference fuselage. Wind velocity should be input as zero, since this is input in STR3. When tail rotor thrust is a trim variable, it is iterated upon and the input value in this module may be an estimated value. Note that when a teetering rotor is modeled, the horizontal tail incidence is coupled to the cyclic rotor control (see STR3 input). Also note that all the moment coefficients in this module are based on the characteristic length of 1 inch.

4.2.5 CLC1 (Linear Constraint). This module provides the necessary constraint of the rigid body flapping modes of the two blades to form the teetering mode. In some cases, this module may also be used to scale the elastic mode which is equivalent to changing the tip deflection of the mode shape to another constant instead of one. This may avoid numerical instability in some situations.

4.2.6 CCE0, CCE1 (Rotor Control System). The use of a control system is mandatory whenever the rotor pitch or elastic twist degrees of freedom are selected.

4.2.7 Other Components. Any other components having a negligible mass may also be included in the model.

4.2.8 STR3 Input. The following comments should assist the user in supplying appropriate input values:

If teetering rotor - Input A and B such that the horizontal tail incidence angle = A + B * cyclic sine control + (C * cyclic sine control)**2 (radians).

Initial Integration Increment (sec) - Depends on system frequencies. If only rigid body modes, an appropriate value is 1/20 of the time for one rotor revolution.

Integration Period (sec) - Normally the time for one rotor revolution.

No. of Iterations - 5 - 10 is typical.

Error Allowed for Each DOF - i.e., allowable tolerance (absolute).

Increment on Each DOF - For calculating partial derivative matrix. .01 radian or .01 inch are typical.

Wind Velocity - In terms of ground fixed system (in./sec). Absolute velocity of air with respect to the ground (not with respect to the fuselage).

Fuselage CG Translational Velocity (in./sec) - In terms of ground fixed system. Include tangential velocity for a turn. Note X velocity is negative in forward flight (see CFM2 coordinate system in User's Manual).

Fuselage Rotational Velocity (rad/sec) - Absolute rotational velocity of fuselage in terms of ground fixed system.

Initial Estimates - May be zero for initial conditions and controls.

4.3 TRIM SIMULATION OF AH-1G

As mentioned in the previous section, the DYSCO trim algorithm involves an analysis which is somewhat more specialized than the general dynamic or aerodynamic analyses often carried out with DYSCO. So, when a trim model is formed, one has to follow the instructions of the previous section or the User's Manual carefully in order to avoid any unnecessary mistakes.

The simulation of the AH-1G by DYSCO includes several component and force modules: elastic rotor CRE3, rotor aerodynamic module FRA3, rotor control system CCEØ, linear constraint module CLC1, fuselage component CFM2, and fuselage aerodynamic module FFC2.

The following is a detailed description of the simulation and its limitations.

Because the derivation of the equations of motion in the aeroelastic rotor component CRE3 is based on the energy method (or its equivalent, the generalized Galerkin method), the input modes need not be orthogonal as long as they satisfy the geometric boundary conditions. In addition to this, these modes may be obtained for each physical degree of freedom separately. In this simulation, the in-plane and out-of-plane elastic modes were obtained from the eigensolution of a B540 blade rotating at 324 rpm with fixed-free boundary conditions. The torsional modes consist of the rigid body mode and a linearly varied elastic mode. All of these modes are superimposed on the out-of-plane

rigid body mode which consists of the modes necessary for a teetering rotor. Note that it is the space spanned by these modes, and not the individual mode, that dominates the accuracy of the result.

Although all data concerning B540 blades are available in Reference 23, the rectangular input for blade distributed properties in Reference 23 is difficult to convert to the data needed for DYSCO, which accepts only the trapezoidal distributed properties.

One way to avoid this problem is to introduce double stations for each radial location. However, this may greatly affect computational efficiency and is not adopted here. Zero value for the precone angle is used in this simulation because the current version of DYSCO cannot handle the transformation when two degrees of freedom are differentiated only by a constant. However, it is expected that the teetering constraint of the two blades may totally cancel the effect of the precone angle to the linear terms and have negligible effect on the trim result.

The simplest control system CCEØ which considers only the control rod stiffness is used to simulate the AH-1G control system because it is a recognized fact that an equivalent spring may be used to reasonably represent a helicopter control system.

In CFM2, four rigid body modes (XCG, ZCG, ROLL, and PTCH) are chosen and no elastic mode is considered.

DYSCO can perform a trim solution for the three force balances and the three moment balances of the fuselage. However, because only the two-dimensional wind effect is considered for the aerodynamic surfaces in the fuselage aerodynamic force module FFC2 and because a tail rotor is not allowed by the trim algorithm, the Y-direction force balance and yaw moment balance of the fuselage are not considered in this simulation. This implies that only four degrees of freedom - XCG, ZCG, PTCH, and ROLL - are assigned to the fuselage.

In CFM2, the rotor shaft angles (forward and lateral) from vertical and the vertical height and horizontal distance of the hub from the CG provide all of the information needed to automatically couple with rotors through rigid massless shafts.

Note that in DYSCO the fuselage CG does not include the contribution from the rotor and is different from the vehicle CG, which is used for helicopter operation.

Note also that the mass moments of inertia of the fuselage, which are required as input, are not used in trim.

A teetering rotor can be formed by using module CLC1 to constrain the rigid flapping modes of the two blades. This module can also be used to scale the coefficient matrices and make the numerical procedure more stable.

Fuselage aerodynamic force module FFC2 only considers the two-dimensional aerodynamic effect by expressing each aerodynamic coefficient as a quadratic function of angle of attack in the plane of the airfoil cross section.

The aerodynamic force on the wing can be calculated using the equations in Reference 24, but this method is not yet available in FFC2 for the current version of DYSCO. A regression procedure is employed to determine the wing aerodynamic coefficients based on the trimmed fuselage aerosurface forces and moments from C81 at various speeds of interest.

4.4 RESULTS AND DISCUSSION

The basic DYSCO model created in this validation effort is AH-1G-35A, which is based on the AH-1G helicopter with a gross weight of 8300 lb, aft CG, and counter number 35A used in the operational loads survey test flight (References 22 and 23). The general characteristics of the AH-1G helicopter are presented in the appendix. The DYSCO trim model AH-1G-35A is demonstrated in Figure 8.

```
* * * * * * * * * * * * * * MODEL AH-1G-35A * * * * * * * * * * * * * * *

AH-1G TRIM SAMPLE CASE

INDEX     COMP      NO.      DATA SET      FORCE      DATA SET

  1       CRE3       1       B2Z1T2        FRA3       FCT1.65
                                        REQUIRED DS/DM=AFD161/AIRFOIL

  2       CCE0       1        3000         NONE
  3       CLC1                COUPLE       NONE
  4       CFM2       1        8300-4       FFC2       AH1G16.5

* * * * * * * * * * * * * * * * * * * * * * * * * * * * * * * * * * * * * *
```

Figure 8. AH-1G-35A Trim Model.

Detailed information for component and force modules associated with the AH-1G-35A model can be seen in the User's Manual. However, for the sake of clarity, some general descriptions of these components and forces are listed below:

1. CRE3, B1Z1T2 - 2 blades; in-plane DOFs, one mode (IP 1110, IP 1210); out-of-plane DOFs, two modes (OP 1110, OP 1120, OP 1210, OP 1220); torsion DOFs, two modes (TOR 1110, TOR 1120, TOR 1210, TOR 1220); 4 hub DOFs (XHUB1000, ZHUB1000, ALFX1000, ALFY1000); 14 degrees of freedom total.
2. FRA3, FCT1.65 - Induced velocity by equation with a 1.65 factor, aerodynamic coefficients by table look-up. Unsteady is off.
3. CCEØ, 3000 - Control system with 3000 lb/in. control rod stiffness, coupled with blade pitch or torsion degrees of freedom.

4. CLC1, COUPLE - Teetering constraint for out-of-plane mode (OP 1110=264*TEET, OP 1210=-264*TEET); scaling for first in-plane mode and second out-of-plane mode (IP 1110=264*IPIP1110, IP 1210=264*IPIP1210, OP 1120=264*OPOP1120, OP 1220=264*OPOP1220).

5. CFM2, 8300-4 - 4 rigid body modes (XCG 1000, ZCG 1000, ROLL1000, PTCH1000); automatically couples to rotor; mass = 7290 lb, station of hub = - .68 in., vertical height of hub = 96.485 in.

6. FFC2, AH1G16.5 - Flat plate drag area is 16.5 square ft. with fuselage, wing, horizontal tail, and vertical tail aerodynamics.

Another DYSCO model AH-1G-36A corresponding to a 9000-lb gross weight, mid-CG location, and counter number 36A in the operational loads survey test flight is shown in Figure 9.

```
* * * * * * * * * * * * * * MODEL AH-1G-36A * * * * * * * * * * * * * *

AH-1G TRIM SAMPLE CASE

INDEX     COMP      NO.       DATA SET       FORCE       DATA SET

  1       CRE3       1        B2Z1T2         FRA3        PCT1.65
                                          REQUIRED DS/DM=AFD161/AIRFOIL

  2       CCE0       1        3000           NONE
  3       CLC1                COUPLE         NONE
  4       CFM2       1        9000-A         FFC2        AH1G16.5

* * * * * * * * * * * * * * * * * * * * * * * * * * * * * * * * * * * * *
```

Figure 9 . AH-1G-36A Trim Model.

Model AH-1G-36A is constructed by simply replacing 8300-4/CFM2 in AH-1G-35A with 9000-4/CFM2, which is the same as 8300-4/CFM2 except that mass = 7990 lb, station of hub = 4.278 in., and vertical height of hub = 95.427 in. Furthermore, in order to compare the differences between rigid rotor CRR2 and elastic rotor CRE3 (with only rigid blade modes) and among aerodynamic modules FRAØ, FRA2 and FRA3, four additional models were created and are illustrated in Figures 10 through 13.

The component and force data sets for the four additional models are described below:

a. CRE3, B1Z1T1 - 2 blades; in-plane DOFs, one rigid mode (IP 1110, IP 1210); out-of-plane DOFs, one rigid mode (OP 1110, OP 1210); torsion DOFs, one rigid mode (TOR 1110, TOR 1210); 4 hub DOFs (XHUB1000, ZHUB1000, ALFX1000, ALFY1000); 10 degrees of freedom total.

b. CRR2, BZT - 2 blades; lag DOFs (ZETA1100, ZETA1200); pitch DOFs (THET1100, THET1200); flapping DOFs (BETA1100, BETA1200); 4 hub DOFs (XHUB1000, ZHUB1000, ALFX1000, ALFY1000), 10 degrees of freedom total; other characteristics are the same as B1Z1T1/CRE3.

c. CLC1, TEET - Teetering constraint of rigid rotor (TEET = BETA1100 = -BETA1200).

d. CLC1, TEETE - Teetering constraint of elastic rotor (TEET = OP1110/264 OP1210/264.

e. CLC1, TSCALE - Scaling component for elastic rotor in-plane mode. (IP 1110 = 264*IPSC1110, IP 1210 = 264*IPSC1210).

f. FRA3, General - Induced velocity factor = 2, Tiplos coefficient = 1, other characteristics are the same as FCC1.65/FRA3.

g. FRA2, Tabular - Characteristics are the same as General/FRA3, but use simple momentum theory to calculate induced velocity; no yaw flow correction for aerodynamic calculation.

```
* * * * * * * * * * * * * * * MODEL ELAST3 * * * * * * * * * * * * * * *

ELAST3:  ELASTIC TEETERING ROTOR AND GENERAL AERODYNAMICS

INDEX     COMP      NO.      DATA SET      FORCE      DATA SET
  1       CRE3       1       B2Z1T2        FRA3       GENERAL
                                        REQUIRED DS/DM=AFD161/AIRFOIL
  2       CCE0       1       3000          NONE
  3       CLC1               TEETE         NONE
  4       CLC1               TSCALE        NONE
  5       CFM2       1       8300-4        FFC2       AH1G16.5

* * * * * * * * * * * * * * * * * * * * * * * * * * * * * * * * * * * * *
```

Figure 10. ELAST3 Trim Model.

```
* * * * * * * * * * * * * * * MODEL ELAST2 * * * * * * * * * * * * * * *

ELAST2:  ELASTIC TEETERING ROTOR AND TABULAR AERODYNAMICS

INDEX     COMP      NO.      DATA SET      FORCE      DATA SET
  1       CRE3       1       B2Z1T1        FRA3       TABULAR
                                        REQUIRED DS/DM=AFD161/AIRFOIL
  2       CCE0       1       3000          NONE
  3       CLC1               TEETE         NONE
  4       CLC1               TSCALE        NONE
  5       CFM2       1       8300-4        FFC2       AH1G16.5

* * * * * * * * * * * * * * * * * * * * * * * * * * * * * * * * * * * * *
```

Figure 11. ELAST2 Trim Model.

```
* * * * * * * * * * * * * * * MODEL ELASTO * * * * * * * * * * * * * * *

ELASTO:  ELASTIC TEETERING ROTOR AND LINEAR AERODYNAMICS

INDEX    COMP     NO.    DATA SET     FORCE     DATA SET
  1      CRE3      1     B1Z1T1       FRA0      LINEAR
  2      CCE0      1     3000         NONE
  3      CLC1            TEETE        NONE
  4      CLC1            TSCALE       NONE
  5      CFM2      1     8300-4       FFC2      AH1G16.5

* * * * * * * * * * * * * * * * * * * * * * * * * * * * * * * * * * * * *
```

Figure 12. ELASTO Trim Model.

```
* * * * * * * * * * * * * * * MODEL RIGIT2 * * * * * * * * * * * * * * *

RIGIT2:  RIGID TEETERING ROTOR AND TABULAR AERODYNAMICS

INDEX    COMP     NO.    DATA SET     FORCE     DATA SET
  1      CRR2      1     BZT          FRA2      TABULAR
                                  REQUIRED DS/DM=AFD161/AIRFOIL
  2      CCE0      1     3000         NONE
  3      CLC1            TEET         NONE
  4      CLC1            ORDER        NONE
  5      CFM2      1     8300-4       FFC2      AH1G16.5

* * * * * * * * * * * * * * * * * * * * * * * * * * * * * * * * * * * * *
```

Figure 13. RIGIT2 Trim Model.

h. FRAØ, Linear - Lift coefficient = .112/deg, drag coefficient = .085, moment coefficient = 0, other characteristics are the same as Tabular/FRA2.

For the AH-1G-35A case (corresponding to flight 35A, clean wing, 8300 lb gross weight, aft CG station 200.6), the comparisons of DYSCO computed and OLS measured flight performance parameters are shown in Figures 14a through 14e. In these figures, the triangle, AH-1G-35A(S), represents the DYSCO model AH-1G-35A with steady aerodynamics; the diamond, AH-1G-35A(U), represents DYSCO model AH-1G-35A with unsteady aerodynamics; and the circle, AH-1G-35A(B1S), stands for the same DYSCO model considering only the rigid out-of-plane mode with steady aerodynamics. As can be seen in these figures, the general trend and agreement between measured and computed results are reasonably good if the irregular test points are neglected. Also, it is observed that the model AH-1G-35A(B1S), which considers only one rigid flapping mode, also gives good prediction as far as trim positions are concerned.

The consideration of unsteady aerodynamics has virtually no effect on the horsepower and has little effect on fuselage pitch or collective and cyclic control angles, as demonstrated in Figures 14a through 14e.

The effect of different modes on the trim result is depicted in Figures 15a through 15e. In Figures 15, the circle, AH-1G-35A(S), represents the DYSCO model AH-1G-35A with steady aerodynamics (shown in Figure 8); the square, AH-1G-35A(B1S), the triangle, AH-1G-35A(B35), and the diamond, AH-1G-35A(B3Z25), represent the same model with one rigid out-of-plane mode, three out-of-plane modes, and three out-of-plane and two in-plane modes, respectively. It is seen in Figure 15a that the collective control position of AH-1G-35A(S) is displaced by a constant value as compared with the other three models. The reason for this is that there is no torsional degree of freedom for the other three models; therefore, the control is directly applied to the blade which is equivalent to being controlled by a control system with infinite spring rate. It is illustrated in Figures 15a through 15e that the

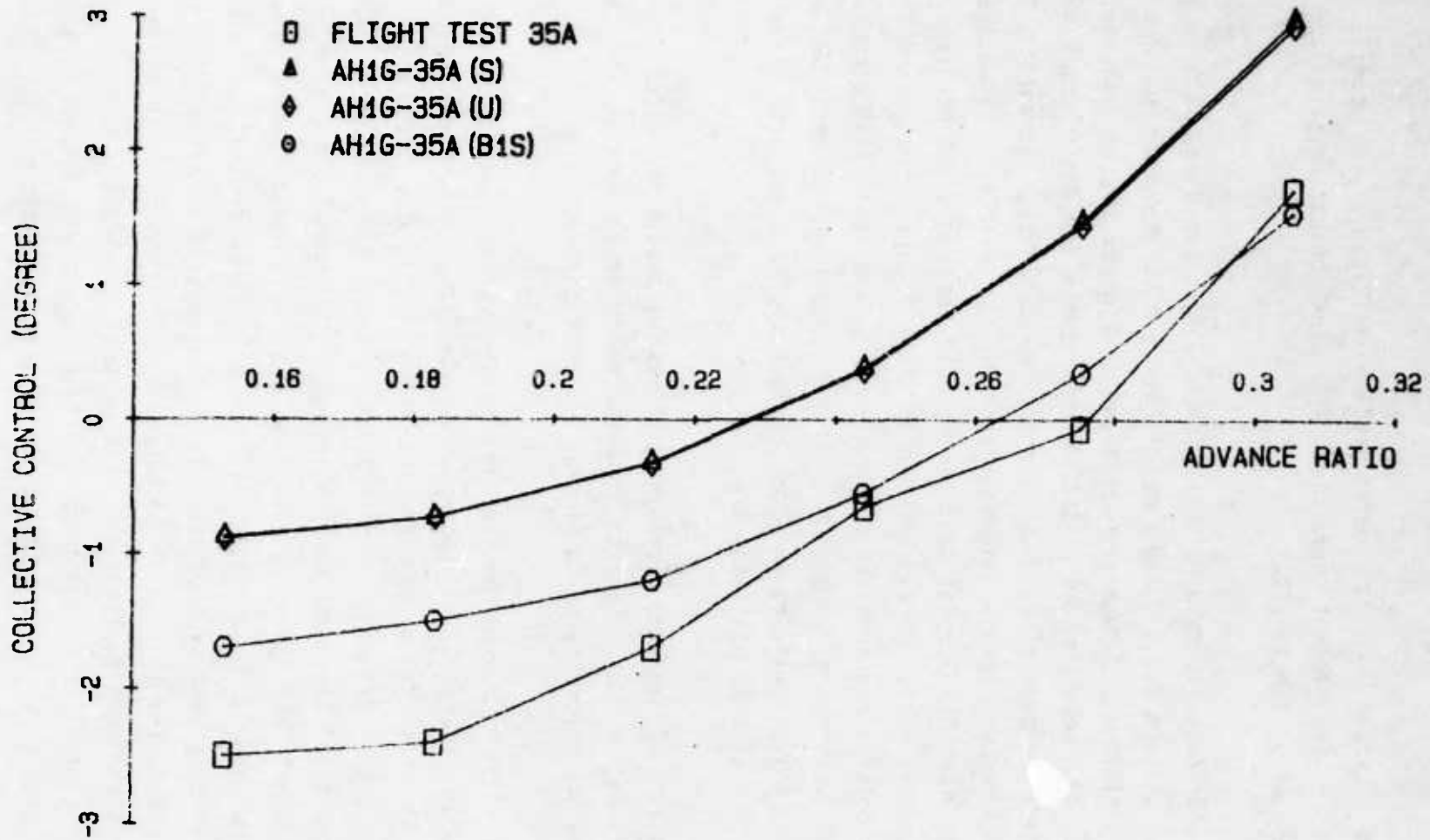

Figure 14a. Comparison Between Flight 35A and DYSCO Simulation, Collective Control vs Advance Ratio.

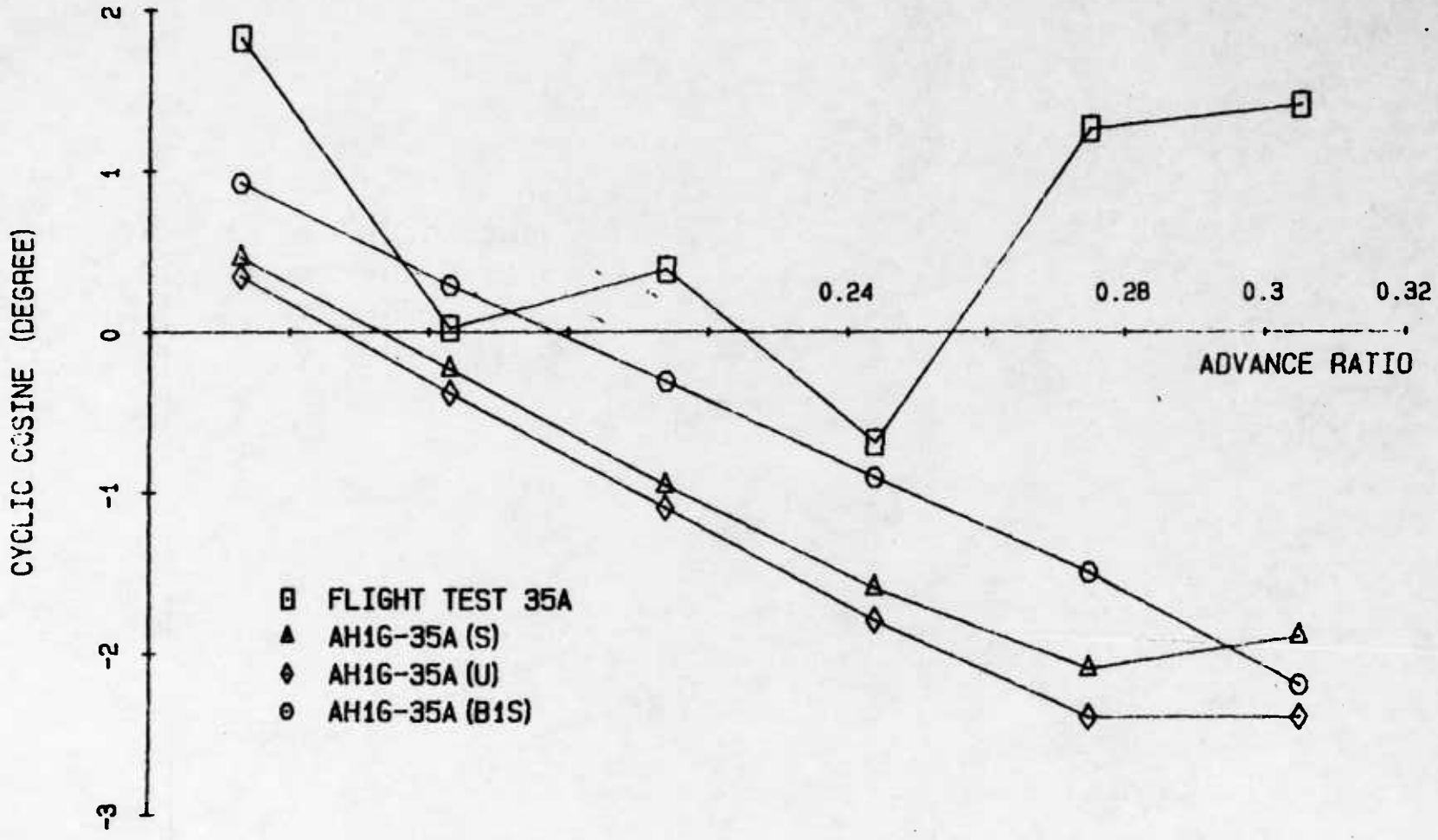

Figure 14b. Comparison Between Flight 35A and DYSCO Simulation, Cyclic Cosine Control vs Advance Ratio.

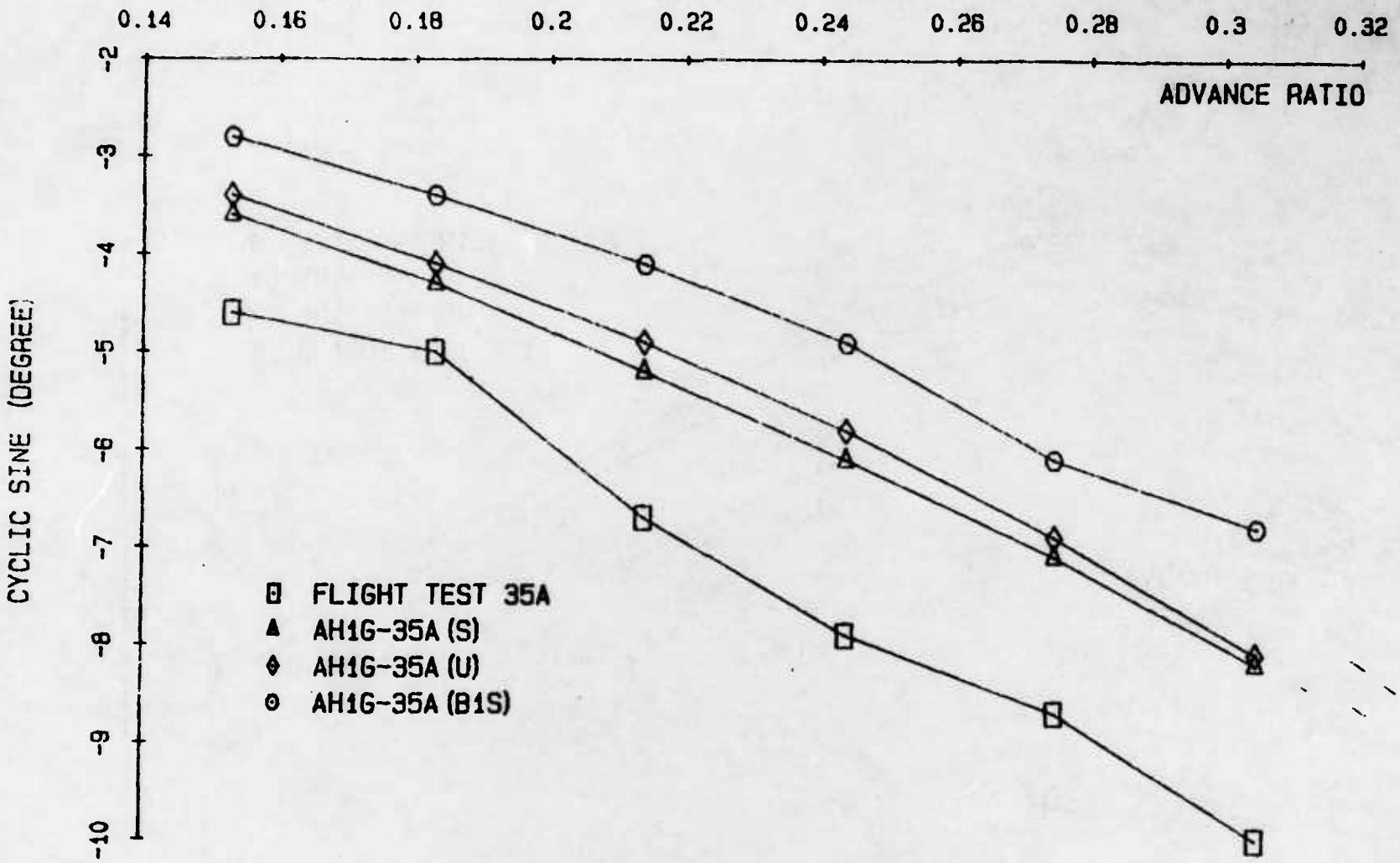

Figure 14c. Comparison Between Flight 35A and DYSCO Simulation, Cyclic Sine Control vs Advance Ratio.

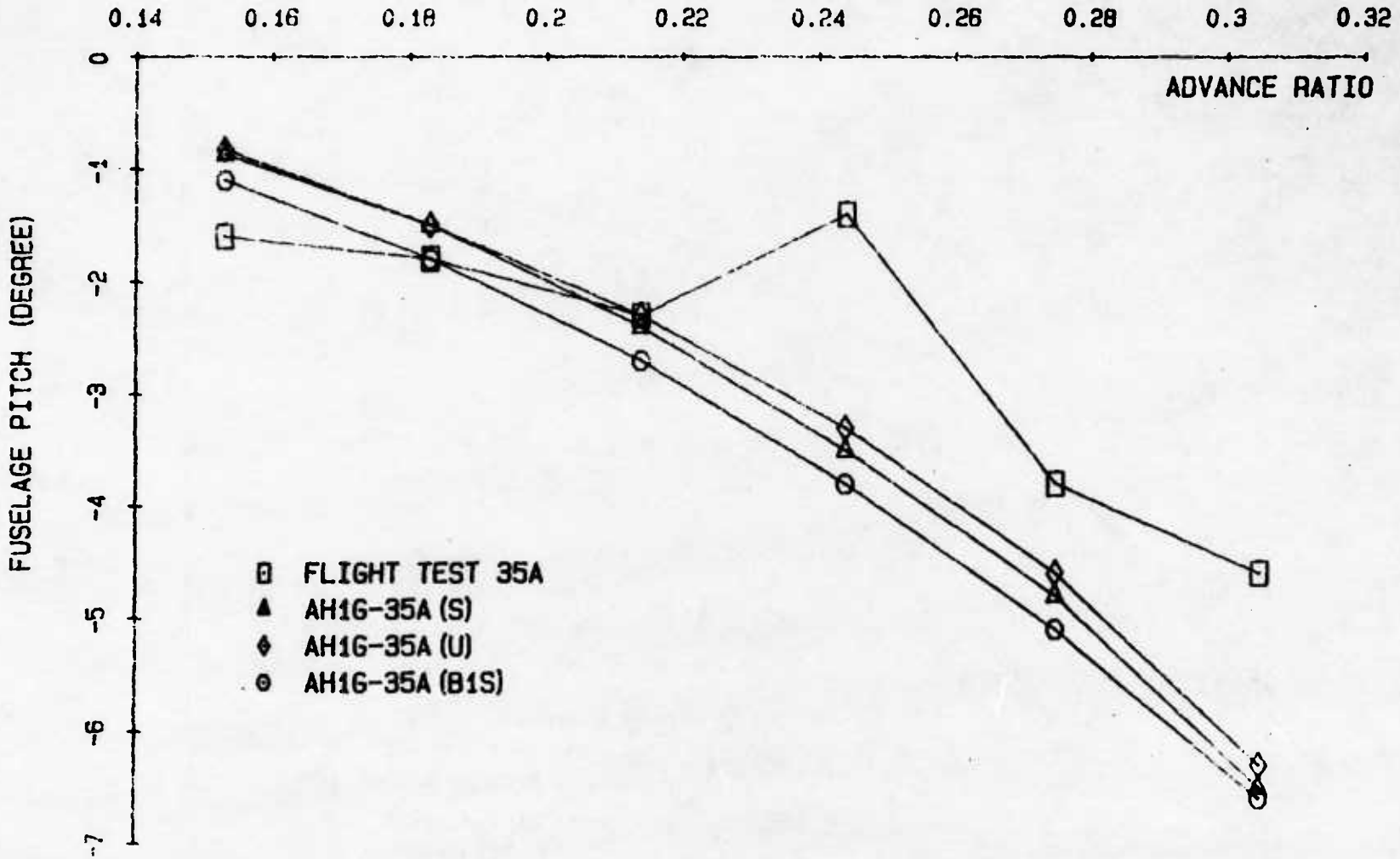

Figure 14d. Comparison Between Flight 35A and DYSCO Simulation, Fuselage Pitch Angle vs Advance Ratio.

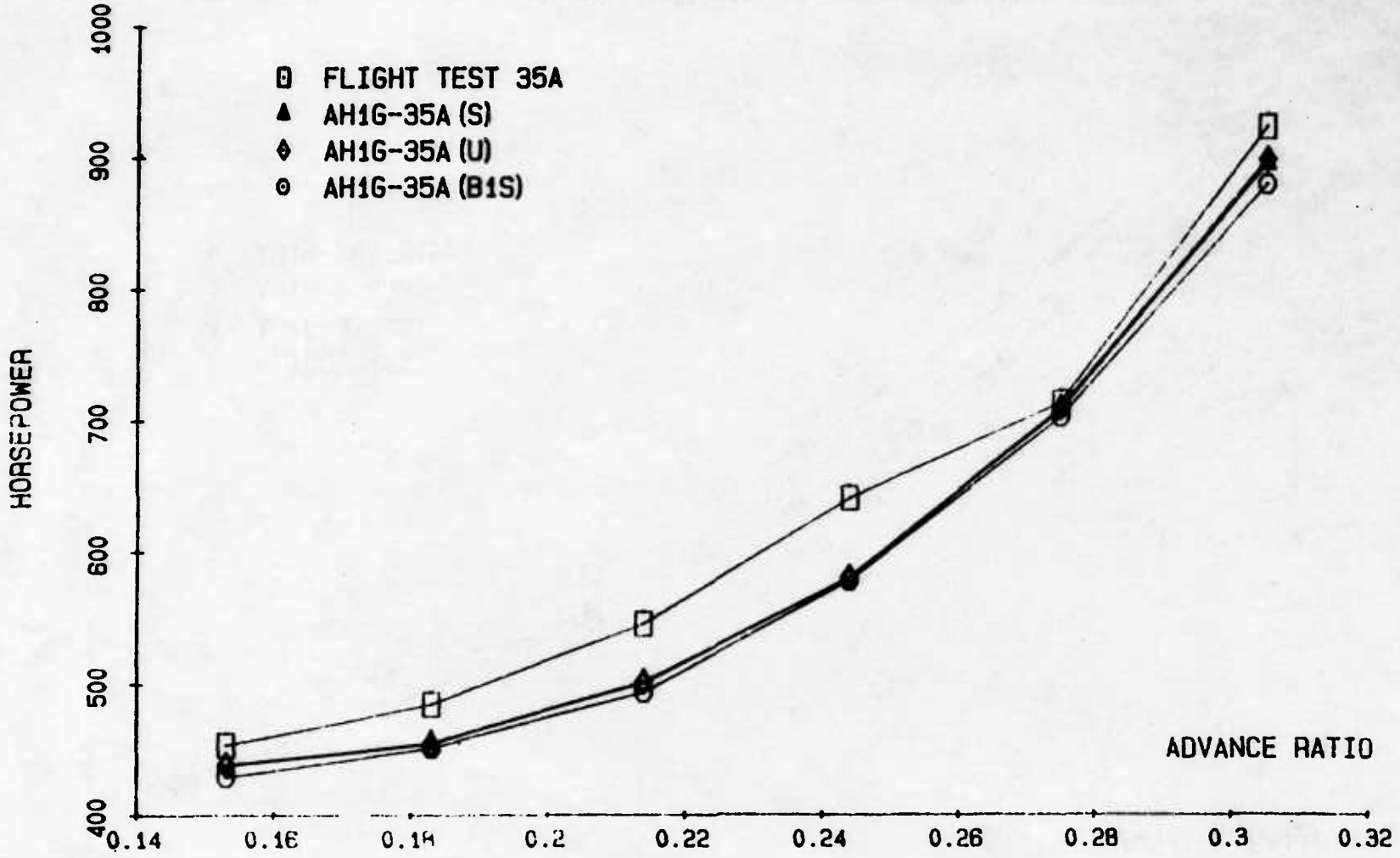

Figure 14e. Comparison Between Flight 35A and DYSCO Simulation, Horsepower vs Advance Ratio.

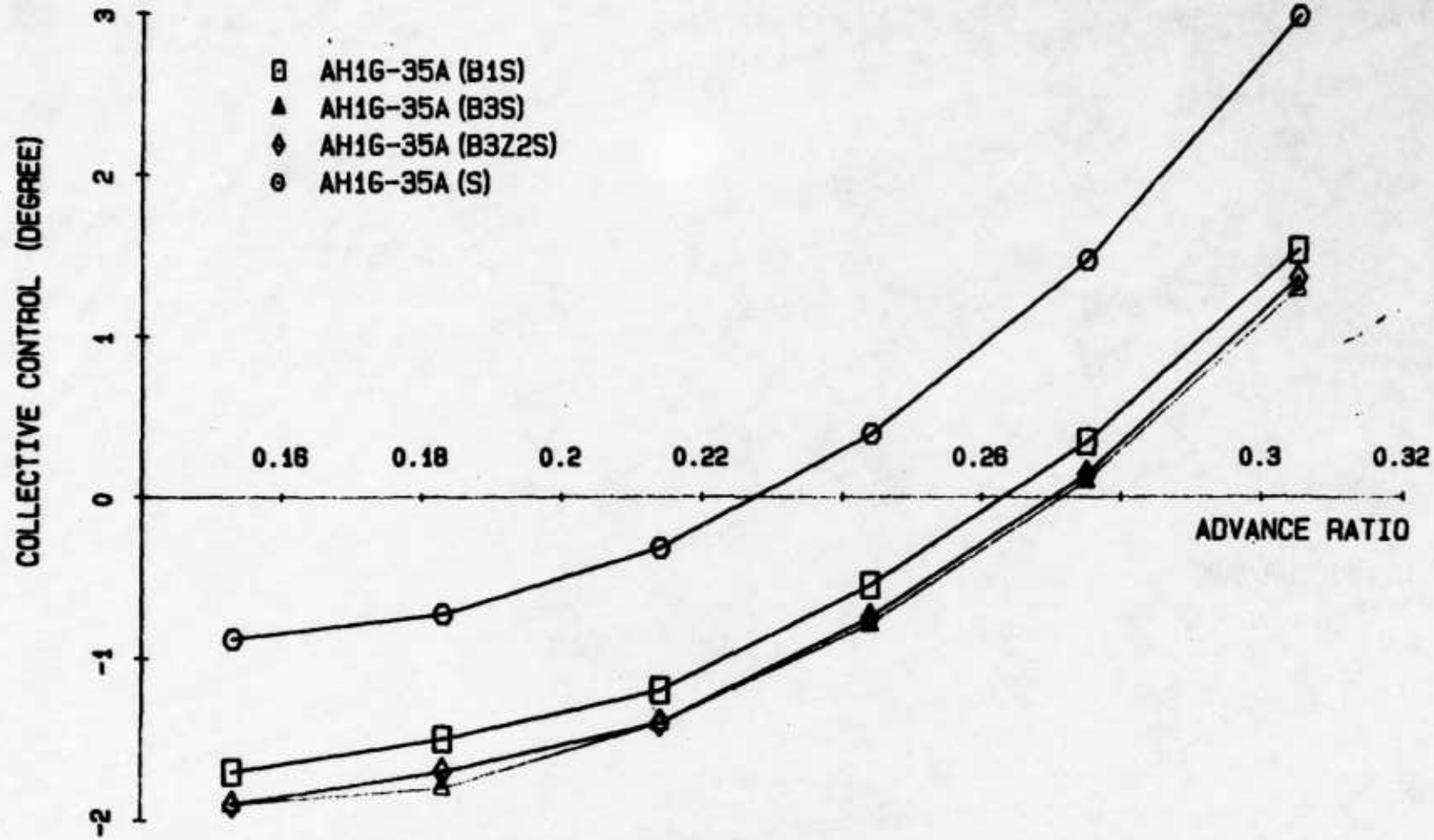

Figure 15a. Degree of Freedom Effect on Trim - Flight 35A Simulation, Collective Control vs Advance Ratio.

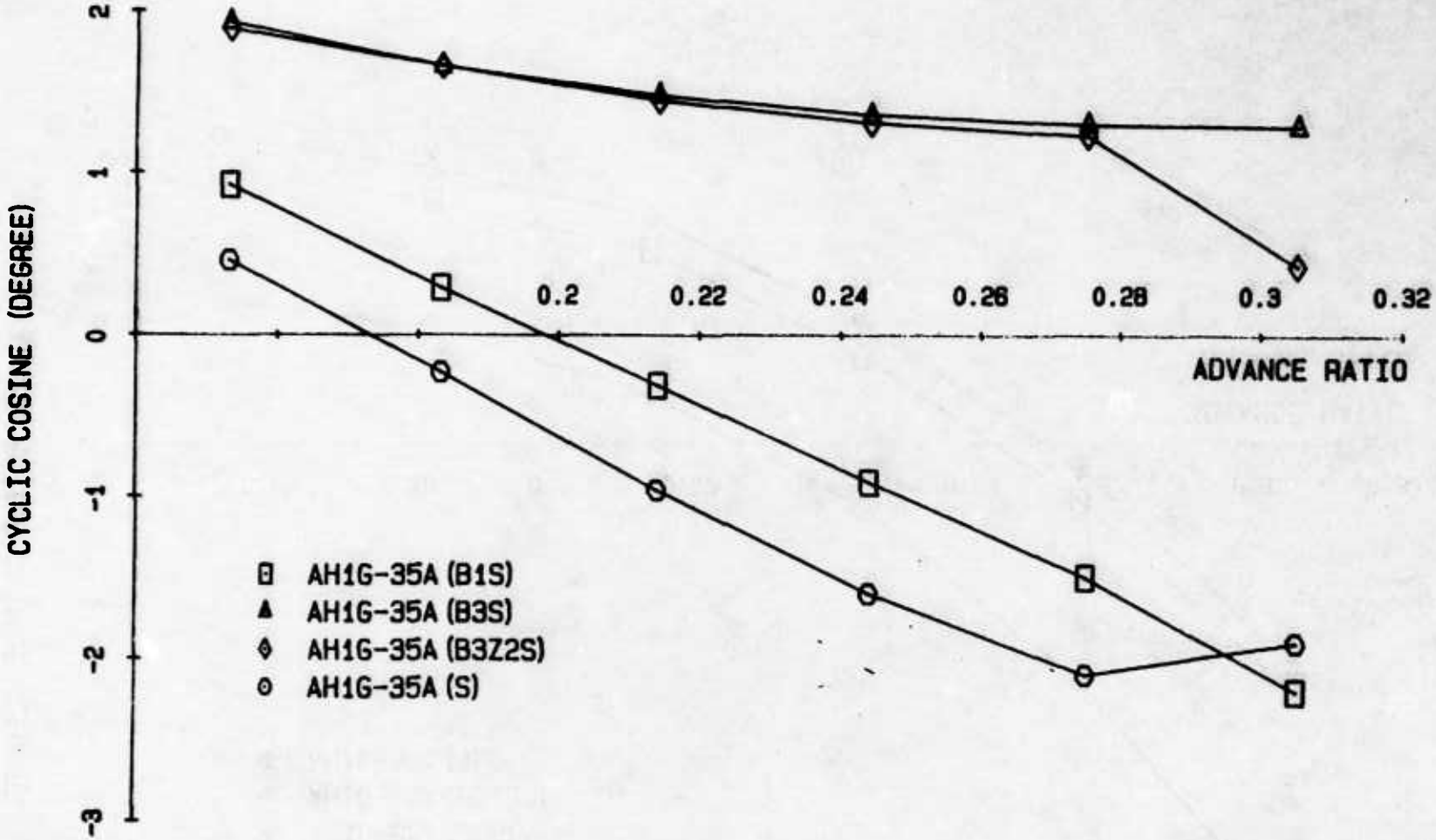

Figure 15b. Degree of Freedom Effect on Trim - Flight 35A Simulation, Cyclic Cosine Control vs Advance Ratio.

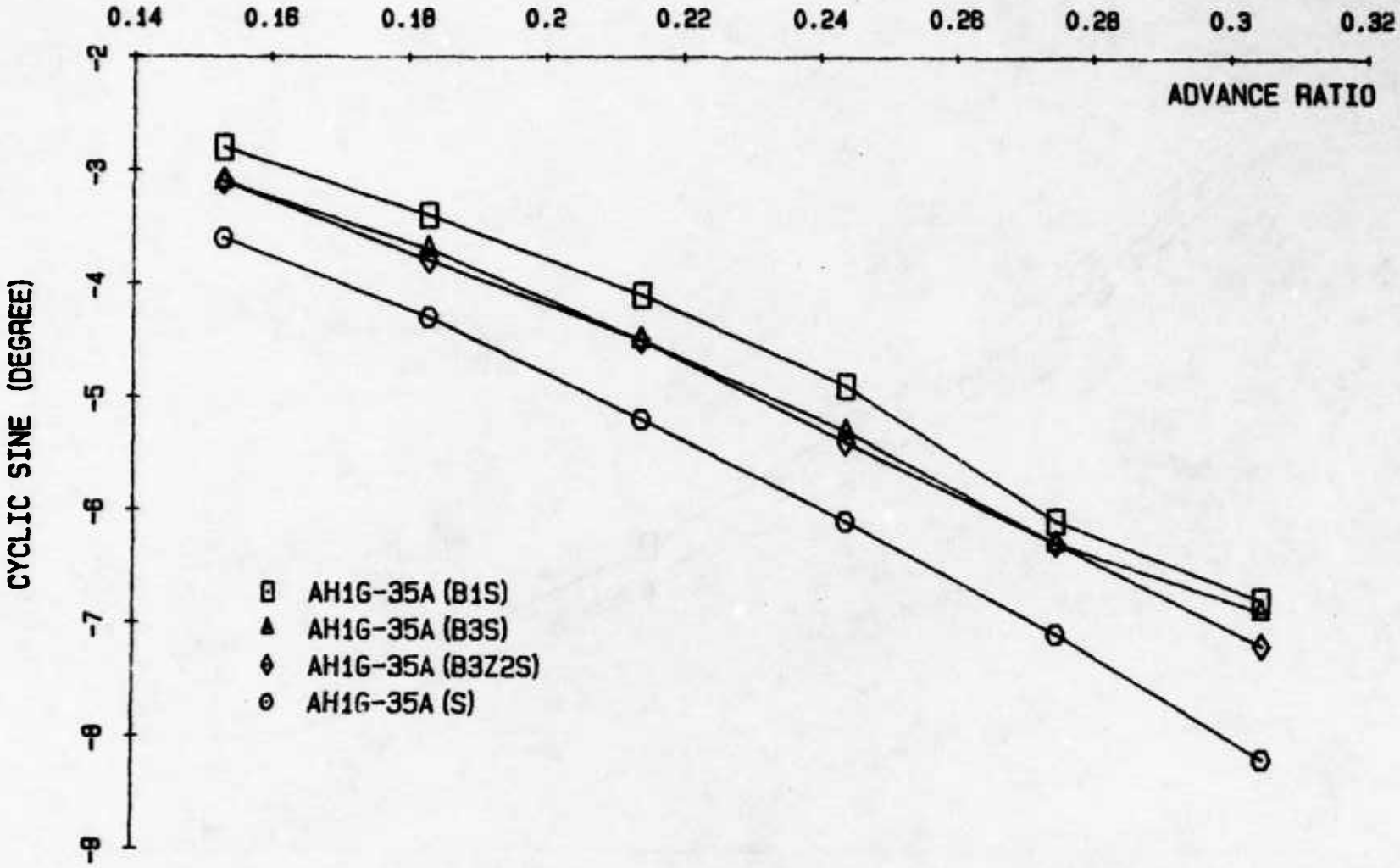

Figure 15c. Degree of Freedom Effect on Trim - Flight 35A Simulation, Cyclic Sine Control vs Advance Ratio.

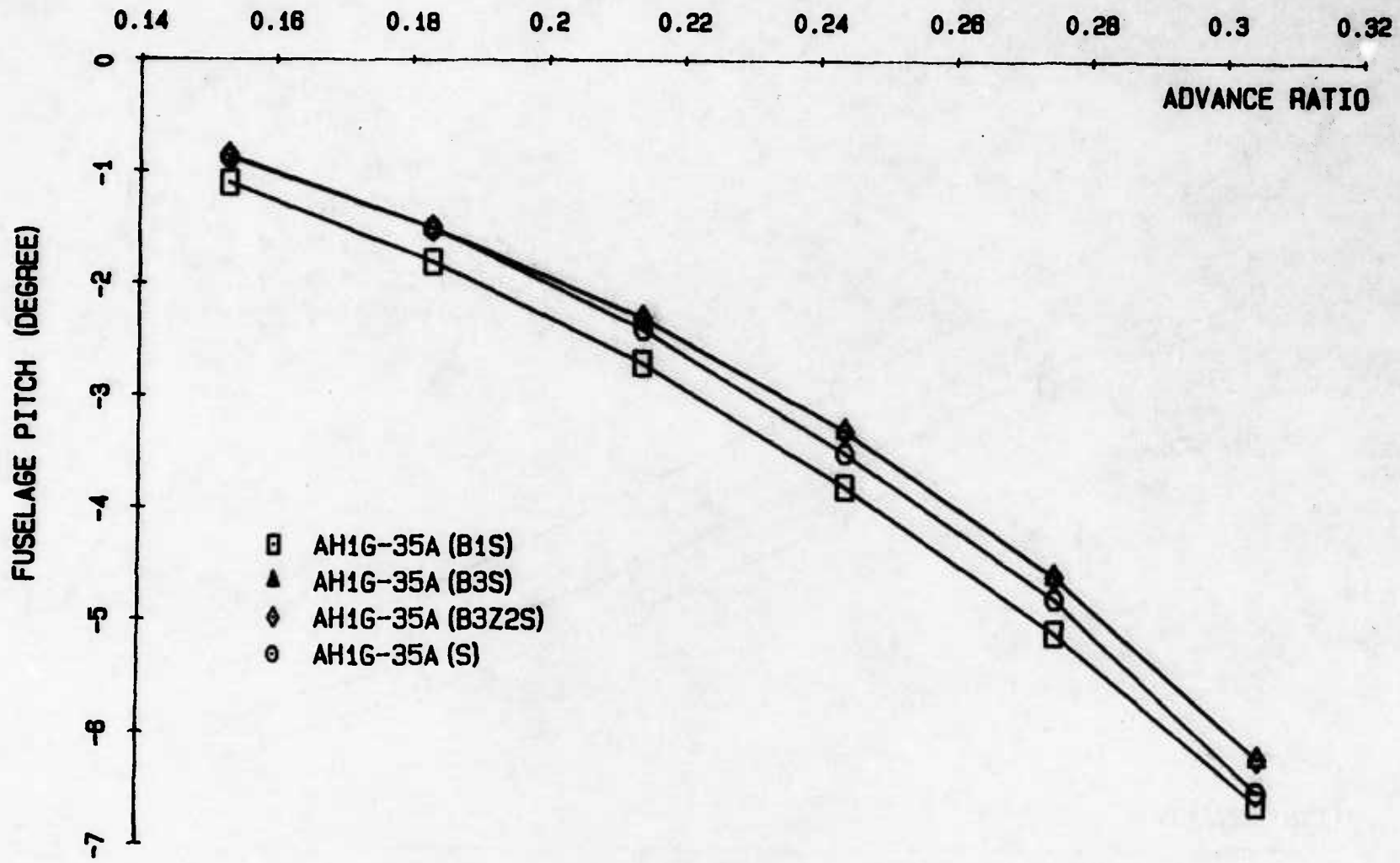

Figure 15d. Degree of Freedom Effect on Trim - Flight 35A Simulation, Fuselage Pitch Angle vs Advance Ratio

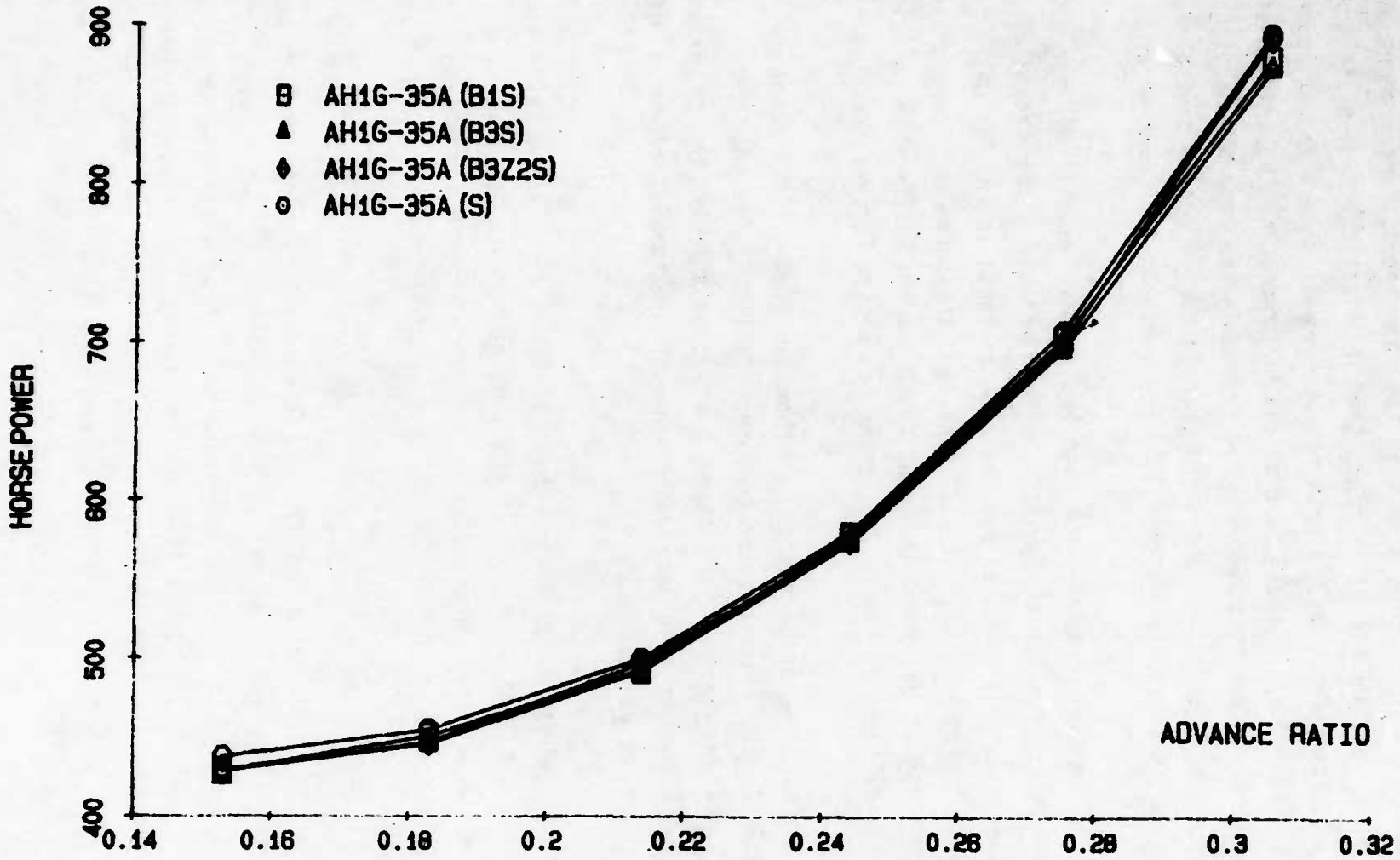

Figure 15e. Degree of Freedom Effect on Trim - Flight 35A Simulation, Horsepower vs Advance Ratio.

in-plane modes have negligible effect on the rotor performance (compare triangle and diamond). On the other hand, the two elastic out-of-plane bending modes have moderate effect on the trim result (compare square and triangle). Despite the differences in these four models in predicting the trim position, it is interesting to see that they require virtually the same amount of horsepower as shown in Figure 15e. The difference in cyclic cosine control angles for various models as shown in Figure 15b, however, requires further study.

The comparison between measured and computed results associated with flight 36A is shown in Figures 16a through 16e. The meanings of the triangle, diamond, and circle in these figures are the same as those in the AH-1G-35A case. As can be seen in Figures 16a, 16c, 16d, and 16e, the agreement among measured and computed results is generally good. Again, the difference in cyclic cosine angles, as shown in Figure 16b, seems to require further investigation.

Four DYSCO models have been created, as shown in Figures 10 through 13. In the model ELAST2, the elastic rotor component B1Z1T1 is assigned three rigid body modes, one for each of the three blade physical degrees of freedom. Therefore, ELAST2 can be used for comparison with the results of model RIGIT2 to achieve a limited validation.

It can also be seen in these figures that the three aeroelastic rotor models ELAST0, ELAST2, and ELAST3 consist of the same components and forces, except for the rotor aerodynamic force module. So, the difference among different aerodynamic algorithms in DYSCO can be observed from the results for these three models.

As can be seen in Figures 17a through 17e, the results for models ELAST2 and RIGIT2 are in good agreement as far as the control positions, fuselage pitch angle, and horsepower consumption are concerned. Figure 17 also shows that the results for FRAØ, FRA2, and FRA3 are reasonably close, except that the horsepower computed for FRA3 is considerably higher than for FRA2 and FRAØ. This may be due to the three-dimensional yaw flow correction and different inflow algorithm of FRA3.

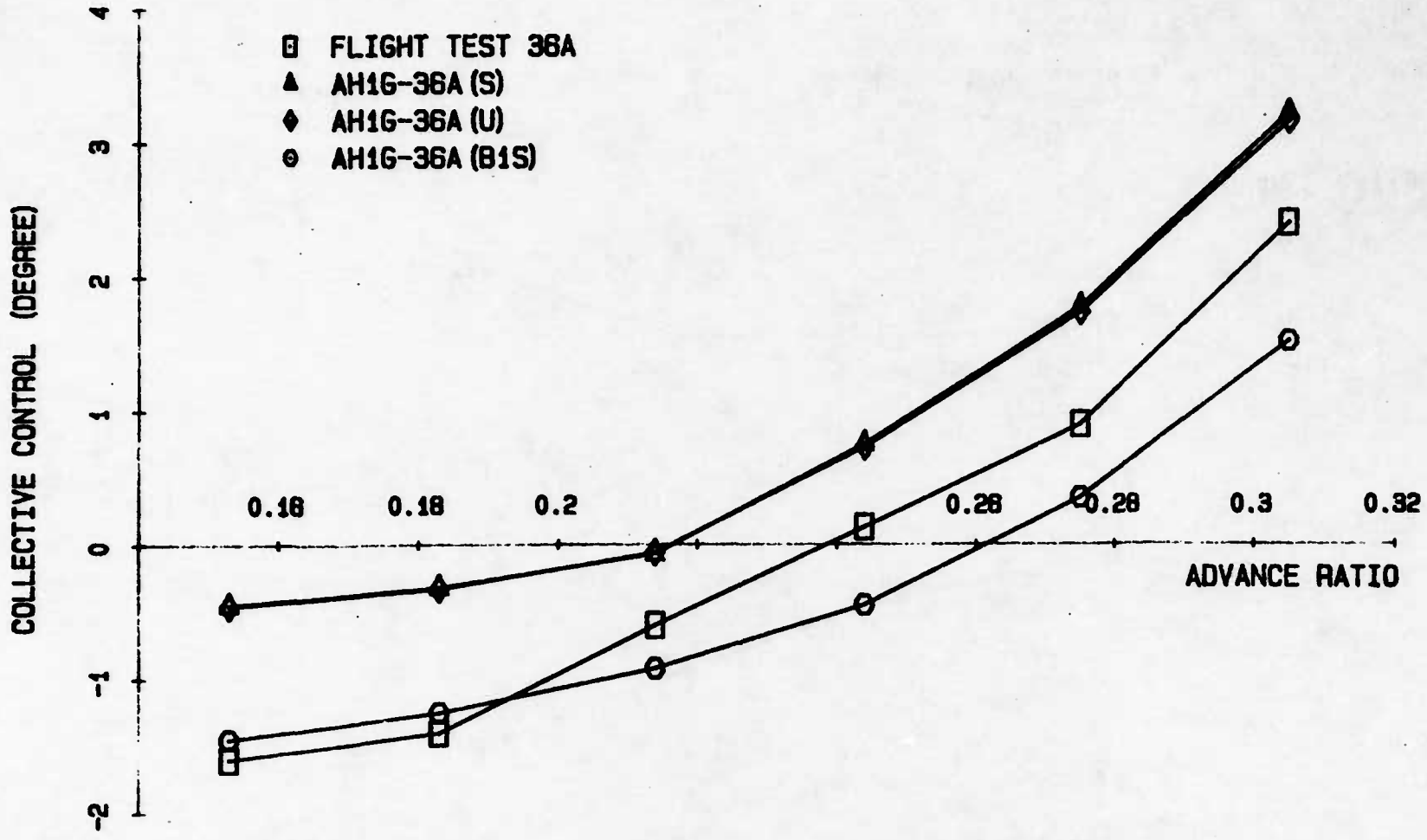

Figure 16a. Comparison Between Flight 36A and DYSCO Simulation, Collective Control vs Advance Ratio.

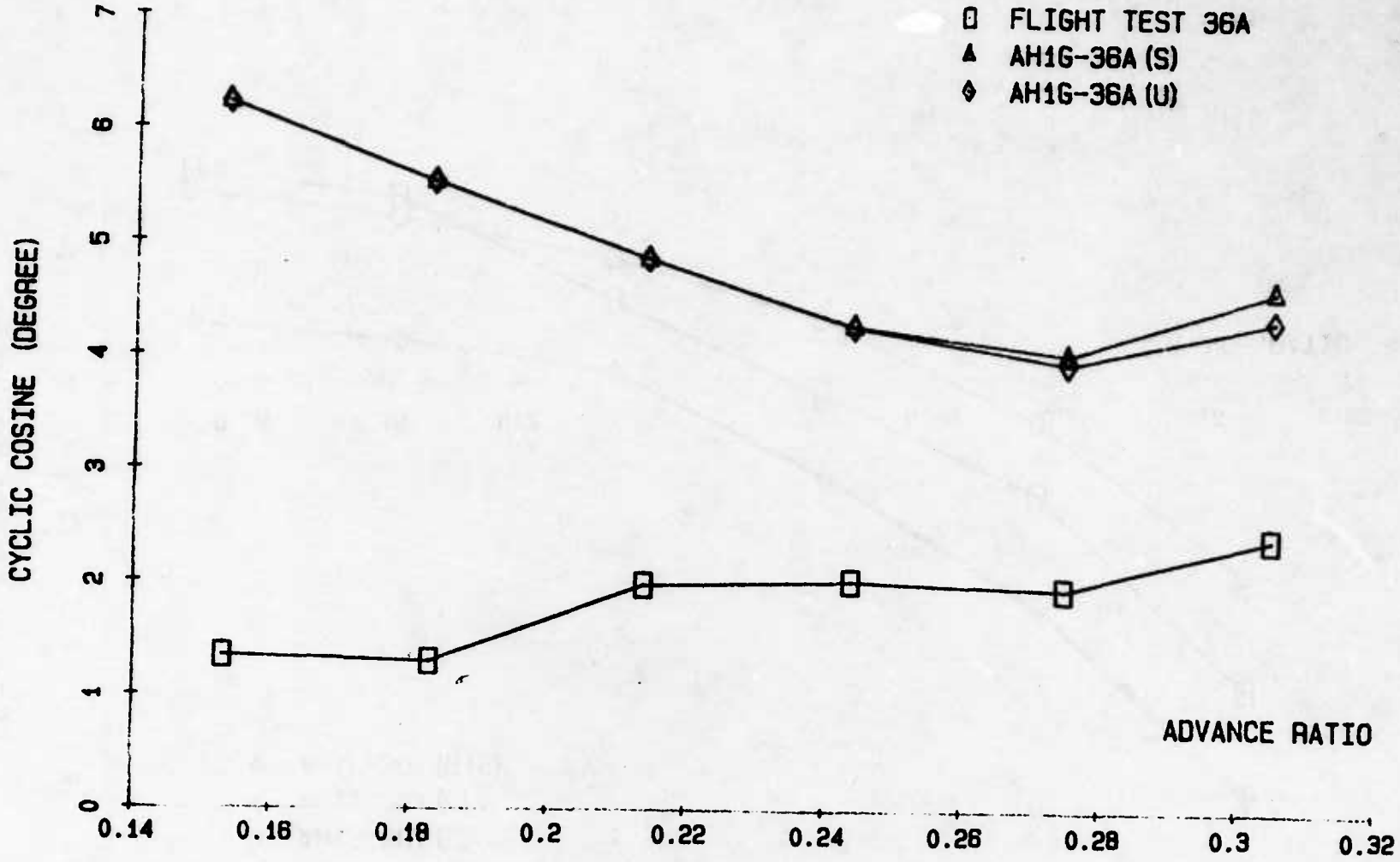

Figure 16b. Comparison Between Flight 36A and DYSCO Simulation, Cyclic Cosine Control vs Advance Ratio.

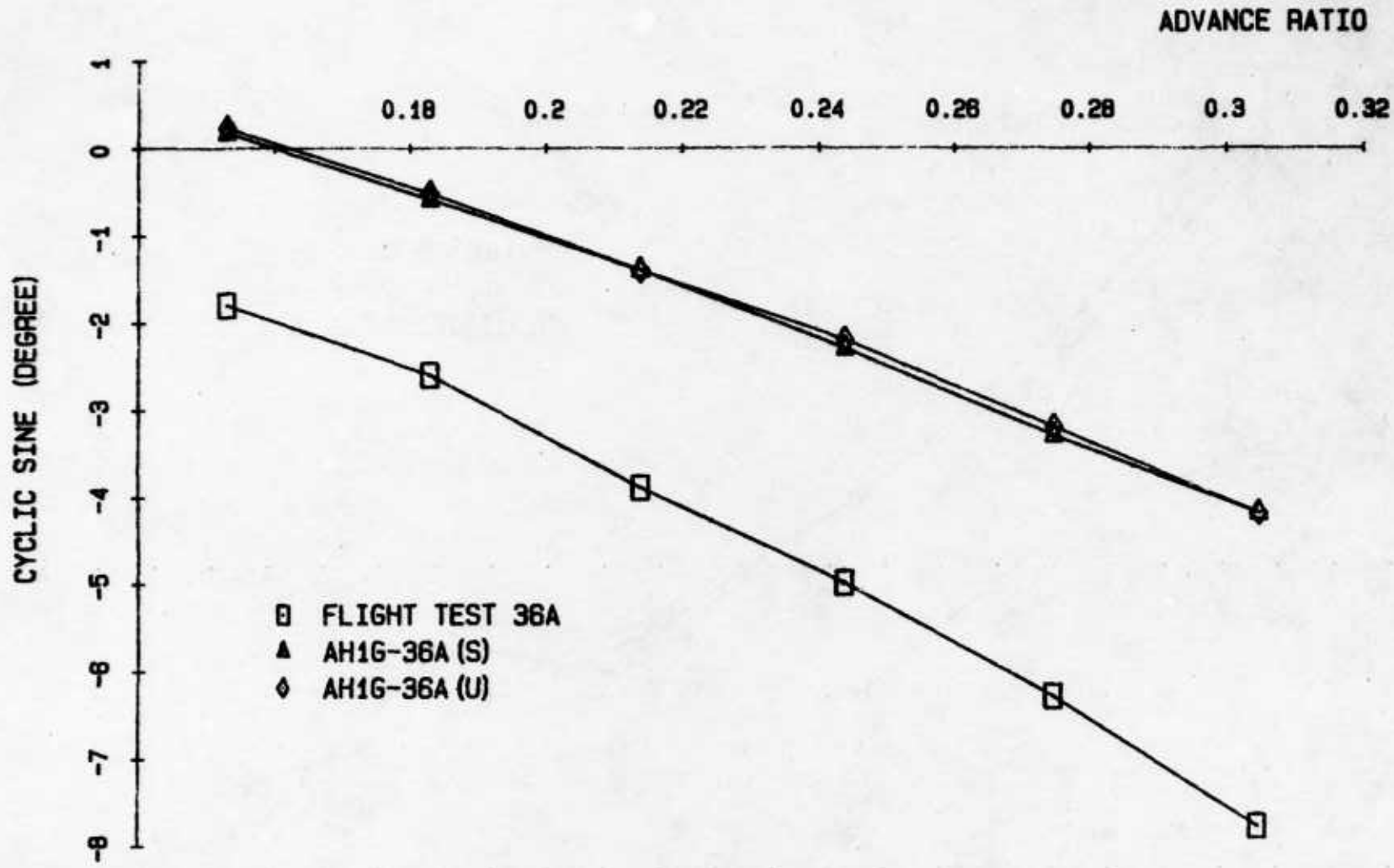

Figure 16c. Comparison Between Flight 36A and DYSCO Simulation, Cyclic Sine Control vs Advance Ratio.

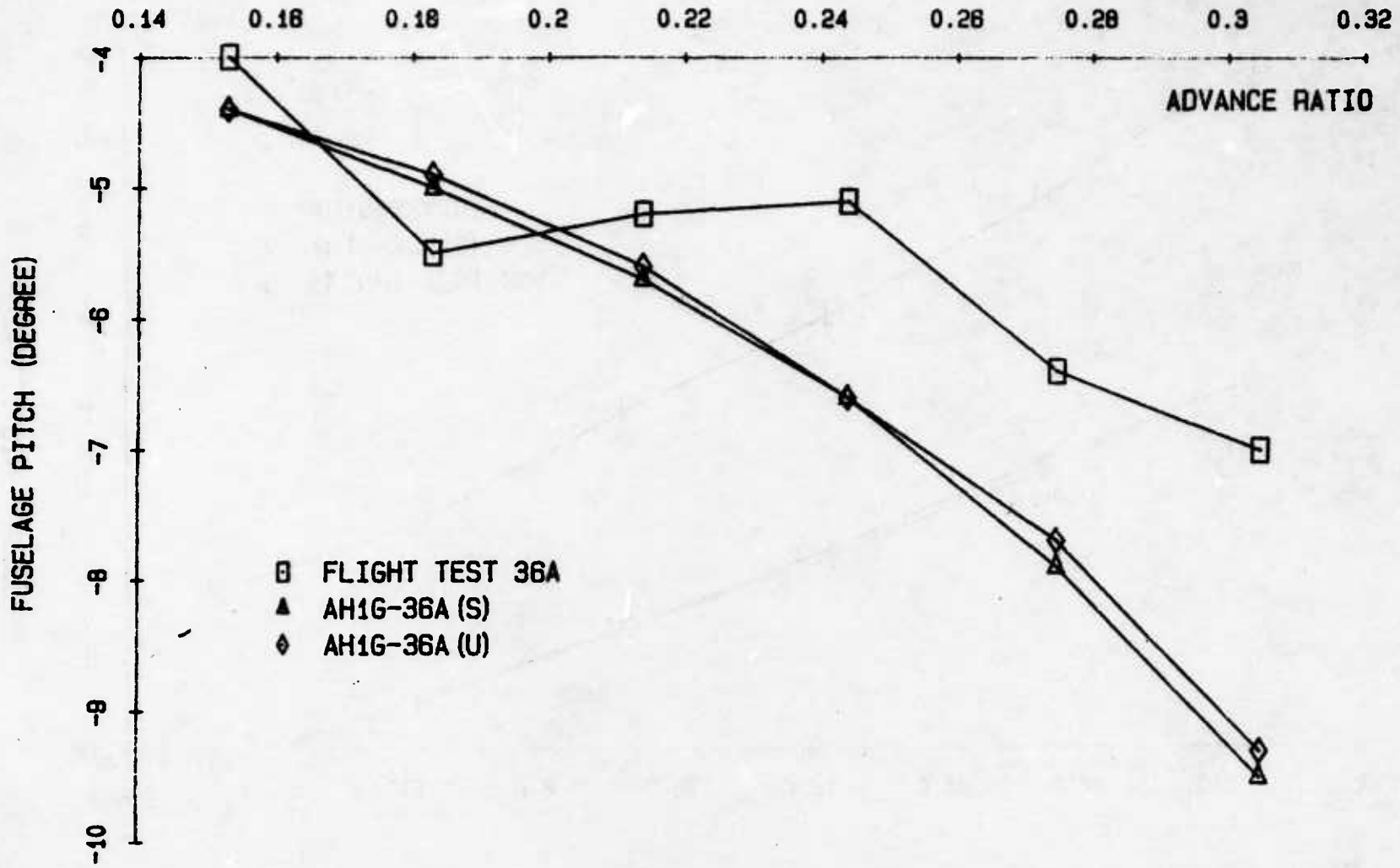

Figure 16d. Comparison Between Flight 36A and DYSCO Simulation, Fuselage Angle vs Advance Ratio.

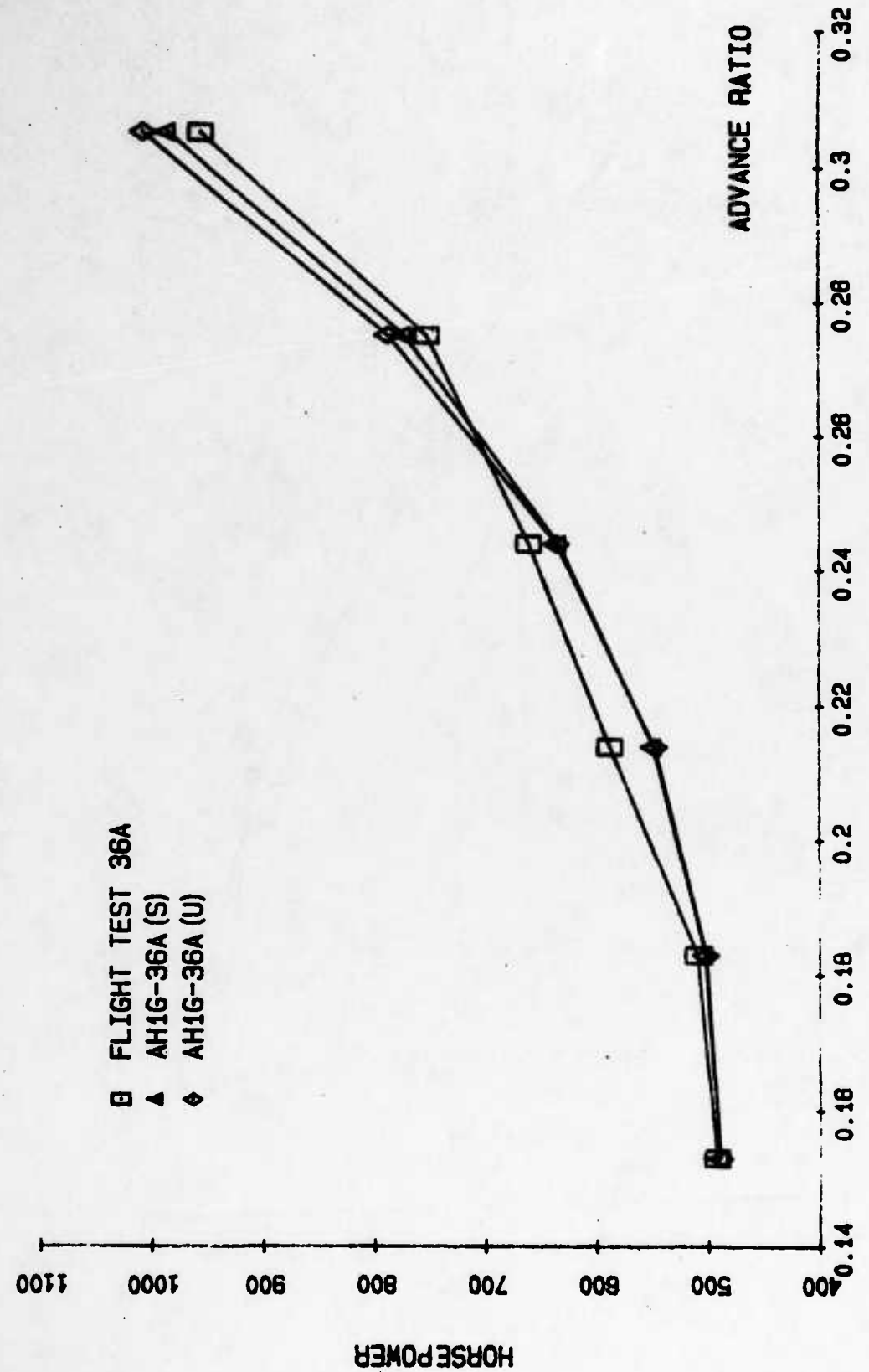

Figure 16e. Comparison Between Flight 36A and DYSCO Simulation, Horsepower vs Advance Ratio.

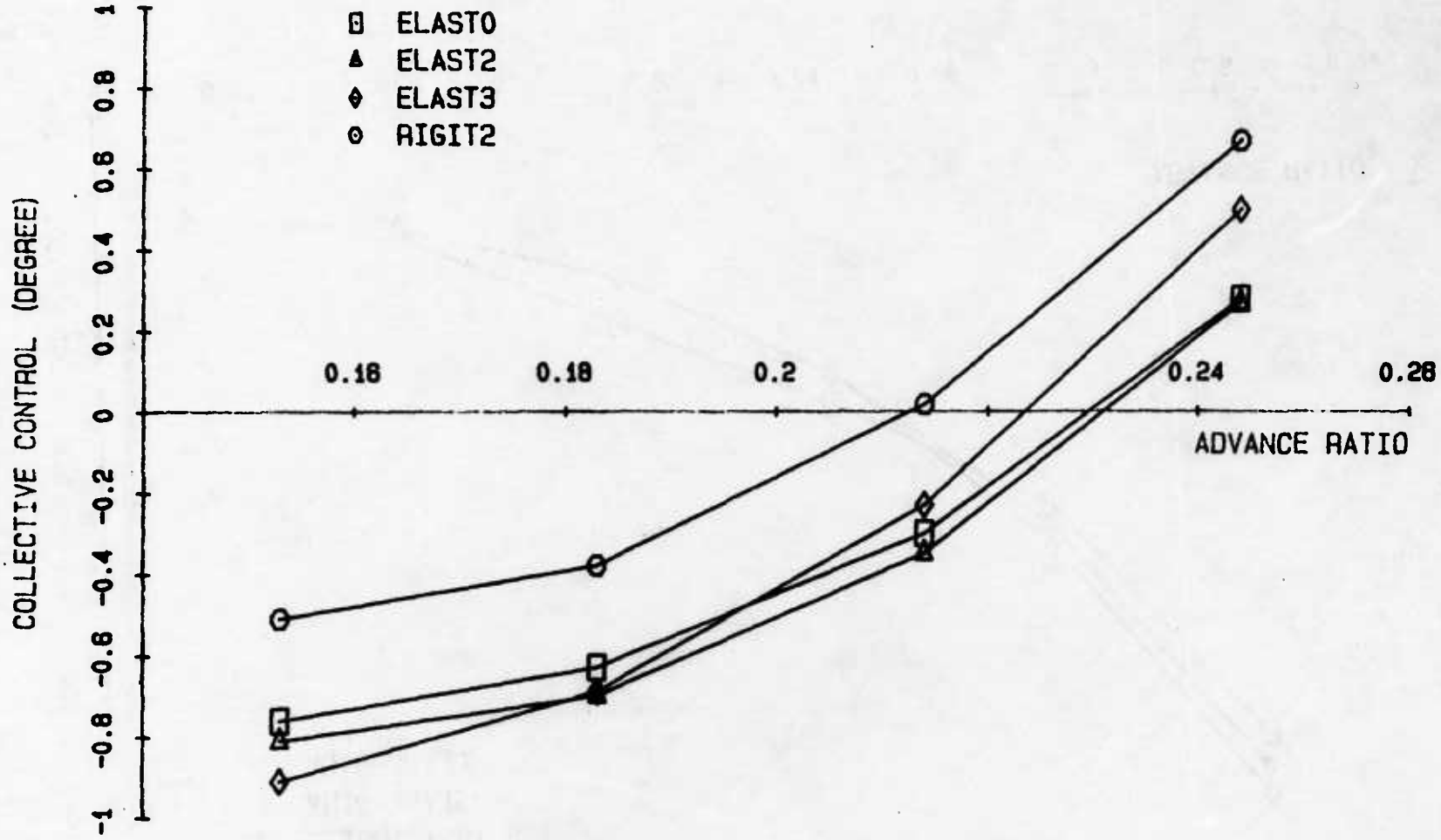

Figure 17a. Effect of Rotor - Aerodynamics Combinations on Trim, Collective Control vs Advance Ratio.

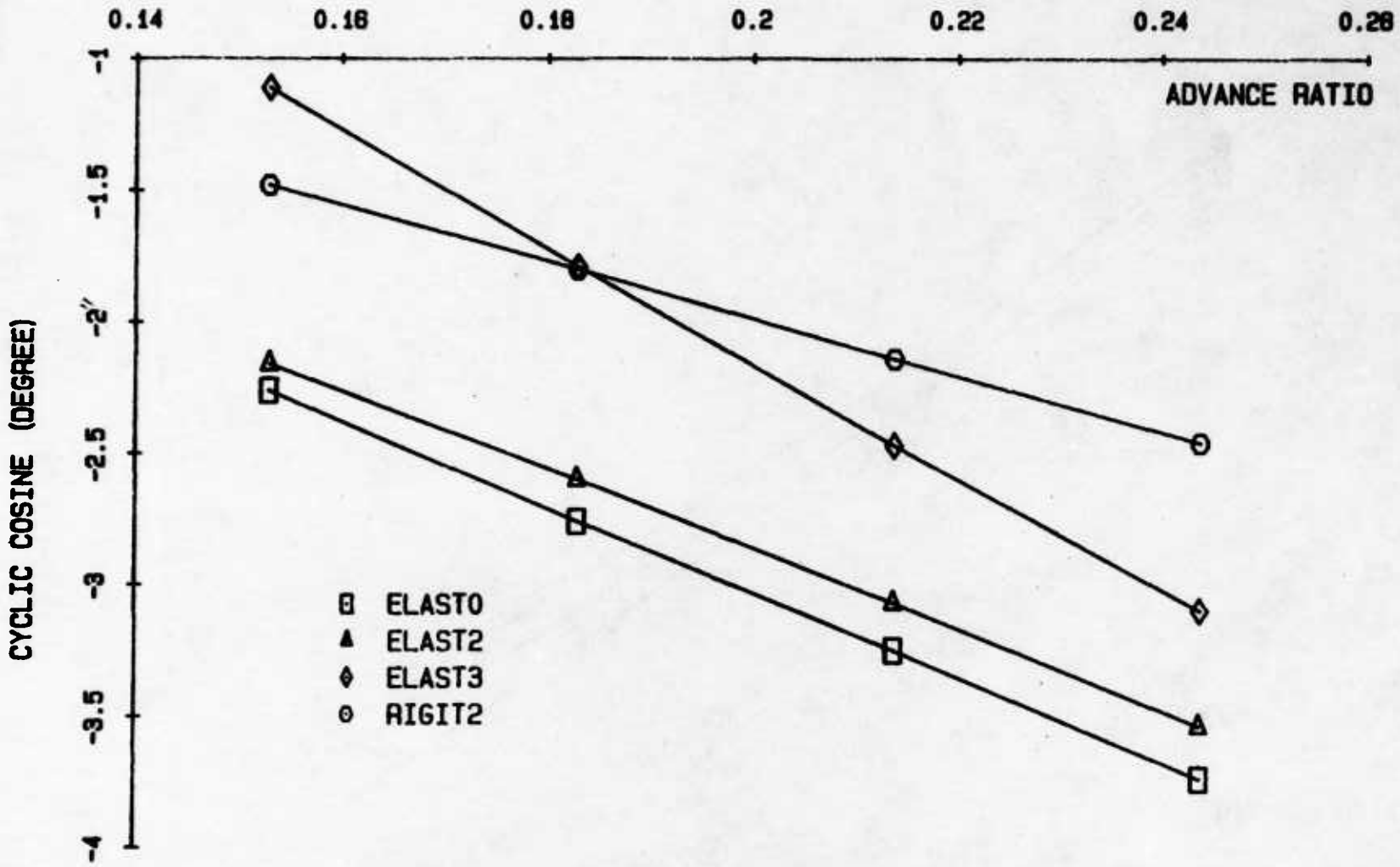

Figure 17b. Effect of Rotor - Aerodynamics Combinations on Trim, Cyclic Cosine Control vs Advance Ratio.

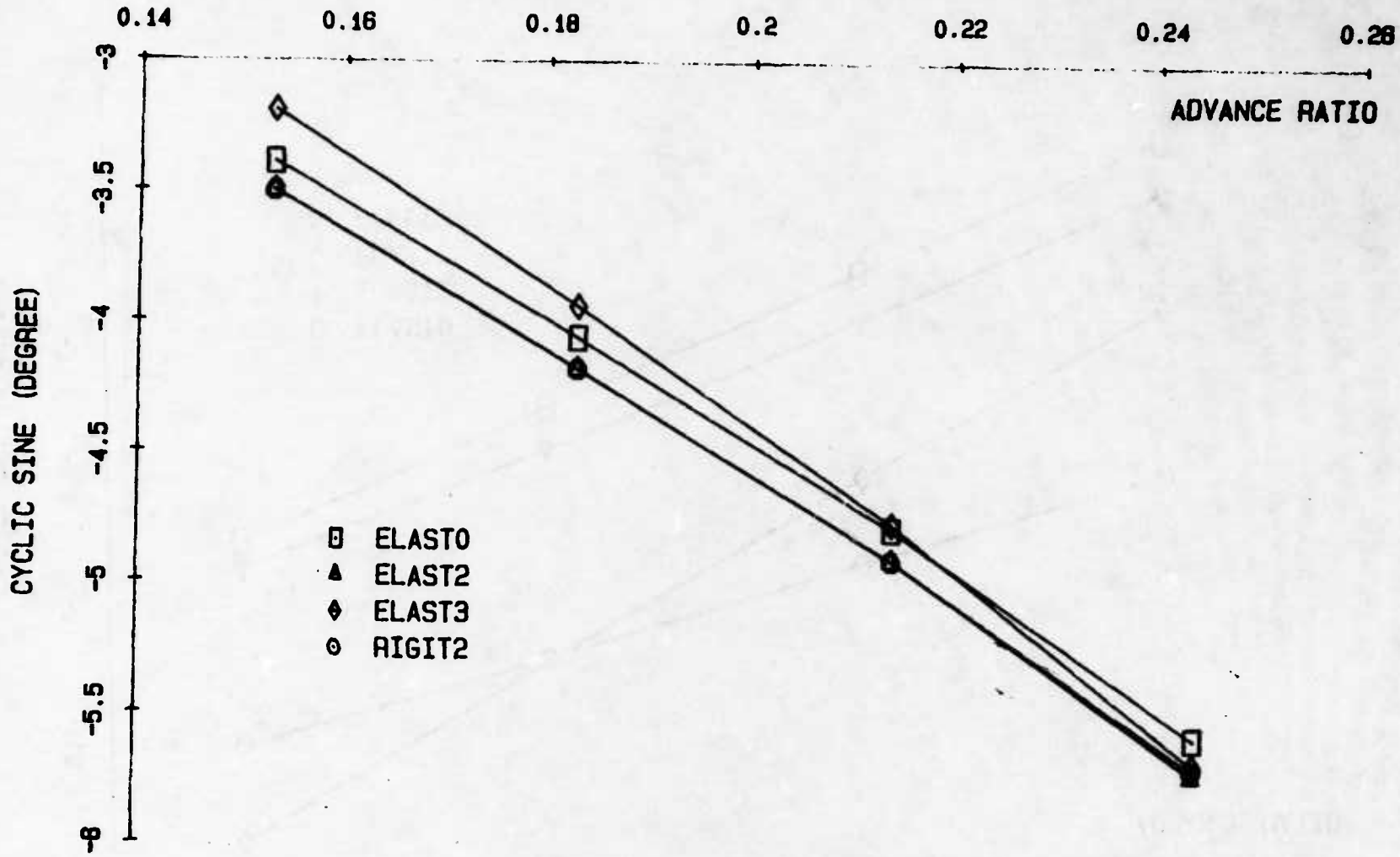

Figure 17c. Effect of Rotor - Aerodynamics Combinations on Trim, Cyclic Sine Control vs Advance Ratio.

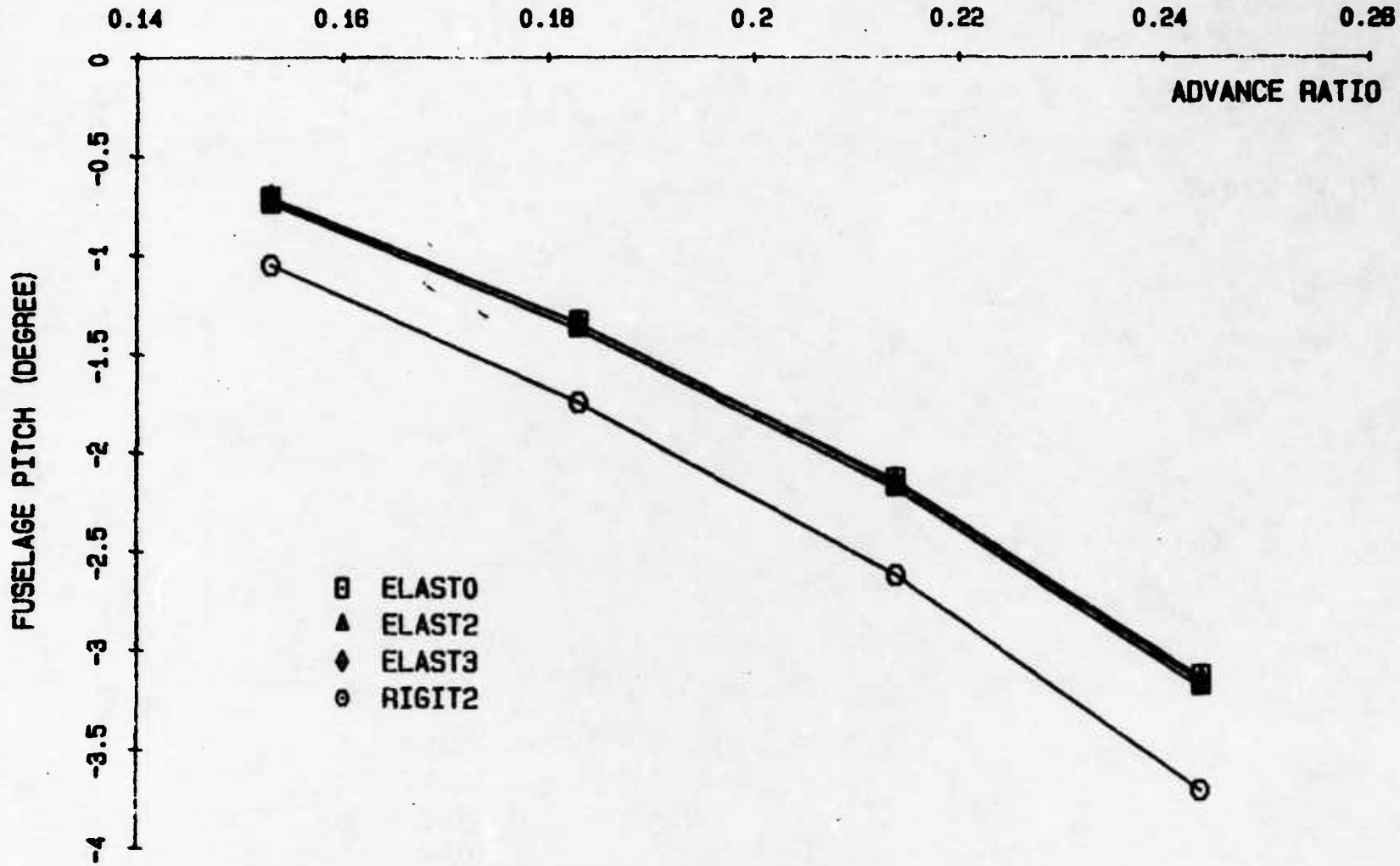

Figure 17d. Effect of Rotor - Aerodynamics Combinations on Trim, Fuselage Pitch Angle vs Advance Ratio.

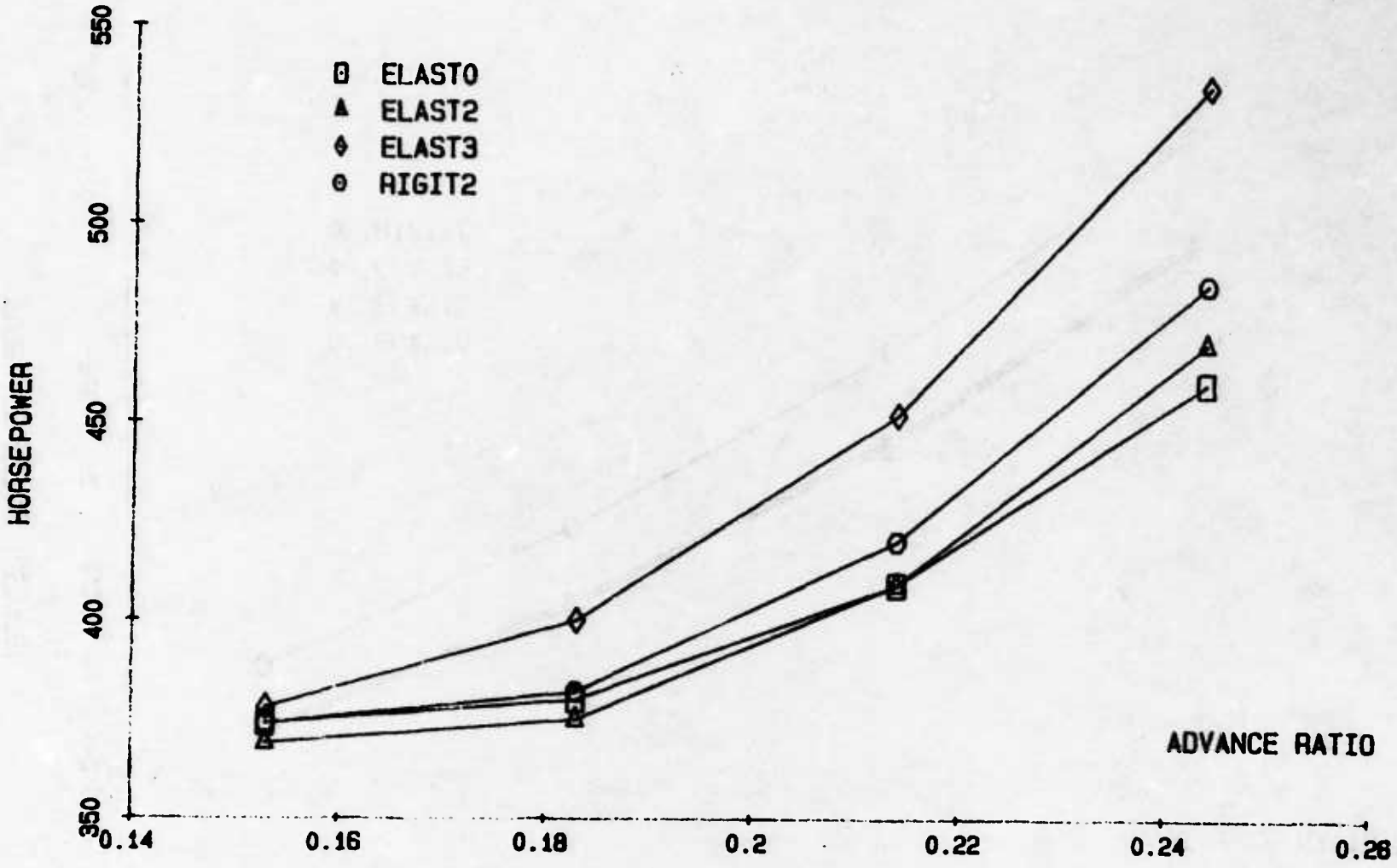

Figure 17e. Effect of Rotor - Aerodynamics Combinations on Trim, Horsepower vs Advance Ratio.

5.0 REFERENCES

1. Houbolt, J.C., and Brooks, G.W., "Differential Equations of Motion for Combined Flapwise Bending, Chordwise Bending, and Torsion of Twisted Nonuniform Rotor Blades," Report 1346, National Advisory Committee for Aeronautics, Langley Aeronautical Laboratory, Langley Field, Virginia, 1958.

2. Hodges, D.H., and Dowell, E.H., "Nonlinear Equations of Motion for the Elastic Bending and Torsion of Twisted Nonuniform Rotor Blades," NASA TN D-7818, National Aeronautics and Space Administration, Washington, D.C., December 1974.

3. Berman, A., Giansante, N., and Flannelly, W.G., "Rotor Dynamic Simulation and System Identification Methods for Application of Vacuum Whirl Data," NASA CR159356, National Aeronautics and Space Administration, Langley Research Center, Hampton, Virginia, September 1980.

4. Bailey, C.D., "A New Look at Hamilton's Principle," Foundations of Physics, Vol. 5, No. 3, 1975.

5. Baruch, M., and Riff, R., "Hamilton's Principle, Hamilton's Law - 6 Correct Formulations," AIAA Journal, 5 May 1982.

6. Peters, D.A., and Ormiston, R.A., "Flapping Response Characteristics of Hingeless Rotor Blades by a Generalized Harmonic Balance Method," NASA, TN D-7856, 1975.

7. McLarty, Tyce T., "Rotorcraft Flight Simulation with Coupled Rotor Aeroelastic Stability Analysis," Bell Helicopter Textron, USAAMRDL-TR-76-41 A and B, Applied Technology Laboratory, U.S. Army Research and Technology Laboratories, Fort Eustis, Virginia, May 1976, AD A042462 and A042908.

8. Livingston, C.L., "Rotor Induced Velocity," Bell Helicopter Company IOM 81:CLL:am-838, 7 October 1966.

9. Drees, J.M., "A Theory of Airflow Through Rotors and Its Applications to Some Helicopter Problems," The Journal of the Helicopter Society of Great Britain, Vol. 3, No. 2, 1949.

10. Carta, F.O., Casellini, L.M., Arcidiacono, P.J., and Elman, H.L., "Analytical Study of Helicopter Rotor Stall Flutter," paper presented at the 26th Annual National Forum of the American Helicopter Society, Washington, D.C., 1970.

11. Scanlan, R.H., and Rosenbaum, R., "Aircraft Vibration and Flutter," New York, New York, MacMillan Co., 1951.

12. Harris, F.D., Tarzanin, F.J., Jr., and Fisher, R.K., Jr., "Rotor High Speed Performance, Theory vs. Test," Journal of AHS, Volume 15, No. 3, July 1970.

13. Hoerner, S.F., "Fluid Dynamic Drag," New York, New York, published by the author, 1958.

14. Bisplinghoff, R.L., Ashley, H., and Halfman, R.L., "Aeroelasticity," Cambridge, Massachusetts, Addison-Wesley Publishing Company, 1955.

15. Multhopp, H., "Methods of Calculating the Lift Distributions of Wings (Subsonic Lifting Surface Theory)," ARC R & M No. 2884, 1950.

16. Multhopp, H.,"Methods of Calculating the Lift Distributions of Subsonic Wings," RAE R&M No.2553, 1950.

17. van Spiegel, E., and Wouters, J. G., "Modification of Multhopp's Lifting Surface Theory with a View to Automatic Computation," NLR Report NLR-TNW.2 (Amsterdam), June 1962.

18. Lamar, J. E., "A Modified Multhopp Approach for Predicting Lifting Pressures and Camber Shape for Composite Planforms in Subsonic Flow," NASA TN D-4427.

19. Ralston and Wilf, "Mathematical Methods for Digital Computers," New York, London, John Wiley and Sons, 1960, pp. 110 - 120.

20. Meirovitch, L., "Analytical Methods in Vibration," New York, The MacMillan Company, 1961, pp. 410 - 412.

21. Moller, C. B., and Stewart, G. W., "An Algorithm for Generalized Matrix Eigenvalue Problems," Siam Journal of Numerical Analysis, No. 10, 1973, pp. 241 - 256.

22. Shockey, G. A., et al., "AH-1G Helicopter Aerodynamic and Structural Loads Survey," Bell Helicopter Textron, USAAMRDL-TR-76-39, Applied Technology Laboratory, U.S. Army Research and Technology Laboratories, Fort Eustis, Virginia, February 1977, AD A036910.

23. Van Gaasbeek, J.R., "Validation of the Rotorcraft Flight Simulation Program (C81) Using Operational Loads Survey Flight Test Data," Bell Helicopter Textron, USAAVRADCOM-TR-80-D-4, Applied Technology Laboratory, U.S. Army Research and Technology Laboratories (AVRADCOM), July 1980, AD A089008.

24. Peters, D.A., and Izadpanah, A.P., "Helicopter Trim by Periodic Shooting with Newton-Raphson Iteration," 37th Annual Forum Proceedings of AHS, May 17 - 20, 1981, New Orleans, Louisiana.

6.0 LIST OF SYMBOLS

a	Distance from midchord to the elastic axis divided by semichord; also lift curve slope
A	Blade cross-sectional area
b	Semichord
B	Rotating coordinate system; also tip loss coefficient
B_1	Rotating coordinate system
B_1^*, B_2^*, C_1, C^*	Blade cross-sectional integrals
c	Blade chord
C_B	Modified thrust coefficient
C_L, C_D, C_M	Blade aerodynamic lift, drag, and pitching moment coefficients
C_{D_N}, C_{D_R}	Blade drag coefficient in the normal and radial directions, respectively
C_T	Thrust coefficient
C_{X_H}, C_{Y_H}, C_{Z_H}, C_{α_x}, C_{α_y}, C_{α_z}	Effective hub damping coefficients
e	Mass centroid offset from elastic axis (positive when centroid is forward)
$\bar{e}$	Hinge offset
e_A	Area centroid offset from elastic axis (positive when centroid is forward)
e_F, e_L	Flap and lag hinge offsets
E	Young's modulus
E_1	$= e_A\, EA\, K_A^2 - EB_2^*$

E_v	Effective in-plane stiffness $= - EA\, e_A^2 \cos\theta + EI_{z'} - (EI_{z'} - EI_{y'}) \sin^2\theta$
E_{vw}, E_{wv}	Coupling stiffness between in-plane and out-of-plane bending $= (EI_{z'} - EI_{y'}) \sin\theta \cos\theta - EA\, e_A^2 \sin\theta$
E_w	Effective out-of-plane stiffness $= - EA\, e_A^2 \sin\theta + EI_{y'} + (EI_{z'} - EI_{y'}) \sin^2\theta$
E_ϕ	Effective torsional stiffness $= GJ + EB_1^* \theta'^2 + K_A^2 T^* - EA\, K_A^4 \theta'^2$
F_N	Induced velocity distribution function
G	Shear modulus
$\vec{i}$, $\vec{j}$, $\vec{k}$	Unit vectors associated with B coordinate system
$I_{y'}$, $I_{z'}$	Blade cross section moment of inertia from y' and z' axes
I_{α_x}, I_{α_y}, I_{α_z}	Effective moments of inertia of hub
J	Torsional rigidity constant
K_A	Area radius of gyration of blade cross section
K_F, K_L, K_ϕ	Blade flap, lag, and pitch spring rate
K_m, K_{m1}, K_{m2}	Mass radius of gyration of blade cross section, polar, from chord, from axis through c.g. perpendicular to chord
K_{X_H}, K_{Y_H}, K_{Z_H}, K_{α_x}, K_{α_y}, K_{α_z}	Effective stiffness of hub
L_u, L_v, L_w, L_{X_H}, L_{Y_H}, L_{Z_H}	Generalized forces applied to blade and hub translational degrees of freedom

m	Blade mass per unit length
M	Mach number
M_{eff}	Effective Mach number
M_{X_H}, M_{Y_H}, M_{Z_H}	Effective hub masses
$M_{y'}$, $M_{z'}$	Bending moment about y′ and z′ axes
M_ϕ, M_{α_x}, M_{α_y}, M_{α_z}, M_{ψ_s}	Generalized applied moments in blade rotational degrees of freedom
p	$= m e \sin \theta$
$P_{x'}$	Warp term in strain energy expression
q	$= m e \cos \theta$
q_i	Generalized degree of freedom
r	Distance along the deformed elastic axis
R	Blade radius; also inertia frame
$S_{x'}$	Twisting moment from shear stress
t	Time; also blade thickness
T	Tension; also kinetic energy
$[T]$	Transformation matrix
T^*	$= \Omega^2 \tau$
$T_{x'}$	Twisting moment from longitudinal stress
u, v, w	Elastic displacements in x, y, z directions
U	Strain energy; also velocity of flow perpendicular to airfoil leading edge
U_T, U_P, U_R	Tangential, vertical, radial velocity components of the air relative to the blade
$\vec{V}_B$	Total velocity of a blade element

$\vec{V}_{OB}$	Velocity of the origin of frame B
V_{sound}	Sound velocity
V_x, V_y, V_z	Components of total velocity of a blade element in B frame
$V_{x'}$	Axial force in the x′ direction
x, y, z	Rotating, undeformed blade coordinate system
x′, y′, z′	Blade fixed coordinate system
x_1, y_1, z_1	Coordinate of a point in the deformed blade
X, Y, Z	Inertia coordinate system
X_h	Hub extent divided by rotor radius
X_H, Y_H, Z_H	Hub translational degrees of freedom
X_u, X_v, $X_{v'}$, X_w, $X_{w'}$, X_ϕ, $X_{\phi'}$, X_{ψ_s}, X_{X_H}, X_{Y_H}, X_{Z_H}, X_{α_x}, X_{α_y}, X_{α_z}	Concise forms for writing the kinetic energy expressions
y_i, z_j, ϕ_k	Generalized coordinates, amplitudes of ith in-plane, jth out-of-plane, and kth torsion modes in Raleigh-Rite/Galerkin method (functions of time only)
Y_i, Z_j, Φ_k	Modal functions used in Raleigh-Rite/Galerkin method (functions of x only)
$Y_{u'}$, $Y_{v'}$, $Y_{v''}$, $Y_{w'}$, $Y_{w''}$, Y_ϕ, $Y_{\phi'}$, $Y_{\phi''}$	Concise forms for writing the potential energy expressions

α	Angle of attack
α_{mod}	Modified angle of attack
α_{RD}	Reference angle of attack for drag
α_{RL}	Reference angle of attack for lift
α_x, α_y, α_z	Hub rotational degrees of freedom
β_{Pc}	Precone angle
$\delta( )$	Variation of ( )
δW	Virtual work of the external forces
ΔC_L, ΔC_M	Increment in lift and moment coefficient due to unsteady aerodynamic effect
ΔE	$= EI_{z'} - EI_{y'} - e_A^2 EA$
ΔK	$= K_{m_2}^2 - K_{m_1}^2$
ϵ	Small parameter
ζ, η	Principal axes of local cross section of blade
$\hat{\zeta}$	$= \zeta + \frac{\partial \lambda}{\partial \eta}$
$\hat{\eta}$	$= \eta - \frac{\partial \lambda}{\partial \zeta}$
θ	Built-in twist
λ	Warp function; also inflow ratio
Λ	Yaw flow angle
μ	Advance ratio
ν	Induced velocity across the rotor disk
$\bar{\nu}$	Averaged induced velocity

$\bar{\nu}^*$	Averaged induced velocity with ground effect
$\vec{\rho}$	Position vector of a deformed blade element in the B frame
σ_{xx}, $\sigma_{x\zeta}$, $\sigma_{x\eta}$	Tensor stress components
τ	Centrifugal tension integral $\int_x^R mx\, dx$
ϕ	Elastic twist about elastic axis
ϕ_A	Inflow angle
ψ	Blade azimuth
ψ_s	Shaft speed perturbation coordinate
$\vec{\omega}_B$	Rotational velocity vector of B frame
Ω	Blade rotational speed
Ω_x, Ω_y, Ω_z	Components of hub angular velocity in B system
$(\,)'$	$= \frac{\partial}{\partial x}(\,)$
$(\dot{})$	$= \frac{\partial}{\partial t}(\,)$

APPENDIX

C81 INPUT PARAMETERS FOR FLIGHT 35A (CLEAN WING, 8320-LB GROSS WEIGHT, AFT C.G.)

BELL HELICOPTER COMPANY ROTORCRAFT FLIGHT SIMULATION PROGRAM AGAJ7407 COMPUTED 10/27/76

AH-1G WITH INSTRUMENTED MAIN ROTOR
FLIGHT 35A 83.00 . 200.0
LEVEL FLIGHT SPEED SWEEP

INPUT DATA

PROGRAM LOGIC GROUP

0	1	0	0	0	2	0	1	-1	3	0	0	0	0
0	1	1	1	2	1	1	0	0	0	1	0	0	0
0	0	0	0	0	0	1	1	0	0	0	0	0	0

FUSELAGE GROUP

8320.000	200.0000	0.0	71.20000	200.0000	0.0	71.00000
2800.000	12500.00	11000.00	947.0000	0.0	15.00000	35.00000
-4.113799	0.0	0.0	0.0	0.0	0.0	-0.1049200E-01
0.1794500E-01	0.2734770	-0.1970000E-02	0.7104990E-03	0.9902999E-02	-0.1530000E-03	0.3050000E-03
5.500000	0.0	150.1000	84.70000	0.0	0.0	-0.2098200E-01
0.4341300E-01	-0.7022095E-01	-0.1970000E-03	0.5780000E-03	0.1200100E-01	0.1000000E-04	0.6599999E-04
-0.990600	0.0	0.0	0.0	300.0000	0.0	0.4389170
-0.7099095E-01	4.849097	0.1390000E-01	-0.8010000E-02	-0.7051300E-01	0.1731000E-02	-0.3101000E-02
0.0	11.76000	45.00000	0.3995340	0.4357100E-01	0.4109999E-03	-0.3099999E-04
1.638453	0.4149800E-01	0.2351000E-02	-0.3571000E-02	-0.2709997E-03	0.2991499E-02	-0.4799999E-04
0.0	-140.0000	45.00000	0.5394999E-02	-0.2259979	-0.1299700E-01	0.8119999E-03
-4.299999	-0.4850000E-01	-0.4200000E-02	0.3611000E-02	-0.8599999E-04	-0.4042000E-02	-0.2020000E-03
600.0000	0.0	0.0	-4.757113	0.8993799E-01	0.7994000E-02	-0.1040000E-02
13.99182	0.1234000E-02	-0.3040000E-02	0.1731300F-01	0.2310000E-02	-0.3025000E-02	-0.1040000E-03
0.0	0.0	0.0	0.0	0.0	0.0	0.0
0.0	0.0	0.0	0.0	0.0	0.0	0.0

RTR AERODYNAMIC GROUP

0.8400000	1.270000.	1.299999	-0.7000000	0.0	0.0	0.7000000
0.9499997E-01	0.0	0.4750000E-01	0.0	0.9999999E-02	0.0	0.3000000E-04
0.4000000E-01	0.3400000	0.9333329E-01	1.000000	0.0	1.000000	0.5000000
0.0	0.0	0.0	0.0	0.0	0.0	0.0
0.0	0.0	0.0	0.0	0.0	0.2500000E-02	0.0
0.8400000	1.270000	1.299999	-0.7000000	0.0	0.0	0.7000000
0.9499997E-01	0.0	0.4750000E-01	0.0	0.9999999E-02	0.0	0.3000000E-04
0.4000000E-01	0.3400000	0.8999997E-01	0.0	0.0	0.0	0.0
0.0	0.0	0.0	0.0	0.0	0.0	0.0
0.0	0.0	0.0	0.0	0.0	0.0	0.0

MAIN ROTOR GROUP

4.000000	4.500000	0.0	22.00000	24.02500	-10.00000	12.00000
206.0000	0.0	157.0200	475.0000	1411.600	0.4910000E-01	0.0
3.000000	0.0	10000.00	0.0	1.000000	0.0	3.400000
2.750000	0.0	0.0	0.0	0.0	0.0	0.0
0.0	0.0	-9.066999	20.39999	0.0	0.0	0.0
0.0	200.0000	0.0	1520.0200	4.000000	-0.2500000	0.0
0.0	0.0	0.0	0.0	0.0	0.0	0.0
42.32399	39.17499	5244.0498	0.7149999	-1.122199	0.0	0.0
107.0640	60.78299	4701.055	5.322000	0.0	-1.122199	0.0

TAIL ROTOR GROUP

2.000000	0.0	0.0	0.2500000	0.4100000	0.0	11.00000
520.7000	-14.85000	118.2700	14.96000	1.399000	0.2509999	0.0
0.0	0.0	10000.00	0.0	1.000000	0.0	0.5000000
1.500000	0.0	30.00000	0.1199999	0.0	0.0	0.2000000
0.0	0.0	0.0	0.0	0.0	0.0	0.0
0.0	0.0	0.0	0.0	0.2500000	0.0	0.4500000
0.0	0.0	90.00000	0.0	0.0	0.0	0.0

WING GROUP

27.79999	192.0000	39.00000	82.00000	14.00000	3.500008	11.00000
3.918000	0.6670000	0.5870000	2.419999	0.0	9.200000	0.0
0.0	0.0	0.0	0.0	0.0	0.0	0.0
0.0	0.0	0.0	0.0	0.0	0.0	0.0
0.5000000	0.5000000	0.0	0.0	0.0	0.0	0.0
0.0	0.0	0.0	0.0	0.0	0.0	0.0
0.8400000	1.250000	1.200000	0.0	0.0	0.0	1.099999
0.1078000	0.0	0.5350000E-01	0.0	0.9999999E-02	0.0	0.3330000E-03
0.0	0.2000000	0.0	0.0	0.0	0.0	0.0
-0.2000000E-02	-0.9000000E-02	0.8200000	0.0	0.0	0.0	0.0

STABILIZER NO. 1 GROUP

7.349999	398.5000	22.06999	56.00000	0.6970470	0.0	14.50000
1.490000	1.367000	0.6600000	0.0	0.0	2.000000	0.0
0.0	0.0	0.0	0.0	0.0	0.0	0.0
0.0	0.0	0.0	0.0	0.0	0.0	0.0
1.500000	0.0	0.0	0.0	0.0	0.0	0.0
0.8400000	1.250000	1.200000	0.0	0.0	0.0	1.200000
0.8699995E-01	0.0	0.4350000E-01	0.0	0.7999999E-02	0.0	0.3329999E-03
0.4000000E-01	0.2000000	0.1500000	0.0	0.3320000E-01	0.0	0.0
-0.2000000E-02	-0.9000000E-02	0.8200000	0.8999999E-01	0.0	0.0	0.0
0.0	0.0	0.0	0.4329350	0.2203640	0.0	0.0
0.0	0.0	0.0	0.0	0.0	0.0	0.0

STABILIZER NO. 2 GROUP

7.349999	398.5000	-22.06999	56.00000	0.6970470	0.0	14.50000
1.490000	1.367000	0.6600000	0.0	0.0	2.000000	0.0
0.0	0.0	0.0	0.0	0.0	0.0	0.0
0.0	0.0	0.0	0.0	0.0	0.0	0.0
1.500000	0.0	0.0	0.0	0.0	0.0	0.0
0.8400000	1.250000	1.200000	0.0	0.0	0.0	1.200000
-0.8699995E-01	0.0	0.4350000E-01	0.0	0.7999999E-02	0.0	0.3329999E-03
0.4000000E-01	0.2000000	0.1500000	0.0	0.3320000E-01	0.0	0.0
-0.2000000E-02	-0.9000000E-02	0.8200000	0.8999999E-01	0.0	0.0	0.0
0.0	0.0	0.0	0.4329350	0.2203640	0.0	0.0
0.0	0.0	0.0	0.0	0.0	0.0	0.0

STABILIZER NO. 3 GROUP

18.59999	201.0000	0.0	56.00000	0.0	40.00000	47.00000
1.359999	0.6670000	0.0	0.0	0.9999999E-01	0.0	0.0
0.0	0.0	0.0	0.0	0.0	0.0	0.0
0.0	0.0	0.0	0.0	0.0	0.1749999	0.2000000E-02
0.0	0.0	0.0	0.0	-40.00000	-20.00000	0.0
0.8400000	1.250000	1.200000	0.0	0.0	0.0	1.200000
0.9999999E-01	0.0	0.4350000E-01	0.0	0.7999999E-02	0.0	0.1370000E-03
0.4000000E-01	0.2000000	0.1500000	0.0	0.3320000E-01	0.0	0.0
-0.2000000E-02	-0.9000000E-02	0.8200000	-0.3000000E-01	0.0	0.0	0.0
0.0	0.0	0.0	0.0	0.0	0.0	0.0
0.0	0.0	0.0	0.0	0.0	0.0	0.0

CONTROLS GROUP

10.00000	9.166659	23.33330	0.0	0.0	0.0	0.0
12.00000	-13.25000	26.66660	0.0	0.0	0.0	0.0
12.00000	-9.366659	16.66663	0.0	0.0	0.0	0.0
5.500000	-10.00000	30.00000	0.0	0.0	0.0	0.0

ITERATION GROUP

41.00000	10.00000	2.000000	0.3000000	0.0	7.000000	0.3000000
0.2000000	0.2000000	1500.000	500.0000	1.000000	0.9999999E-01	2000.000
50.00000	50.00000	50.00000	100.6000	100.0000	100.0000	10.00000

FLIGHT CONSTANTS GROUP

141.8000	0.0	0.0	460.0000	-1.554274	-3.111987	0.0
24.83376	83.72459	39.78268	49.34368	0.0	0.0	0.0
-2.695279	-0.6137535	3.213921	-0.9134431	8025.777	421.8851	0.0
2.000000	0.0	1080.000	6600.000	101.0000	0.8789999	1137.920

MAIN ROTOR AEROELASTIC BLADE DISTRIBUTIONS AND DATA

BLADE STATION NUMBER	WEIGHT (LB/IN)	BEAMWISE INERTIA (IN-LB-SEC**2/IN)	CHORDWISE INERTIA (IN-LB-SEC**2/IN)
1	4.6800	0.0	0.0
2	7.2500	0.0	0.0
3	5.6900	0.0	0.0
4	4.6000	0.0	0.0
5	0.9520	0.0	0.0
6	0.7610	0.0	0.0
7	0.8580	0.0	0.0
8	0.8360	0.0	0.0
9	0.8760	0.0	0.0
10	0.7620	0.0	0.0
11	0.7260	0.0	0.0
12	0.8750	0.0	0.0
13	1.1470	0.0	0.0
14	1.0620	0.0	0.0
15	1.0390	0.0	0.0
16	1.2660	0.0	0.0
17	1.1860	0.0	0.0
18	1.2690	0.0	0.0
19	1.1490	0.0	0.0
20	1.1600	0.0	0.0

TOTAL BLADE WEIGHT = 503.96 LB MAIN TIP WEIGHT = 0.0 LB FLAPPING INERTIA/BLADE = 1657.7 SLUG-FT**2

MAIN ROTOR

MODE SHAPE FOR MODE 1

STA	OUT-OF-PLANE	INPLANE	TORSION
0	0.0	0.0	0.0
1	0.0500	0.0	0.0
2	0.1000	0.0	0.0
3	0.1500	0.0	0.0
4	0.2000	0.0	0.0
5	0.2500	0.0	0.0
6	0.3000	0.0	0.0
7	0.3500	0.0	0.0
8	0.4000	0.0	0.0
9	0.4500	0.0	0.0
10	0.5000	0.0	0.0
11	0.5500	0.0	0.0
12	0.6000	0.0	0.0
13	0.6500	0.0	0.0
14	0.7000	0.0	0.0
15	0.7500	0.0	0.0
16	0.8000	0.0	0.0
17	0.8500	0.0	0.0
18	0.9000	0.0	0.0
19	0.9500	0.0	0.0
20	1.0000	0.0	0.0

MODE SHAPE FOR MODE 2

OUT-OF-PLANE	INPLANE	TORSION
0.0	0.0	0.0
-0.0211	0.0037	0.0
-0.0478	0.0165	0.0
-0.0774	0.0348	0.0
-0.1041	0.0708	0.0
-0.1196	0.1076	0.0
-0.1222	0.1504	0.0
-0.1157	0.1982	0.0
-0.1033	0.2447	0.0
-0.0877	0.3041	0.0
-0.0703	0.3610	0.0
-0.0520	0.4199	0.0
-0.0333	0.4806	0.0
-0.0144	0.5428	0.0
0.0045	0.6062	0.0
0.0233	0.6707	0.0
0.0420	0.7359	0.0
0.0606	0.8016	0.0
0.0791	0.8678	0.0
0.0976	0.9338	0.0
0.1161	1.0000	0.0

MODE SHAPE FOR MODE 3

OUT-OF-PLANE	INPLANE	TORSION
0.0	0.0	0.0
-0.1283	-0.0021	0.0
-0.2286	-0.0095	0.0
-0.3164	-0.0229	0.0
-0.3977	-0.0398	0.0
-0.4686	-0.0567	0.0
-0.5247	-0.0723	0.0
-0.5579	-0.0863	0.0
-0.5726	-0.0984	0.0
-0.5692	-0.1084	0.0
-0.5435	-0.1162	0.0
-0.4947	-0.1217	0.0
-0.4208	-0.1245	0.0
-0.3204	-0.1246	0.0
-0.1945	-0.1220	0.0
-0.0416	-0.1169	0.0
0.1383	-0.1094	0.0
0.3353	-0.0999	0.0
0.5465	-0.0892	0.0
0.7729	-0.0778	0.0
1.0000	-0.0661	0.0

MODE SHAPE FOR MODE 4

STA	OUT-OF-PLANE	INPLANE	TORSION
0	0.0	0.0	0.0
1	0.0219	-0.0007	0.0
2	0.0658	-0.0014	0.0
3	0.1116	-0.0021	0.0
4	0.1588	-0.0027	0.0
5	0.2071	-0.0030	0.0
6	0.2569	-0.0031	0.0
7	0.3078	-0.0030	0.0
8	0.3596	-0.0027	0.0
9	0.4118	-0.0023	0.0
10	0.4645	-0.0019	0.0
11	0.5174	-0.0015	0.0
12	0.5705	-0.0010	0.0
13	0.6238	-0.0005	0.0
14	0.6773	0.0000	0.0
15	0.7306	0.0005	0.0
16	0.7844	0.0011	0.0
17	0.8384	0.0016	0.0
18	0.8922	0.0022	0.0
19	0.9461	0.0027	0.0
20	1.0000	0.0033	0.0

MODE SHAPE FOR MODE 5

OUT-OF-PLANE	INPLANE	TORSION
0.0	0.0	0.0
-0.0624	-0.0184	0.0
-0.1648	-0.0367	0.0
-0.2751	-0.0546	0.0
-0.3754	-0.0714	0.0
-0.4635	-0.0856	0.0
-0.5326	-0.0957	0.0
-0.5807	-0.1016	0.0
-0.6075	-0.1034	0.0
-0.6126	-0.1012	0.0
-0.5968	-0.0950	0.0
-0.5620	-0.0848	0.0
-0.4819	-0.0703	0.0
-0.3831	-0.0516	0.0
-0.2660	-0.0294	0.0
-0.0975	-0.0045	0.0
0.0879	0.0272	0.0
0.2969	0.0596	0.0
0.5231	0.0938	0.0
0.7645	0.1288	0.0
1.0000	0.1634	0.0

MODE SHAPE FOR MODE 6

OUT-OF-PLANE	INPLANE	TORSION
0.0	0.0	0.0
0.1036	0.0351	0.0
0.2432	0.0692	0.0
0.3584	0.1004	0.0
0.4484	0.1274	0.0
0.4857	0.1419	0.0
0.4504	0.1406	0.0
0.3511	0.1255	0.0
0.2045	0.1002	0.0
0.0224	0.0683	0.0
-0.1694	0.0330	0.0
-0.3548	-0.0022	0.0
-0.4884	-0.0340	0.0
-0.5071	-0.0541	0.0
-0.4304	-0.0752	0.0
-0.2618	-0.0808	0.0
-0.0316	-0.0756	0.0
0.1275	-0.0604	0.0
0.2107	-0.0392	0.0
0.2456	-0.0136	0.0
1.0000	0.0136	0.0

MODE NUMBER	1	2	3	4	5	6
MODE TYPE	RIGID BODY	CYCLIC	CYCLIC	COLLECTIVE	COLLECTIVE	COLLECTIVE
DAMPING RATIO	0.0	0.20000E-01	0.20000E-01	0.20000E-01	0.20000E-01	0.20000E-01
GENERALIZED INERTIA	0.21843E 01	0.24894E 01	0.21931E 01	0.24691E 01	0.21867E 01	0.21466E 01
NATURAL FREQUENCY,/REV	0.10000E 01	0.14196E 01	0.26679E 01	0.10429E 01	0.27555E 01	0.46562E 01
LEAD-LAG HINGE DISPLACEMENT,DEG	0.0	0.0	0.0	0.0	0.0	0.0
CHARACTERISTIC COEFFICIENTS AT BLADE ROOT						
BEAM BENDING MOMENT,FT-LB	-0.18750E 00	0.46647E 02	0.44330E 03	0.66200E 04	-0.19041E 05	0.24422E 02
CHORD BENDING MOMENT,FT-LB	0.0	0.13710E 06	-0.78443E 05	0.12320E 01	0.12193E 05	-0.18203E 04
TORSIONAL MOMENT,FT-LB	0.0	0.0	0.0	0.0	0.0	0.0
VERTICAL SHEAR,LB	0.59097E 04	-0.12274E 04	-0.21255E 05	0.57655E 04	-0.21008E 05	0.46699E 05
INPLANE SHEAR,LB	0.0	0.12966E 05	-0.71360E 04	-0.34934E 02	-0.43307E 04	0.16512E 05
MOMENT COEFFICIENTS AT R = 39.60 IN.						
BEAM BENDING MOMENT,FT-LB	-0.14063E 00	-0.60647E 04	0.18704E 05	0.16942E 04	0.77894E 04	-0.47814E 05
CHORD BENDING MOMENT,FT-LB	0.0	0.99429E 05	-0.58152E 05	-0.16021E 03	0.53094E 04	-0.31944E 05
TORSIONAL MOMENT,FT-LB	0.0	0.0	0.0	0.0	0.0	0.0

SUPER 540 EXT*DSUPER 540 EXT*D CLCD DATA TABLES USED

CL

ALPHA/MACH	0.0	0.30000	0.50000	0.60000	0.65000	0.70000	0.75000	0.80000	0.85000	0.90000	1.00000
-180.00000	0.0	0.0	0.0	0.0	0.0	0.0	0.0	0.0	0.0	0.0	0.0
-172.00000	0.78000	0.78000	0.78000	0.78000	0.78000	0.78000	0.78000	0.78000	0.78000	0.78000	0.78000
-161.00000	0.62000	0.62000	0.62000	0.62000	0.62000	0.62000	0.62000	0.62000	0.62000	0.62000	0.62000
-147.00000	1.00000	1.00000	1.00000	1.00000	1.00000	1.00000	1.00000	1.00000	1.00000	1.00000	1.00000
-129.00000	1.00000	1.00000	1.00000	1.00000	1.00000	1.00000	1.00000	1.00000	1.00000	1.00000	1.00000
-49.00000	-1.18000	-1.18000	-1.18000	-1.18000	-1.18000	-1.18000	-1.18000	-1.18000	-1.18000	-1.18000	-1.18000
-39.00000	-1.18000	-1.18000	-1.18000	-1.18000	-1.18000	-1.18000	-1.18000	-1.18000	-1.18000	-1.18000	-1.18000
-21.00000	-0.80000	-0.81000	-0.85000	-0.85000	-0.85000	-0.85000	-0.71500	-0.68000	-0.66400	-0.64000	-0.64100
-18.00000	-0.65600	-0.65600	-0.66200	-0.67000	-0.67000	-0.66400	-0.75400	-0.72200	-0.69800	-0.67000	-0.66400
-14.00000	-1.17000	-1.17000	-0.92800	-0.87100	-0.87200	-0.85300	-0.84100	-0.80100	-0.76700	-0.72600	-0.72600
-12.00000	-1.22000	-1.22000	-0.93500	-0.86700	-0.86700	-0.83900	-0.84000	-0.81800	-0.77800	-0.74000	-0.73700
-11.00000	-1.18000	-1.18000	-0.93400	-0.86200	-0.86000	-0.82900	-0.83200	-0.81200	-0.77700	-0.74000	-0.72600
-10.00000	-1.07000	-1.07000	-0.93000	-0.85300	-0.85400	-0.81500	-0.82000	-0.80300	-0.77000	-0.73400	-0.70500
-9.00000	-0.96800	-0.96800	-0.92000	-0.83800	-0.84000	-0.80500	-0.80100	-0.78100	-0.75200	-0.71800	-0.67200
-8.00000	-0.86000	-0.86000	-0.89000	-0.81300	-0.81900	-0.77600	-0.76000	-0.75300	-0.73000	-0.69000	-0.63200
-7.00000	-0.75300	-0.75300	-0.83000	-0.78400	-0.78500	-0.75400	-0.74200	-0.72000	-0.70400	-0.65200	-0.58100
-6.00000	-0.64500	-0.64500	-0.71000	-0.74500	-0.72200	-0.72100	-0.67900	-0.67200	-0.66800	-0.60100	-0.52000
-4.00000	-0.43000	-0.43000	-0.47400	-0.52400	-0.55600	-0.58900	-0.56500	-0.56000	-0.52000	-0.45000	-0.36000
-2.00000	-0.21500	-0.21500	-0.23700	-0.26200	-0.27800	-0.29800	-0.31200	-0.31200	-0.26000	-0.22500	-0.18000
0.0	0.0	0.0	0.0	0.0	0.0	0.0	0.0	0.0	0.0	0.0	0.0
2.00000	0.21500	0.21500	0.23700	0.26200	0.27800	0.29800	0.31200	0.31200	0.26000	0.22500	0.18000
4.00000	0.43000	0.43000	0.47400	0.52400	0.55600	0.58900	0.56500	0.56000	0.52000	0.45000	0.36000
6.00000	0.64500	0.64500	0.71000	0.74500	0.72200	0.72100	0.67900	0.67200	0.66800	0.60100	0.52000
7.00000	0.75300	0.75300	0.83000	0.78400	0.78500	0.75400	0.74200	0.72000	0.70400	0.65200	0.58100
8.00000	0.86000	0.86000	0.89000	0.81300	0.81900	0.77600	0.76000	0.75300	0.73000	0.69000	0.63200
9.00000	0.96800	0.96800	0.92000	0.83800	0.84000	0.80500	0.80100	0.78100	0.75200	0.71800	0.67200
10.00000	1.07500	1.07500	0.93000	0.85300	0.85400	0.81500	0.82000	0.80300	0.77000	0.73400	0.70500
11.00000	1.18400	1.18400	0.93400	0.86200	0.86000	0.82900	0.83200	0.81200	0.77700	0.74000	0.72600
12.00000	1.22000	1.22000	0.93500	0.86700	0.86700	0.83900	0.84000	0.81800	0.77800	0.74000	0.73700
14.00000	1.17200	1.17200	0.92800	0.87100	0.87200	0.85300	0.84100	0.80100	0.76700	0.72800	0.72800
18.00000	0.65600	0.65600	0.66200	0.87000	0.87000	0.86400	0.75400	0.72200	0.69800	0.67000	0.66400
21.00000	0.80000	0.81000	0.85000	0.85000	0.85000	0.85000	0.71500	0.68000	0.66400	0.64000	0.64100
39.00000	1.18000	1.18000	1.18000	1.18000	1.18000	1.18000	1.18000	1.18000	1.18000	1.18000	1.18000
49.00000	1.18000	1.18000	1.18000	1.18000	1.18000	1.18000	1.18000	1.18000	1.18000	1.18000	1.18000
129.00000	-1.00000	-1.00000	-1.00000	-1.00000	-1.00000	-1.00000	-1.00000	-1.00000	-1.00000	-1.00000	-1.00000
147.00000	-1.00000	-1.00000	-1.00000	-1.00000	-1.00000	-1.00000	-1.00000	-1.00000	-1.00000	-1.00000	-1.00000
161.00000	-0.62000	-0.62000	-0.62000	-0.62000	-0.62000	-0.62000	-0.62000	-0.62000	-0.62000	-0.62000	-0.62000
172.50000	-0.78000	-0.78000	-0.78000	-0.78000	-0.78000	-0.78000	-0.78000	-0.78000	-0.78000	-0.78000	-0.78000
180.00000	0.0	0.0	0.0	0.0	0.0	0.0	0.0	0.0	0.0	0.0	0.0

SUPER 540 EXT'DSUPER 540 EXT'D CLCD DATA TABLES USED

CD

ALPHA/MACH	0.0	0.30000	0.50000	0.60000	0.65000	0.70000	0.75000	0.80000	0.85000	0.90000	1.00000
-180.00000	0.02200	0.02200	0.02200	0.02200	0.02200	0.02200	0.02200	0.02200	0.02200	0.02200	0.02200
-175.00000	0.06200	0.06200	0.06200	0.06200	0.06200	0.06200	0.06200	0.06200	0.06200	0.06200	0.06200
-170.00000	0.13200	0.13200	0.13200	0.13200	0.13200	0.13200	0.13200	0.13200	0.13200	0.13200	0.13200
-165.00000	0.24200	0.24200	0.24200	0.24200	0.24200	0.24200	0.24200	0.24200	0.24200	0.24200	0.24200
-160.00000	0.30200	0.30200	0.30200	0.30200	0.30200	0.30200	0.30200	0.30200	0.30200	0.30200	0.30200
-140.00000	1.04200	1.04200	1.04200	1.04200	1.04200	1.04200	1.04200	1.04200	1.04200	1.04200	1.04200
-120.00000	1.65200	1.65200	1.65200	1.65200	1.65200	1.65200	1.65200	1.65200	1.65200	1.65200	1.65200
-110.00000	1.85200	1.85200	1.85200	1.85200	1.85200	1.85200	1.85200	1.85200	1.85200	1.85200	1.85200
-100.00000	2.00200	2.00200	2.00200	2.00200	2.00200	2.00200	2.00200	2.00200	2.00200	2.00200	2.00200
-90.00000	2.02200	2.02200	2.02200	2.00200	2.00200	2.00200	2.00200	2.00200	2.00200	2.00200	2.00200
-80.00000	1.96200	1.96200	1.96200	1.96200	1.96200	1.96200	1.96200	1.96200	1.96200	1.96200	1.96200
-70.00000	1.84200	1.84200	1.84200	1.84200	1.84200	1.84200	1.84200	1.84200	1.84200	1.84200	1.84200
-60.00000	1.66200	1.66200	1.66200	1.66200	1.66200	1.66200	1.66200	1.66200	1.66200	1.66200	1.66200
-50.00000	1.39200	1.39200	1.39200	1.39200	1.39200	1.39200	1.39200	1.39200	1.39200	1.39200	1.39200
-30.00000	0.60000	0.60000	0.60000	0.60000	0.60000	0.60000	0.60000	0.60000	0.60000	0.60000	0.60000
-28.00000	0.54000	0.54000	0.56300	0.57800	0.57800	0.58100	0.58100	0.58100	0.58100	0.58100	0.58100
-26.00000	0.48000	0.48000	0.52200	0.54500	0.54500	0.54700	0.55800	0.55800	0.55800	0.55800	0.55800
-24.00000	0.42000	0.42000	0.46900	0.50200	0.50200	0.51200	0.52600	0.52600	0.52600	0.52600	0.52600
-22.00000	0.35800	0.35800	0.40900	0.44800	0.46100	0.47200	0.48900	0.49100	0.49100	0.49100	0.49100
-20.00000	0.29900	0.29900	0.35100	0.39600	0.41400	0.43100	0.45100	0.45300	0.45300	0.45300	0.45300
-18.00000	0.24000	0.24000	0.30000	0.34500	0.37000	0.38600	0.40700	0.41400	0.41900	0.41400	0.41900
-16.00000	0.19100	0.19100	0.25300	0.30000	0.32600	0.34100	0.35800	0.36700	0.38100	0.38900	0.38900
-15.00000	0.16700	0.16700	0.23200	0.27500	0.30300	0.31800	0.33300	0.34.00	0.36500	0.37.00	0.37200
-13.50000	0.13500	0.13500	0.20200	0.24400	0.27100	0.28300	0.29900	0.30900	0.33900	0.35000	0.35100
-12.50000	0.10050	0.10050	0.17500	0.22000	0.24900	0.26100	0.27400	0.28500	0.32100	0.33500	0.33600
-11.50000	0.06800	0.06800	0.14200	0.18400	0.22600	0.23800	0.25100	0.26100	0.30200	0.31900	0.32100
-10.50000	0.02600	0.02600	0.11000	0.15800	0.19500	0.21200	0.22960	0.24000	0.28700	0.30200	0.30500
-9.50000	0.01750	0.01750	0.07600	0.12700	0.16400	0.18600	0.20400	0.21800	0.26400	0.28700	0.29100
-8.50000	0.01250	0.01250	0.04900	0.09600	0.13300	0.16200	0.18000	0.19500	0.25000	0.26900	0.27300
-7.50000	0.01020	0.01020	0.02740	0.06800	0.10200	0.13200	0.15500	0.17100	0.23000	0.25000	0.25700
-6.50000	0.00920	0.00920	0.01440	0.04900	0.07100	0.10200	0.12700	0.14600	0.21000	0.23000	0.23900
-5.50000	0.00850	0.00850	0.01000	0.02230	0.04150	0.07150	0.09850	0.12000	0.18700	0.21100	0.22000
-4.50000	0.00800	0.00800	0.00940	0.01340	0.02000	0.04300	0.07000	0.10000	0.16600	0.19000	0.19900
-3.50000	0.00740	0.00740	0.00780	0.00940	0.01280	0.02600	0.04500	0.07000	0.14100	0.16600	0.17600
-2.50000	0.00740	0.00740	0.00780	0.00780	0.00930	0.01650	0.02700	0.04200	0.11000	0.14000	0.15000
-1.50000	0.00710	0.00710	0.00710	0.00700	0.00730	0.00980	0.01650	0.02650	0.07000	0.10500	0.12000
-0.50000	0.00680	0.00680	0.00680	0.00670	0.00650	0.00720	0.00890	0.01280	0.05000	0.07200	0.09500
0.0	0.00680	0.00680	0.00670	0.00660	0.00650	0.00680	0.00740	0.01500	0.04500	0.06900	0.09300
0.50000	0.00680	0.00680	0.00680	0.00670	0.00650	0.00720	0.00840	0.01660	0.05000	0.07400	0.09500
1.50000	0.00710	0.00710	0.00710	0.00700	0.00730	0.00980	0.01650	0.02650	0.07000	0.10500	0.12000
2.50000	0.00740	0.00740	0.00780	0.00780	0.00930	0.01650	0.02700	0.04200	0.11000	0.14000	0.15000
3.50000	0.00740	0.00740	0.00860	0.00940	0.01280	0.02600	0.04500	0.07000	0.14100	0.16600	0.17600
4.50000	0.00800	0.00800	0.00940	0.01340	0.02000	0.04300	0.07000	0.10000	0.16600	0.19000	0.19900
5.50000	0.00850	0.00850	0.01000	0.02230	0.04150	0.07150	0.09850	0.12000	0.18700	0.21100	0.22000
6.50000	0.00920	0.00920	0.01440	0.04900	0.07100	0.10200	0.12700	0.14600	0.21000	0.23000	0.23900
7.50000	0.01020	0.01020	0.02740	0.06800	0.10200	0.13200	0.15500	0.17100	0.23000	0.25000	0.25700
8.50000	0.01250	0.01250	0.04900	0.09600	0.13300	0.16200	0.18000	0.19500	0.25000	0.26900	0.27300
9.50000	0.01750	0.01750	0.07600	0.12700	0.16400	0.18600	0.20400	0.21800	0.26400	0.28700	0.29100
10.50000	0.02600	0.02600	0.11000	0.15800	0.19500	0.21200	0.22960	0.24000	0.28700	0.30200	0.30500
11.50000	0.04600	0.04600	0.14200	0.18400	0.22600	0.23800	0.25100	0.26100	0.30200	0.31900	0.32100
12.50000	0.10050	0.10050	0.17500	0.22000	0.24900	0.26100	0.27400	0.28500	0.32100	0.33500	0.33600
13.50000	0.13500	0.13500	0.20200	0.24400	0.27100	0.28300	0.29900	0.30900	0.33900	0.35000	0.35100
15.00000	0.16700	0.16700	0.23200	0.27500	0.30300	0.31800	0.33300	0.34200	0.36500	0.37200	0.37200
16.00000	0.19100	0.19100	0.25300	0.30000	0.32600	0.34100	0.35800	0.36700	0.38100	0.38900	0.38900
18.00000	0.24000	0.24000	0.30000	0.34500	0.37000	0.38600	0.40700	0.41400	0.41900	0.41400	0.41900
20.00000	0.29900	0.29900	0.35100	0.39600	0.41400	0.43100	0.45100	0.45300	0.45300	0.45300	0.45300
22.00000	0.35800	0.35800	0.40900	0.44800	0.46100	0.47200	0.48900	0.49100	0.49100	0.49100	0.49100
24.00000	0.42000	0.42000	0.46900	0.50200	0.50200	0.51200	0.52600	0.52600	0.52600	0.52600	0.52600
26.00000	0.48000	0.48000	0.52200	0.54500	0.54500	0.54700	0.55800	0.55800	0.55800	0.55800	0.55800
28.00000	0.54000	0.54000	0.56300	0.57800	0.57800	0.58100	0.58100	0.58100	0.58100	0.58100	0.58100
30.00000	0.60000	0.60000	0.60000	0.60000	0.60000	0.60000	0.60000	0.60000	0.60000	0.60000	0.60000
50.00000	1.39200	1.39200	1.39200	1.39200	1.39200	1.39200	1.39200	1.39200	1.39200	1.39200	1.39200
60.00000	1.66200	1.66200	1.66200	1.66200	1.66200	1.66200	1.66200	1.66200	1.66200	1.66200	1.66200
70.00000	1.84200	1.84200	1.84200	1.84200	1.84200	1.84200	1.84200	1.84200	1.84200	1.84200	1.84200
80.00000	1.96200	1.96200	1.96200	1.96200	1.96200	1.96200	1.96200	1.96200	1.96200	1.96200	1.96200
90.00000	2.02200	2.02200	2.02200	2.00200	2.00200	2.00200	2.00200	2.00200	2.00200	2.00200	2.00200
100.00000	2.00200	2.00200	2.00200	2.00200	2.00200	2.00200	2.00200	2.00200	2.00200	2.00200	2.00200
110.00000	1.85200	1.85200	1.85200	1.85200	1.85200	1.85200	1.85200	1.85200	1.85200	1.85200	1.85200
120.00000	1.65200	1.65200	1.65200	1.65200	1.65200	1.65200	1.65200	1.65200	1.65200	1.65200	1.65200
140.00000	1.04200	1.04200	1.04200	1.04200	1.04200	1.04200	1.04200	1.04200	1.04200	1.04200	1.04200
160.00000	0.30200	0.30200	0.30200	0.30200	0.30200	0.30200	0.30200	0.30200	0.30200	0.30200	0.30200
165.00000	0.24200	0.24200	0.24200	0.24200	0.24200	0.24200	0.24200	0.24200	0.24200	0.24200	0.24200
170.00000	0.13200	0.13200	0.13200	0.13200	0.13200	0.13200	0.13200	0.13200	0.13200	0.13200	0.13200
175.00000	0.06200	0.06200	0.06200	0.06200	0.06200	0.06200	0.06200	0.06200	0.06200	0.06200	0.06200
180.00000	0.02200	0.02200	0.02200	0.02200	0.02200	0.02200	0.02200	0.02200	0.02200	0.02200	0.02200

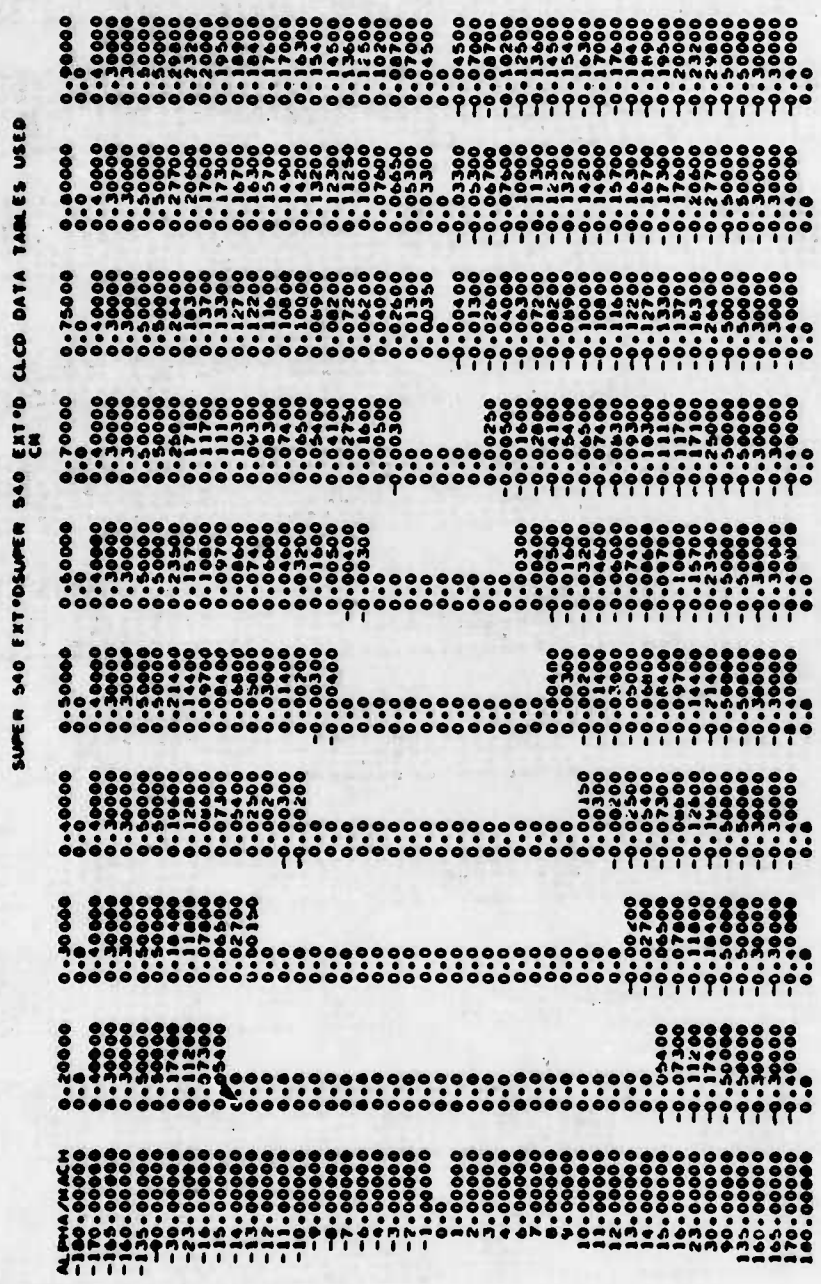
SUPER 540 EXT'D CLCD DATA TABLES USED
CM